

ALMA MATER STUDIORUM – UNIVERSITA' DI BOLOGNA
SCUOLA DI INGEGNERIA E ARCHITETTURA
SEDE DI BOLOGNA
CORSO DI LAUREA MAGISTRALE IN INGEGNERIA DELLE
TELECOMUNICAZIONI

Elaborated in
COMMUNICATION SYSTEMS: THEORY AND MEASUREMENT M

SIMULATION OF VISIBLE LIGHT COMMUNICATIONS IN
VEHICULAR NETWORKS

Candidate

Alex Calisti

Supervisor

Oreste Andrisano

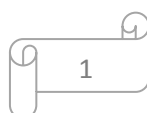
Correlators

Barbara Mavi Masini

Alessandro Bazzi

ACADEMIC YEAR 2013-2014

SESSION II



ABSTRACT

The rapid development in the field of lighting and illumination allows low energy consumption and a rapid growth in the use, and development of solid-state sources. As the efficiency of these devices increases and their cost decreases there are predictions that they will become the dominant source for general illumination in the short term. The objective of this thesis is to study, through extensive simulations in realistic scenarios, the feasibility and exploitation of visible light communication (VLC) for vehicular ad hoc networks (VANETs) applications. A brief introduction will introduce the new scenario of smart cities in which visible light communication will become a fundamental enabling technology for the future communication systems. Specifically, this thesis focus on the acquisition of several, frequent, and small data packets from vehicles, exploited as sensors of the environment. The use of vehicles as sensors is a new paradigm to enable an efficient environment monitoring and an improved traffic management. In most cases, the sensed information must be collected at a remote control centre and one of the most challenging aspects is the uplink acquisition of data from vehicles.

My thesis discusses the opportunity to take advantage of short range vehicle-to-vehicle (V2V) and vehicle-to-roadside (V2R) communications to offload the cellular networks. More specifically, it discusses the system design and assesses the obtainable cellular resource saving, by considering the impact of the percentage of vehicles equipped with short range communication devices, of the number of deployed road side units, and of the adopted routing protocol.

When short range communications are concerned, WAVE/IEEE 802.11p is considered as standard for VANETs. Its use together with VLC will be considered in urban vehicular scenarios to let vehicles communicate without involving the cellular network. The study is conducted by simulation, considering both a simulation platform (SHINE, simulation platform for heterogeneous interworking networks) developed within the Wireless communication Laboratory (Wilab) of the University of Bologna and CNR, and

network simulator (NS3). trying to realistically represent all the wireless network communication aspects. Specifically, simulation of vehicular system was performed and introduced in ns-3, creating a new module for the simulator. This module will help to study VLC applications in VANETs. Final observations would enhance and encourage potential research in the area and optimize performance of VLC systems applications in the future.

TABLE OF CONTENTS

- CHAPTER 1: INTRODUCTION 6
- CHAPTER 2: INTELLIGENT TRANSPORTATION SYSTEM (ITS) 9
 - 2.1 Introduction 9
 - 2.2 Architecture 10
 - 2.3 Radio systems restriction..... 13
- CHAPTER 3: VEHICULAR NETWORKS..... 14
 - 3.1 Introduction 14
 - 3.2 Vehicular network architecture 15
 - 3.3 Vehicular network characteristics 18
 - 3.4 Vehicular networks security and routing algorithms..... 20
 - 3.5 Vehicular networks applications 22
- CHAPTER 4: VISIBLE LIGHT COMMUNICATION 24
 - 4.1 VLC systems 24
 - 4.2 VLC architecture 31
 - 4.3 LEDs..... 36
 - 4.4 Dimming, flickering and eye safety 44
 - 4.5 Luminance intensity 47
 - 4.6 VLC channel..... 60
 - 4.7 Modulation system 70
 - 4.8 Future trends..... 86
- CHAPTER 5: VEHICULAR NETWORKS..... 94
 - 5.1 VLC in ITS 94
 - 5.2 IEEE 802.15.7 98
- CHAPTER 6: SIMULATION OF VLC IN VEHICULAR NETWORKS AND COMPARISON WITH IEEE802.11p
..... 107
 - 6.1 IEEE 802.11p..... 107
 - 6.2 Ns-3 simulator 112
 - 6.3 Implementation of VLC in ns-3 120
 - 6.4 Comparison between VLC in vehicular networks and IEEE 802.11p systems..... 135

CHAPTER 7: CONCLUSION 137
TABLE OF FIGURES..... 138
REFERENCES 141

CHAPTER 1: INTRODUCTION

Wireless communications are enabling the paradigm of the smart cities and networked society, where people, knowledge, devices, and information are networked or the growth of society, life and business [1]. This is happening at a breath taking development speed of technologies and standards toward the 5th generation (5G) [2]. Mobility of people and goods is vital to urban economy and quality of life. It is estimated that people will increase their need of mobility around 35% per decade for the next 3 decades. People and goods travelling will be connected and aware of their location and context. Today the number of networked devices is equal to the global population. By 2015, the number of connected devices will double the global population. A survey conducted by Adobe in 2013, demonstrates that 71% of people use mobile to access social media, so moving people and devices will generate most of the future data traffic so much so that vehicular networks are becoming new key enablers of the future networked society and as the future mobile wireless access for the fifth generation (5G) systems. Most of the future data traffic will be generated and demanded by moving people and devices that produce more and more context-aware data and demand for a variety of new applications [3]. This new scenario changes the classical concepts of communications highlighting new demands for very high level performance networks with extremely low latency. From Shannon's initial work in information theory, it is clear that the capacity of a wireless link is directly proportional to the available bandwidth. On one hand, the system capacity in previous generations of cellular networks was diminished by limiting the spatial reuse of frequencies in an attempt to minimize interference. On the other hand, the most recent generation of wireless technologies, Long-Term Evolution (LTE) and beyond, rely on full frequency reuse along with advanced interference management algorithms to maximize the system capacity. Nonetheless, in spite of employing interference management, there is a trade-off between bandwidth use and link connectivity. Future networks are moving toward more heterogeneous architectures where multiple access points (APs) are available in each cell [4]. This will lead to even denser spatial reuse of resources. These heterogeneous networks (HetNets) provide

enhanced coverage in standard cellular networks and improve the capacity of the system. Unfortunately, the increased frequency reuse introduces both inter- and intracell interference, which limits the achievable capacity of the network. To this extent, the conventional methods for capacity improvement, enhanced spatial reuse and intercell interference coordination (ICIC), will be unable to support the growing demand for mobile communications. Therefore, a new radio frequency-orthogonal communication medium is required to fill the ever increasing capacity gap. Also the demands for solutions for traffic problem such as jams, accidents and environmental impact are increasing. Roads are becoming more congested every year due to insufficient road development to accommodate the increasing number of vehicles; apart from inconvenience to users, heavy economical losses are caused by traffic congestion. Road crashes are the second leading cause of death globally among young people aged five to 29 and the third leading cause of death among people aged 30 to 44 years. Over 1.2 million people are killed annually because of road accidents [5]. Studies predicted that road accidents would become the sixth largest cause of death in the world in 2020 even with the use of many safety devices, whereas it was the ninth largest cause of death in 1990. Intelligent Transportation Systems (ITS) [6] have drawn a lot of attention to solve these (and many others) traffic problems. An excellent solution can be brought by visible light communication (VLC) based on Light Emitting Diodes (LEDs), that is an emerging research area. VLC is a novel kind of Optical Wireless Communication (OWC) [7] which uses white and coloured LEDs to provide information transport through visible light. The combined lighting and switching feature of LEDs is unique and opens the door for very important applications in ITS where the switching characteristics of LEDs are used for data communication without interruption to its normal function of human-visible signalling or lighting. LED-based traffic lights and VLC systems can become an integrated component of ITS and play a key role in road safety applications by broadcasting traffic information in advance to drivers running vehicles which incorporates a low cost LED receiver. In this thesis, we have investigated VLC systems, we have analysed its structure, the modulations systems, the LEDs characteristics and its optical channel. Subsequently a simulation of networking it was created and implemented in a commercial and

open software (NS-3) in order to assesses the obtainable cellular resource saving in vehicular networks (VNs), by considering the impact of the percentage of equipped vehicles, of the number of deployed road side units, and of the adopted routing protocol. The use of the simulator give us the opportunity to create a complete scenario that it can take into account of any characteristics of the environment and because it is open software, it is possible to distribute the visible light communication module to each person making known the potential of the VLC. I have argued this thesis because the VLC systems have many potential to be an integral part of ITS, because of ubiquitous infrastructures support have not been deeply investigated. Recent progress and advancement in LED technology has challenged the most popular and reasonably inexpensive conventional lamps, the Compact Fluorescent Lamp [8]. LEDs have been gradually replacing traffic lights and other conventional lamps because of their merits of huge energy saving, long life, low maintenance cost, better visibility and low temperature generation. Therefore, there is a great need to explore this research area and analyse its novel applications. Furthermore, VLC systems are cost effective, use LEDs and the unregulated visible spectrum, hence they are expected to offer broad potential applications.

CHAPTER 2: INTELLIGENT TRANSPORTATION SYSTEM (ITS)

2.1 Introduction

The application of information and communication technology (ICT) to surface transport is called “Intelligent Transportation Systems”. ITS provides the ability to gather, organize, analyse, use, and share information about transportation systems.

ITS interrelates humans, roads, and vehicles through state-of-art Information Technology (IT), are new information systems for the purpose of the solution of road transportation problems in order to reduce the environment load and aiming efficient traffic flow.

To minimize road accidents and fatalities, vehicle-to-infrastructure (V2I), vehicle-to-vehicle (V2V) and infrastructure-to-vehicle (I2V) vehicular mode communications are being investigated. Emergence of IEEE 802.11p standard [9] for short to medium range inter-vehicle communication and the allocation of a dedicated frequency band for ITS communication in Europe have paved the way for future implementations of communication-based ITS safety applications.

The standard 802.11p for vehicular environment [10] or WiMax currently contribute to road safety. The Car2Car Communication Consortium [11] is dedicated to the objective of further increasing road traffic safety and efficiency by means of cooperative ITS with Inter-Vehicle Communications supported by Vehicle-2-Roadside Communications and vice versa. With the growth of population and its corresponding increase in number of cars, the traffic is becoming totally chaotic. The problem of congestions not only affects the day-to-day life of citizens but also has a great impact on business and economic activities[12].

The future systems will allow cooperation and coexistence among heterogeneous devices and data in VNs, in which the user is a central aspect of transportation systems, forcing architectures to become adaptable and accessible by different means so as to meet different requirements and a wide range of purposes.

Future transport systems must make decisions automatically, analysing input information and acting accordingly, triggering coordinated actions to improve

system performance with flexibility and freedom in the choice in order to create multi-modal heterogeneous networks with an optimal management of resources. In this chapter we will see how a VLC system can be efficiently deployed in ITS and play key role in ever increasing road safety applications and it discussed important differences over most popular radio frequency solutions.

2.2 Architecture

European Telecommunications Standards Institute (ETSI) has contributed significantly towards development of ISO TC 204 ITS architecture [13].

The COMeSafety project [14] defines a common European ITS communication architecture as a basis for future development and standardization as a reference protocol architecture of ITS systems. The ITS represents a generic component for vehicles and roadside communication infrastructures. The reference protocol architecture basically obeys the ISO/OSI reference model, vertically extended by a management and security layer (Figure 1).

The ITS standards [6, 15] promise to offer various access technologies. This family of standards specifies a common architecture, network protocols and communication interface definitions for wired and wireless communications using various access technologies including cellular 3G, LTE, satellite, infrared, 5GHz micro-wave, 60GHz millimetre-wave, and mobile wireless broadband. These and other access technologies that can be incorporated are designed to provide broadcast, unicast and multicast communications between mobile stations, between mobile and fixed stations and between fixed stations in the ITS sector.

Networking and Transport layer offers Internet connectivity and routing and consists of many basic transport protocols and Internet protocol (IPv4-IPv6). For communication support, application support, service announcement and so on, facility layer is included into the model while safety related, efficient traffic relay and value added dedicated applications are handled using application layer.

A security layer monitors and offer authentication for extended services and applications.

A management and control layer becomes necessary for the reference model for proper control and operation of various components.

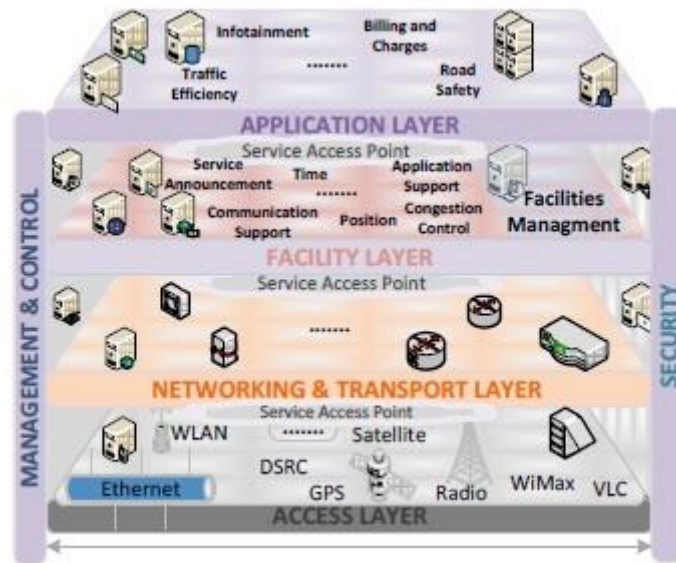


Figure 1: ITS architecture.

In this way is more simple integrated radio-access technologies enabling the 5G networked society for new ideas toward an efficient handling of a very large number of devices with widely varying requirements.

It can also be implemented with the design of advanced PHYs for the coexistence of heterogeneous data flows (high rate flows and several low rate flows) still maintain high the efficiency. A generic communication architecture for ITS is given (Figure 2); it contain the following subsystem:

- the vehicle station, the vehicle require a vehicle gateway connected to the vehicle manufacturer’s proprietary network and to the vehicle station;
- the mobile station, the communication between the vehicle subsystem component and the mobile subsystem component are performed over a short range wireless or wired communication media;
- the roadside station, vehicle communication systems interact with RSUs which consist of many communication infrastructures and access networks. Access point routers, variable message sign and gateways are

responsible for offering information data connectivity between mobile units and Internet;

- the central station, that collect and manage all data.

ITS communication architecture contains the ITS subsystem components and usually a vehicle gateway connecting the ITS Station to legacy systems, these components are inter-linked by a communication network. However, these radio systems are not cost effective. It is very difficult to use wireless based access point all along the road at small intervals, differently from the VLC systems that are deployed everywhere.

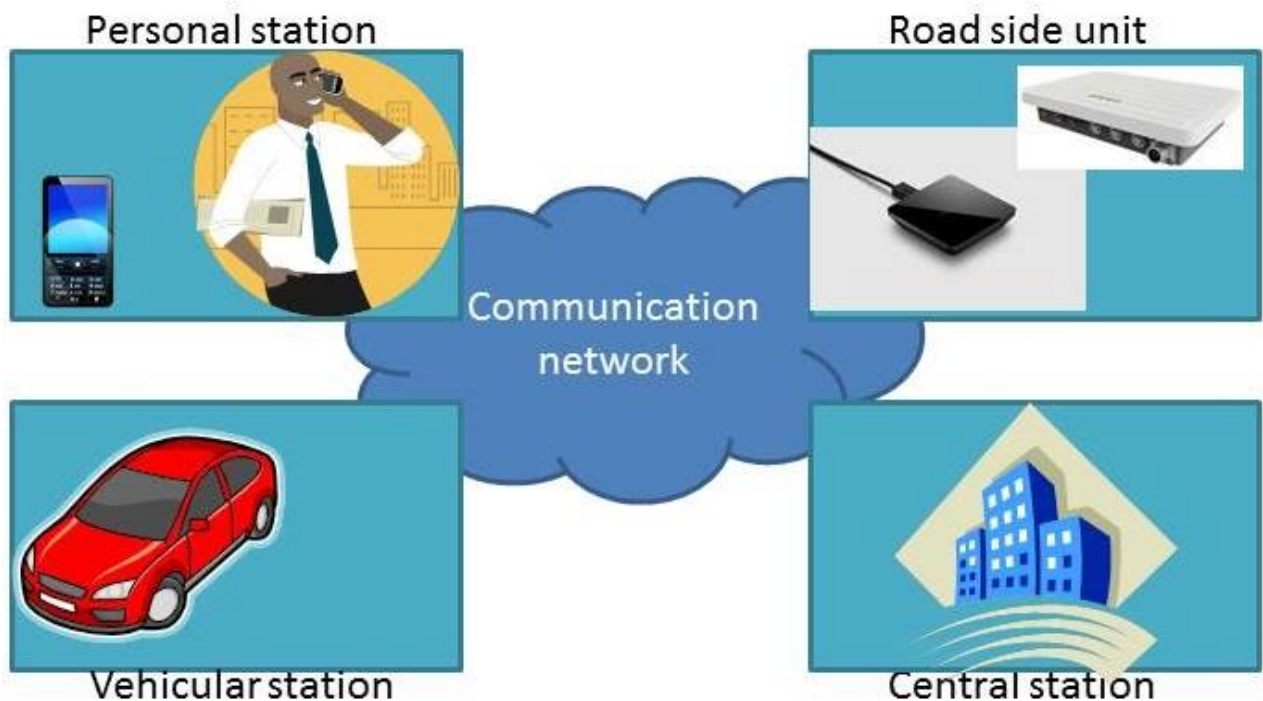


Figure 2: ITS communication architecture

2.3 Radio systems restriction

Visible light communication systems can play a key role in ITS from broadcasting traffic information via visible light through vehicular-to-vehicular (V2V) and vehicular-to-infrastructure (V2I) systems. The Radio Law does restrict the free usage of the radio wave wireless communication, while the VLC does not require any license at present. Due to the limited licensed bandwidth, the radio spectrum is becoming increasingly congested. In addition the electric transmission power cannot be increased because of harm effects to the human health which has been acknowledged by WHO recently [16] and due to radio wave restrictions, frequency bands are licensing congested.

These problems are effectively mitigated by VLC, a LED-based VLC system has no licensing requirement or tariffs for ITS utilization, contrary to RF radiation visible light is very safe for humans and consume less energy reducing carbon emissions, that is an excellent characteristic in a green era. VLC has a large bandwidth , which enables very high data rates and the lights are set everywhere; then wireless transmission can be easily established through VLC device attached to the LED infrastructures.

CHAPTER 3: VEHICULAR NETWORKS

3.1 Introduction

Intervehicle communication (IVC) is attracting considerable attention from the research community and the automotive industry, where it is beneficial in providing intelligent transportation system (ITS) as well as drivers and passengers' assistant services. In this context, vehicular ad hoc networks (VANETs) are emerging as a new class of wireless network, spontaneously formed between moving vehicles equipped with wireless interfaces that could have similar or different radio interface technologies, employing short-range to medium-range communication systems. A VANET is a form of mobile ad hoc network, providing communications among nearby vehicles and between vehicles and nearby fixed equipment on the roadside. This chapter gives an overview of vehicular networks (also known as VANETs), showing their potential architectures and possible deployment scenarios.

Both academia and car manufacturers are progressively paying more and more attention to Vehicular Communications (VC), that allow vehicles to connect to each other and with the roadside infrastructure to form a Vehicular Ad-hoc Network (VANET). VANETs [17, 18] are special types of mobile ad-hoc networks (MANETs) [19], where wireless-equipped vehicles spontaneously form a network while traveling along the road. The nodes of a VANET that constitute the network infrastructure, can be:

- On-Board Units (OBU), that are radio devices installed on vehicles;
- Road-Side Units (RSU), that are placed along the roadside.

VC will enable the development of systems to support several services, for instance road safety, traffic information diffusion, automatic tolling and entertainment [20].

So, vehicular networks are spontaneously formed between moving vehicles equipped with wireless interfaces that could be of homogeneous or heterogeneous technologies. These networks, also known as VANETs, are considered as one of the ad hoc network real-life application enabling

communications among nearby vehicles as well as between vehicles and nearby fixed equipment.

Vehicles networks can be either private, belonging to individuals or private companies, or public.

Indeed, vehicular networks are promising in allowing diverse communication services to drivers and passengers. These networks are attracting considerable attention from the research community as well as the automotive industry. High interest for these networks is also shown from governmental authorities and standardization organizations. In this context, dedicated short-range communications (DSRC) system has emerged in North America, where 75 MHz of spectrum was approved by the U.S. FCC (Federal Communication Commission) in 2003 for such type of communication that mainly targets vehicular networks [21]. Car-to-Car Communication Consortium (C2C-CC) has been initiated in Europe by car manufacturers and automotive OEMs (original equipment manufacturers), with the main objective of increasing road traffic safety and efficiency by means of intervehicle communication [22]. IEEE is also advancing within the IEEE 1609 family of standards for wireless access in vehicular environments.

3.2 Vehicular network architecture

Vehicular network can be deployed by network operators and service providers or through integration between operators, providers, and a governmental authority. Recent advances in wireless technologies and the current and advancing trends in ad hoc network scenarios allow a number of deployment architectures for vehicular networks, in highway, rural, and city environments. Such architectures should allow communication among nearby vehicles and between vehicles and nearby fixed roadside equipment. Three alternatives architecture can be deployed:

- Pure vehicle-to-vehicle ad hoc networks (V2V) without infrastructure support.

As we can see in figure (Figure 3) [23], each car can communicate with the other via wireless system;



Figure 3: V2V communication

- Wired backbone with wireless last hops. In which the wireless systems is used only for the last part of the architecture (Figure 4);

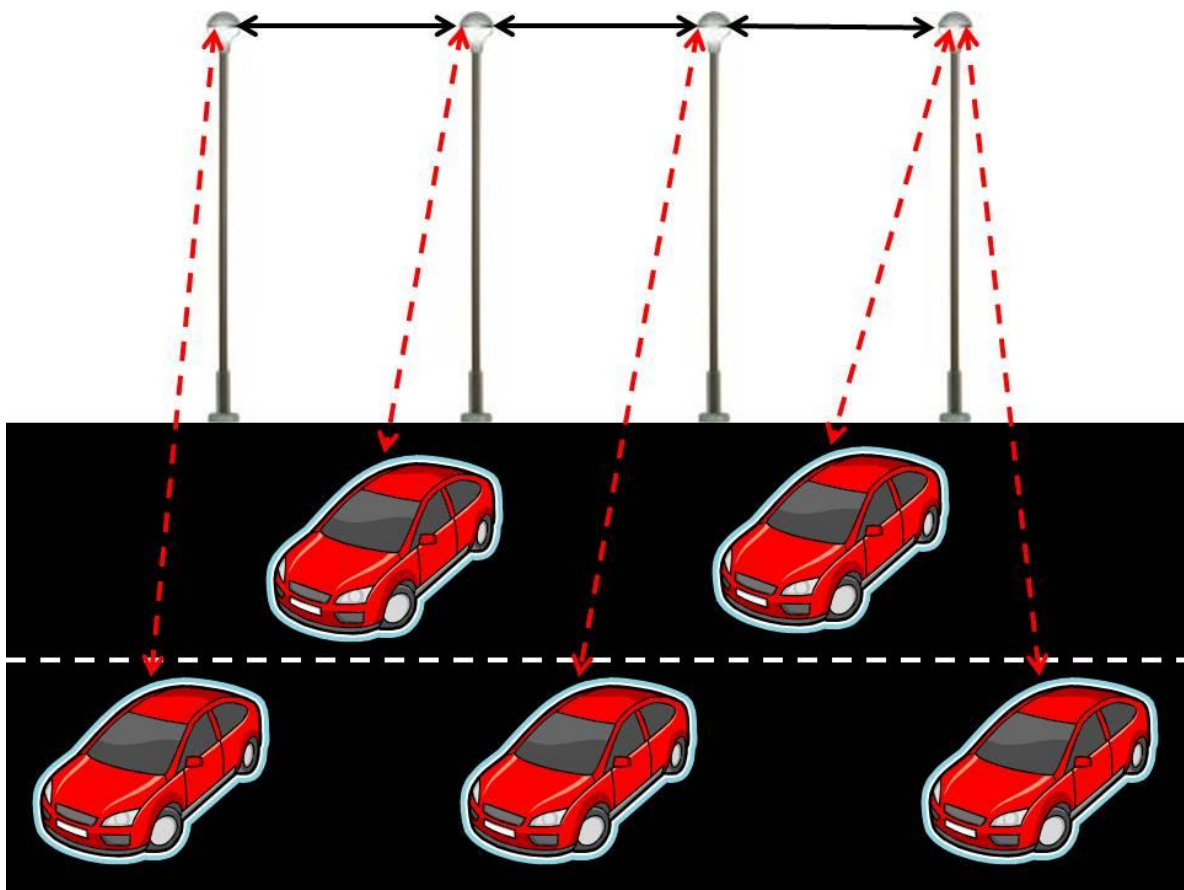


Figure 4: C2C communication with wired backbone.

- Hybrid vehicle-to-road (V2R) that can be exploit in order to improve the performance and service access. Vehicles can communicate with the infrastructure either in a single hop or multihop fashion according to the vehicles' positions with respect to the point of attachment with the infrastructure. Actually the V2I architecture implicitly includes V2V communication (Figure 5) [22].



Figure 5:V2I communication

A reference architecture for vehicular networks is proposed within the C2C-CC, distinguishing between three domains: in-vehicle, ad hoc and infrastructure domain [25] (Figure 6). The in-vehicle domain refers to a local network inside each vehicle logically composed of on-board unit (OBU) and one or more application units (AUs). An OBU is a device in the vehicle having communication capabilities (wireless and/or wired), while an AU is a device executing a single or a set of applications while making use of the OBU's communication capabilities [26]. Indeed, an AU can be an integrated part of a vehicle and be permanently connected to an OBU. It can also be a portable device such as a laptop or PDA that can dynamically attach to an OBU. The AU and OBU are usually connected with a wired connection, while wireless connection is also possible. This distinction between AU and OBU is logical and they can also reside in a single physical unit.

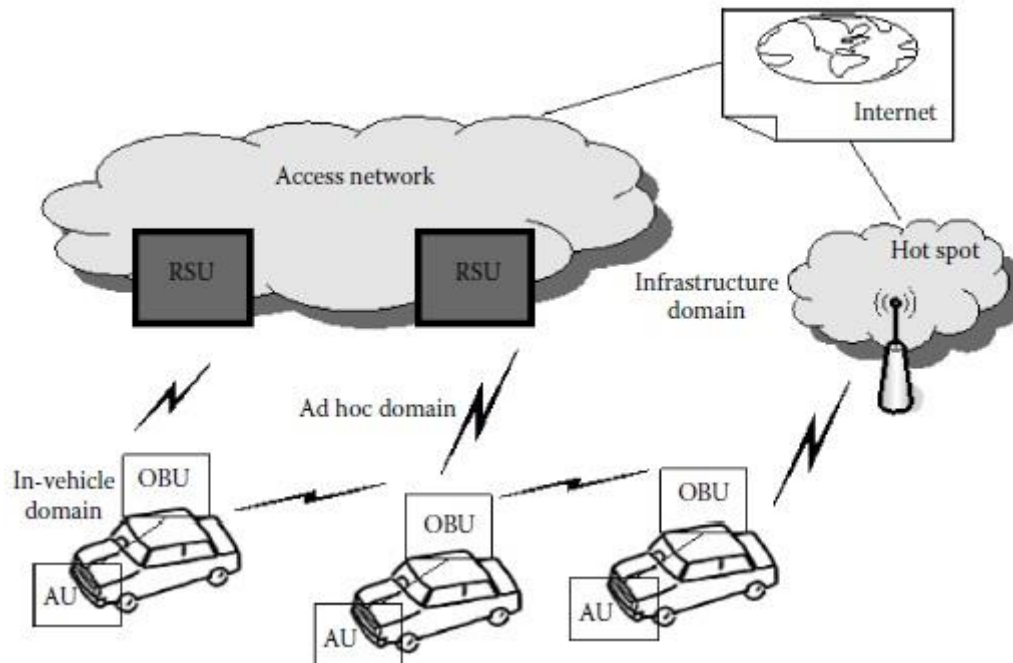


Figure 6: C2C-CC architecture

The ad hoc domain is a network composed of vehicles equipped with OBUs and road side units (RSUs) that are stationary along the road. OBUs of different vehicles form a mobile ad hoc network (MANET), where an OBU is equipped with communication devices, including at least a short range wireless communication device dedicated for road safety. OBUs and RSUs can be seen as nodes of an ad hoc network, respectively, mobile and static nodes. An RSU can be attached to an infrastructure network, which in turn can be connected to the Internet. RSUs can also communicate to each other directly or via multihop, and their primary role is the improvement of road safety, by executing special applications and by sending, receiving, or forwarding data in the ad hoc domain. The infrastructure domain can be access by RSU or via public, commercial, private hot spots (Wi-Fi hot spots). In the absence of RSUs and hot spots, OBUs can utilize communication capabilities of cellular radio networks (GSM, GPRS, UMTS, WiMax, and 4G) if they are integrated.

3.3 Vehicular network characteristics

Vehicular networks have excellent characteristic and special behaviour respect the other types of mobile networks.

In comparison to other communication networks, vehicular networks come with unique attractive features, as follows [27]:

- Unlimited transmission power: mobile device power issues are usually not a significant constraint in vehicular networks as in the case of classical ad hoc or sensor networks, since the node (vehicle) itself can provide continuous power to computing and communication devices.
- Higher computational capability: indeed, operating vehicles can afford significant computing, communication, and sensing capabilities.
- Predictable mobility: unlike classic mobile ad hoc networks, where it is hard to predict the nodes' mobility, vehicles tend to have very predictable movements that are limited to roadways. Roadway information is often available from positioning systems and map based technologies such as GPS. Given the average speed, current speed, and road trajectory, the future position of a vehicle can be predicted.

However, vehicular networks have to face with some challenging [28], which include:

- Potentially large scale: unlike most ad hoc networks studied in the literature that usually assume a limited network size, vehicular networks can in principle extend over the entire road network and so include many participants.
- High mobility: the environment in which vehicular networks operate is extremely dynamic, and includes extreme configurations.
- Partitioned network: vehicular networks will be frequently partitioned. The dynamic nature of traffic may result in large intervehicle gaps in sparsely populated scenarios, and hence in several isolated clusters of nodes.
- Network topology and connectivity: vehicular network scenarios are

very different from classic ad hoc networks. Since vehicles are moving and changing their position constantly, scenarios are very dynamic. Therefore the network topology changes frequently as the links between nodes connect and disconnect very often. Indeed, the degree to which the network is connected is highly dependent on the range of wireless links and the fraction of vehicles on the road that could be equipped with wireless interfaces.

3.4 Vehicular networks security and routing algorithms

As the demand for service discovery is growing, passengers may use services in foreign networks and create immense security problems for themselves and for other network users.

Then, it is important to propose innovative solutions for secure communication between participants as well as authorized and secure service access. To enhance the vehicular network access ubiquity, these solutions should take advantage of the ad hoc multihop authentication and communication concepts, which on one hand allow secure communication and on the other hand extend the infrastructure coverage with the minimum deployment cost for the network operator, and the distributed-based authentication. Appropriate security architectures should be in place providing communication between vehicles and allowing different service access. A set of security mechanisms suitable for any vehicular network environment should be developed, providing trust, authentication, access control, authorized and secure service access. Node behaviour is an important issue that can threaten the security of communication and service delivery in vehicular networks, and hence is worth consideration. Due to the open and dynamic environment of vehicular networks, nodes cooperation is an important aspect that should be satisfied for allowing successful communication between vehicles [26]. In this context, authentication optimization is important to be studied for both infrastructure-based and infrastructure-less communications, aiming to facilitate the re-authentication process that may need to take place during the vehicle mobility.

A security system for safety messaging in a VANET should satisfy the following requirements:

- **Authentication:** vehicle reactions to events should be based on legitimate messages, therefore we need to authenticate the senders of these messages.

- Verification of data consistency: the legitimacy of messages also encompasses their consistency with similar ones.
- Availability: even assuming a robust communication channel, some attacks can bring down the network; therefore, availability should be also supported by alternative means.
- Non-repudiation: drivers causing accidents should be reliably identified; a sender should not be able to deny the transmission of a message.
- Privacy: people are increasingly wary of Big Brother enabling technologies. Hence, the privacy of drivers against unauthorized observers should be guaranteed.
- Real-time constraints: at the very high speeds typical in VANETs, strict time constraints should be respected.

With that characteristic the networks can be secure and we can concentrate on the routing algorithm in order to forward packets how much is possible. Vehicular networks differ from conventional ad hoc wireless networks by not only experiencing rapid changes in wireless link connections, but also having to deal with different types of network densities [30]. Vehicular networks are expected to handle a wide range of applications ranging from safety to leisure. Consequently, routing and dissemination algorithms should be efficient and should adapt to vehicular network characteristics and applications, permitting different transmission priorities according to the application type. Until now, most of vehicular network research has focused on analysing routing algorithms to handle the broadcast storm problem in a highly dense network topology [31, 32], under the oversimplified assumption that a typical vehicular network is a well-connected network in nature. In the future, these networks are expected to observe high penetration with lesser infrastructure support and it is important in this case to consider the disconnected network problem which is a crucial research challenge for developing a reliable and efficient routing protocol that can support highly diverse network topologies.

In no safety-related applications, message transfer through unicast or multicast transmission is more suitable [29].

3.5 Vehicular networks applications

This section discusses major vehicular networking applications and use cases. A use case represents the utilization of a vehicular networking application in a particular situation with a specific purpose [33]. In vehicular networks there are many and many applications, from road safety applications that are employed to decrease the probability of loss of life and traffic accidents [34, 35, 36, 37, 38, 39] to infotainment applications like cooperative local services [35, 36, 39, 40] and global internet services.

The Vehicular networks can be used for:

Control loss warning: the vehicles determine the relevance of the event and provide a warning to the drivers only if appropriate.

Intersection collision warning: the risk of lateral collision for vehicles that are approaching road intersection is detected by vehicles or road side units.

Hazardous location notification: like construction work or obstacles on the road.

Lane change assistance: the risk of lateral collision for vehicles that are accomplishing a lane change is reduced.

Collision risk warning: a road side unit detects a risk of collision between two or more vehicles that do not have the capability to communicate.

Emergency electronic brake lights.

Overtaking vehicle warning: aims to prevent collision between vehicles in an overtaken situation.

Signal violation warning: one or more devices detect a traffic signal violation and informs all vehicles in the neighbourhood.

Head on collision warning: the risk of a head on collision is reduced by sending early warning to the vehicles that are travelling in opposite directions [29].

Rear end collision warning: the risk of rear-end collisions is reduced.

Traffic condition warning: any vehicle that detects some rapid traffic evolution, informs other vehicles about this situation.

Cooperative forward collision warning: a risk of forward collision accident is detected through the cooperation between vehicles.

Wrong way driving warning.

Emergency vehicle warning: an active emergency vehicle informs other vehicles to free an emergency corridor.

Pre-crash sensing: it is considered that a crash is unavoidable and will take place, but vehicles and RSU can share information to predict collision and alarm other vehicles.

Stationary vehicle warning: any vehicle that is disabled due to an accident, breakdown or any other reason, informs other vehicles and RSU about this situation.

CHAPTER 4: VISIBLE LIGHT COMMUNICATION

4.1 VLC systems

After the invention of the mobile phone, the popularity of short-range radio communications has increased. More and more mobile devices have appeared with an increasing need to exchange data wirelessly. This massive increase in the number of mobile devices is provoking a shortage of radio spectrum resources.

Under this scenario, the efforts of the research community have been redirected toward the exploration of novel solutions that could guarantee an efficient usage of the available spectrum. As a consequence, new paradigms such as cognitive radio, spectrum sharing and spectrum refarming have emerged. This scenario also offers a new opportunity for optical wireless communications (OWC) to regain the attention of the wireless industry by providing additional spectrum resources.

OWC had a slow but constant evolution during the last century. Most OWC applications are related to short-range and low-data-rate communication.

They use infrared light and can be found in our daily life, where the best known example is the remote control of electronic domestic appliances. However, in the last few years, visible light communication (VLC), a new paradigm of OWC, has captured the attention of the research community. As the name suggests, VLC uses beams of visible light to send information. The main challenge of VLC systems consists of finding a source of artificial light that can easily be modulated [41]. The recent development of high-power light-emitting diodes (LEDs) has provided a cost-effective technical solution to the aforementioned challenge.

Visible light communications (VLC) has a long history dating back to ancient signal fires, followed by the 1880 Alexander Graham Bell photophone, which transmitted speech wirelessly using modulated reflected sunlight, also in 1979, Gfeller and Bapst suggested the first system using infrared (IR) LEDs for wireless data transmission. But it was the emergence of solid state light sources that sparked the imagination of researchers, such as those at Nakagawa Laboratories at Keio University around the turn of the 21st century, to demonstrate that solid state light sources could be used for secondary purposes such as data transmission and positioning.

It is expected that by 2020, 70 percent of residential and 90 percent of architectural lighting will be LED-based [42].

As a matter of fact, these appliances might not serve only as illumination devices. During the last decade, the interest of the communications research community in LED devices has increased because white-LEDs can be also used as data transmitters without losing their main functionality as illumination sources [43, 44], enabling the appearance of VLC. Visible light communications are the offspring of well-studied infrared wireless systems and can form a promising enhancement of future illumination infrastructures with communication functionalities. This technology presents several advantages regarding radio wave communications systems. Among them, robustness against electromagnetic interference and a high level of protection against eavesdropping can be highlighted. The research community is not the only one gaining interest in this new technology (Figure 7) [45].

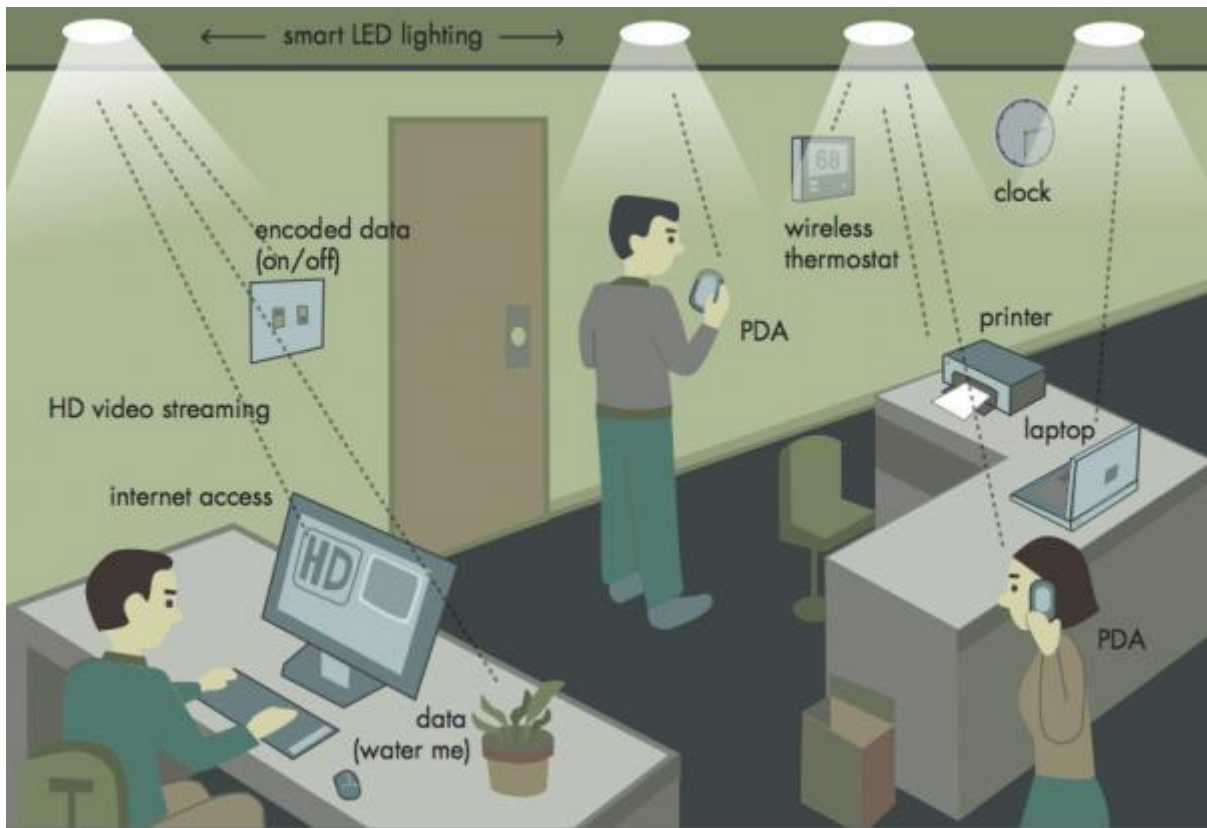


Figure 7: VLC application

The vision of LED-based illumination as the future of lighting systems motivates continuous effort within the lighting industry to maximize the efficiency and minimize the fabrication costs of LED luminaires. Since the early days of VLC there has been much research demonstrating increased unidirectional data rates, with increasingly sophisticated modulation formats, today approaching 1 Gb/s and over this same timeframe we have seen several VLC standards generated specifying data rates approaching 100 Mb/s. LEDs electrically behave as solid-state diodes that allow for rapid switching times down to tens of nanoseconds. Such fast response is an attractive quality, which inspired the transmission of information by means of LED light modulation.

Since then, IR wireless communications were standardized and applied in special settings such as remote control applications and short range line-of-sight

links, but have not evolved to a widespread alternative for broadband access networks.

With a view toward green technologies and operational cost reduction, the work on IR wireless systems was recently revitalized by the emergence of HB-LEDs that allow for simultaneous operation as illumination and communication sources (Figure 8) [46].



Figure 8: VLC applications

Visible light communications (VLC), as this field is called today, covers optical wavelengths between 380 and 780 nm, and is similar in many respects to IR wireless communications [47]. In essence, there is no difference in the radiation propagation and interaction with reflecting surfaces between visible and IR wavelengths, despite the strong similarities between IR and VLC systems, there are also distinct differences. Traditional radio frequency (RF) communication below 6 GHz is rapidly running out of spectrum bandwidth for high data-rate communication.

With ~300 THz of bandwidth available for VLC, multi-gigabit-per second data

rates could be provided over short distances, for example, using arrays of LEDs in a multiple-input multiple-output (MIMO) fashion [3,4]. In addition, communication is provided in conjunction with lighting providing gigabit-per-second data rates with only simple LEDs and photodetectors (PDs) compared to expensive RF solutions that require high power consumption for transmitting, sampling and processing gigabit-per-second data.

VLC already offers almost 500 Mb/s with low-complexity on-off keying (OOK) [50] and more than 1 Gb/s with optical versions of orthogonal frequency-division multiplexing (OOFDM) [51]. For the same emitted power, narrowband IR systems have better immunity to broadband noise from ambient light sources than VLC systems. On the other hand, the broadband nature of white light offers some degree of wavelength diversity in spectrally selective reflection from colored surfaces that absorb specific wavelengths. Furthermore, IR radiation is invisible to the human eye, allowing continuous operation of IR wireless systems without being perceived, while VLC systems cannot operate when no lighting is desired and the LED luminaires are turned off. The potential use of the same device for simultaneous data transmission and illumination is tempting and fascinating. At first glance, the power and money already invested in providing illumination could be reused to facilitate high- data-rate communication between light sources and users.

LED luminaires could act as network access points, turning VLC into a direct competitor to broadband radio technologies such as WiFi, third/fourth generation (3G/4G) systems and WiGig. The Visible Light (VL) spectrum is unlicensed and currently largely unused for communication, the availability of this free spectrum creates an opportunity for low-cost broadband communication that can help the more used bands. The VL systems have excellent isolation propriety, because the fact that they cannot pass through wall or obstacles that can be seen as a limit but if we have some applications like point-to-point or vehicular systems in which only nearby cars must communicate this result like a deletion of interfering signals and they do not suffer multipath fading. This systems with current technology is a non-coherent mode of communication [52], the front-end components are relatively simple and cheap devices that operate in the baseband and do not require frequency mixers or sophisticated algorithms for the correction. The wavelength of light is in the sub-micron range (Figure 9) [53], so accurate direction-of-arrival estimation is achievable with

photodiodes arrays, which enables accurate indoor positioning of mobile devices.

On the other end the achievable data rate falls sharply with increasing the distance, since VLC is a non-coherent form of communication the path loss is inversely proportional to the distance raised to the power of four, there is shot noise if the photodiodes are exposed to direct sunlight and the light have to be powered on in order to transmit data at link rates that approach those of WIFI.

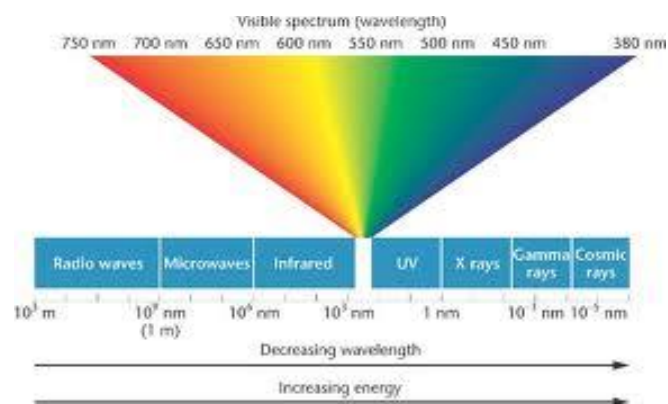


Figure 9: VLC wavelength

VLC systems have multiple benefits, however a number of complex challenging issues need to be addressed. The first and the foremost, while the requirement of line of sight link can be thought of as a drawback of the system, it becomes advantageous in the indoor from one room to another room or cell based links without interference from each other. Some challenges are outlined as follows:

- Long Range Limitation: because of LoS path requirement, the technology is suitable for short range communication;
- Ambient and other sources of intense noise: especially in outdoor applications;
- Increasing data rate: the limited bandwidth of LEDs is another major challenge for high-speed communication;

- Provision of Uplink: using illumination sources is naturally suited to broadcast applications, providing uplink communication will be problematic;
- Complex modulation: the most simple and useful modulation technique based on direct detection intensity modulation is too weak to overcome many challenges. A complex modulation technique would be needed to support effective and desirable data communication;
- Complex receiver based on equalizer: As an extension of IR, some studies proposed the use of equalizers at the receiver at the cost of increased complexity;
- Regulatory challenges: VLC is subject to regulation by non-communication standard, so coordination across regulatory bodies and frameworks become challenging.

To better understand the benefit of the visible light communication, in (Table 1) we can see a comparison between VLC and radio systems.

Until now, we have seen what is visible light communication and see the benefit that it can introduce.

Then, now in this chapter we will describe the visible light communication system architectures, the LED illumination, the optical channel and its possible applications in vehicular network, in order to better understand this now excellent system.

| Parameters | RF | VLC |
|-------------------------|--|---|
| Bandwidth | 300 GHz | 300 THz |
| Spectrum regulation | Licensed | Unlicensed |
| Data rate | Few 100 Mbps | Depend on distance and limited by LED switching speed |
| Line of sight | No | Yes |
| Standards | Matured | Beginning |
| Hazard | Yes | No |
| Safety issue | Susceptible to the biological damages to humans by the electromagnetic way | No danger to eyes or biological effects. Easily used with medical instruments or even on airplane |
| Usage | Everywhere with cell phones or wireless devices | on all possible things with a LED |
| Suitability | Wide applications and popularity. restricted in hospital and airplane | Short and medium, both indoor and outdoor |
| Visibility | No | Yes |
| Implementation and cost | Complex, costly | Cost effective, used on existing infrastructure or with slight modification |
| Security | Many complex algorithm needed | Secured |

Table 1: comparison between Radio Frequency and Visible Light Communication

4.2 VLC architecture

In this section, we introduce the architecture system of a VLC transceiver and next we described each part that compose it.

The block diagram representation of VLC systems architecture is shown in (Figure 10) [54, 55].

Devices such as laptop, mobile phones or cars can be used for transmitting and receiving information signal.

The transmitter part consists of a light source, modulator and a pulse shaper to switch the LEDs at the rate of data transmission. The light source emits data using light wave as the medium while illuminating and the data is sent between two or more terminals.

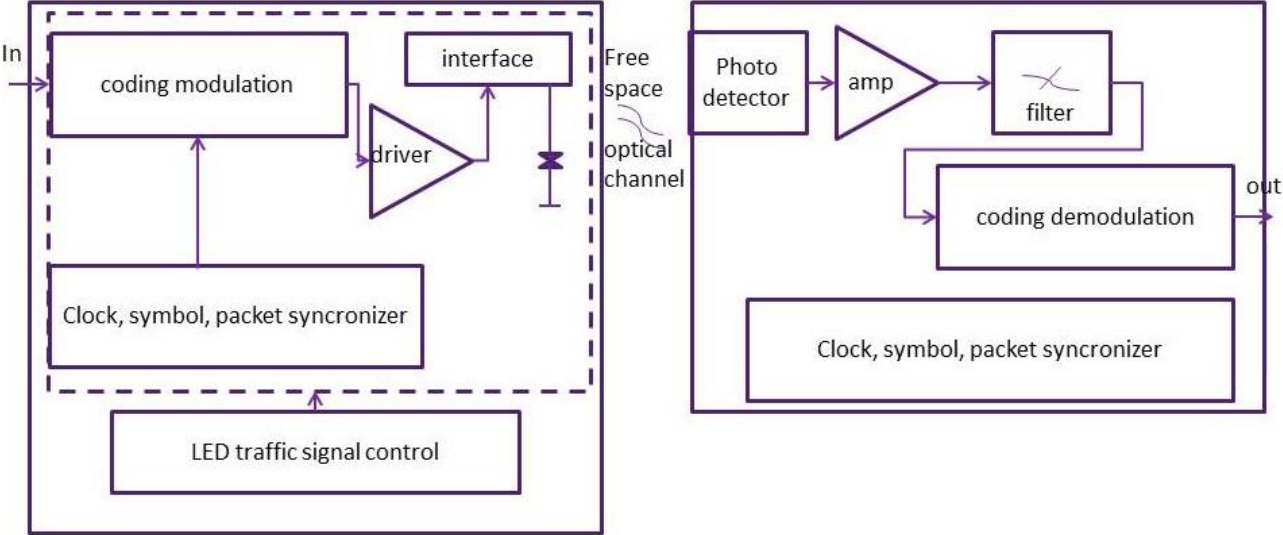


Figure 10: VLC system architecture

The VLC transmitter is different from conventional communication transmitter in viewpoint that it must act as a communication transmitter and an illumination device simultaneously.

The digital data signal is passed to a data encoder that modulates the signal with the purpose to switch the LEDs at the expected rate of data transmission. The modulation method used must offer high robustness to background light and at the same time, light should be as bright as possible.

Intensity modulation/direct detection (IM/DD) often used in IR can also be used in VLC, next we will see also modulation formats.

In a practical aspect, the modulator also receives information from the traffic control unit so that it can hold information while the light colour changes. This ensures that there is no transmission in the brief period of change in traffic signal and the transmission is synchronized.

The resulting signal is then used to control the switching of the LED through the output driver.

To modulate the LEDs, the drive current is fed into the LEDs with the appropriate DC bias.

For modulating an LED directly, a transistor is switched for feeding the LED or an FET can be used (56), or also, integrated circuit (IC) based driver chip can be used.

Since the drive current contains the DC current for illumination or the dimming current for data signal, a bias Tee can be used for mixing the DC current and digital data for low data rate application.

To design an appropriate driver circuit for VLC system, the following items must be considered:

- Current requirement of LED: bias current and modulation depth;
- Rise and fall times of components: related to maximum bit rate;
- Illumination compatibility with communication;
- Design approach: whether driver IC is used or not;
- Power dissipation and thermal design of the transmitter.

VLC data rate is limited by the switching speed of the emitter LEDs. On the other hand, long distance communication is limited by the transmitted power and background light sources.

The VLC receiver is composed of receiving optical elements including optical concentrator and optical filter, photodiode (or LEDs), amplifier and signal recovery circuit as shown in figure (Figure 10).

Basically, the VLC system is designed to employ direct detection at the photodiode, the optical concentrator is used to compensate for high spatial attenuation due to the beam divergence from the LEDs to illuminate large area. The detector is characterized by the parameter field of view (FOV) (Figure 11) [56]; for a larger service area, a receiver with a wider FOV is preferable. However, a wider FOV leads to performance degradation because of possibilities of receiving unwanted light signals.

By using the appropriate concentrator, the effective collection area can be increased. The methods using compound parabolic concentrator (CPC) and imaging lens for infrared communications are described in [57, 58].

Since the wavelength range is different from the infrared communication, the specific design parameters for the VLC system will be changed from the design for the infrared communication.

The VLC system is vulnerable to the sunlight and other illuminations, and therefore, it is important to employ appropriate optical filter to reject unwanted DC noise components in the recovered data signal.

There are many photodiodes whose bandwidths are over 200 MHz and is much wider than the VLC LED transmitter.

There are several types of signal amplification circuits; among them, high impedance amplifier and transimpedance amplifier [59] are briefly described. The high impedance amplification is simple to implement, the series resistor is connected to the anode of the photodiode and the high input-impedance amplifier senses the voltage across the series resistor and amplifies it. The transimpedance amplifier provides current-to-voltage conversion by using shunt feedback resistor around an inverting amplifier.

The resulting voltage is then applied to a low-pass filter to remove any high-frequency noise.

The signal is then further amplified in the final voltage amplifier stage. Also, DC signal filtering is applied at the input of the amplifying and filtering stages, which helps reduce the DC noise component of the captured signal as well as low-frequency components.

The final voltage signal should correspond to the received light pulses which are then decoded in the final decoder block, thus extracting the digital data. This final block performs the inverse function of the emitter's encoder block, but it can also be implemented with a microprocessor or, even better, an FPGA. The demodulation scheme will depend on the modulation scheme used in emitter side.

A practical down-conversion technique that can be considered is direct detection. Clock recovery is necessary to synchronize the receiver with the transmitter, in addition, the system will also need the protocol management unit and data/clock recovery block for the synchronization of received packets.

Generally, the noise in the VLC receiver is similar to the usual optical communication receiver, for example, the thermal noise from the load resistor and the photodiode, the shot noise in the photodiode, the excess noise from the amplifier.

The main noise components are the sunlight and the other illumination light.

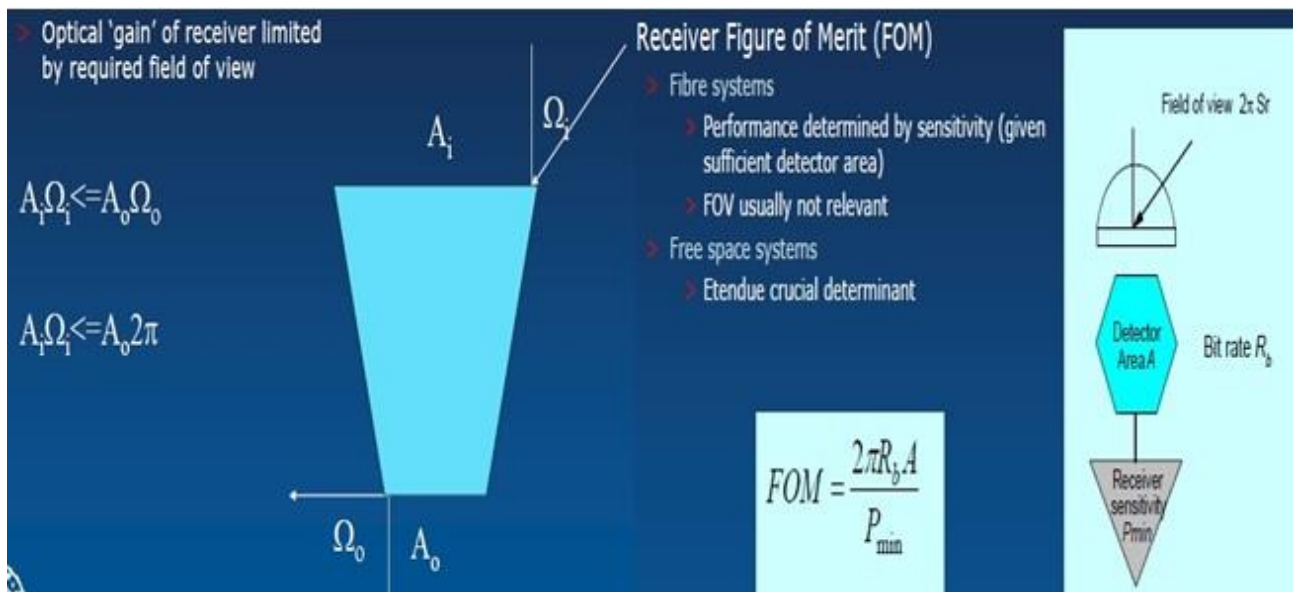


Figure 11: Receiver properties.

Devices that use a slotted VLC scheme to communicate need to operate in a time-synchronized way: VLC devices in range of each other are synchronized if the beginning of each slot occurs at the same time for all devices. Synchronization errors such as clock shift and jitter are undesirable and reduce the system performance [65].

Using an LED in reverse bias acting as a receiver leads to low sensitivity to optical energy (in comparison with photodetectors).

This setup makes obtaining an accurate synchronization more difficult.

A possible solution is to leave devices un-synchronized and transmit a dedicated synchronization preamble before each frame [66, 67].

If a portion of time is dedicated to the transmission of the preamble for synchronisation, the overhead increases.

When powered on, a VLC device performs an initial measurement that typically lasts for a few milliseconds, the device measures the current light intensity over several measurement slots.

After the initial measurement, every VLC device continuously measures the amount of light detected in measurement slots and compares the values of two consecutive measurements.

If the amount of light measured during two consecutive slots is close to each other and if it is also similar to the ambient light measured earlier, the device can

conclude that either there is no other device in its vicinity, or that it is synchronized to the other nearby devices.

However, if the device detects that the two consecutive measurement values deviate (with some hysteresis), this might mean that there is another light-emitting device in the vicinity.

4.3 LEDs

A light-emitting diode (Figure 12: coloured LEDs.) [60] is a two-lead semiconductor light source, it is a basic pn-junction diode, which emits light when activated. When a fitting voltage is applied to the LEDs, electrons are able to recombine with electron holes within the device, releasing energy in the form of photons. This effect is called electroluminescence, and the color of the light (corresponding to the energy of the photon) is determined by the energy band gap of the semiconductor. An LED is often small in area and integrated optical components may be used to shape its radiation pattern. Appearing as practical electronic components in 1962, the earliest LEDs emitted low-intensity infrared light.

Infrared LEDs are still frequently used as transmitting elements in remote-control circuits, such as those in remote controls for a wide variety of consumer electronics. The first visible-light LEDs were also of low intensity and limited to red, modern LEDs are available across the visible, ultraviolet, and infrared wavelengths, with very high brightness. Early LEDs were often used as indicator lamps for electronic devices, replacing small incandescent bulbs. Recent developments in LEDs permit them to be used in environmental and task lighting, LEDs have many advantages over incandescent light sources including lower energy consumption, longer lifetime, improved physical robustness, smaller size, and faster switching. LEDs have allowed new text, video displays, and sensors to be developed, while their high switching rates are also useful in advanced communications technology.

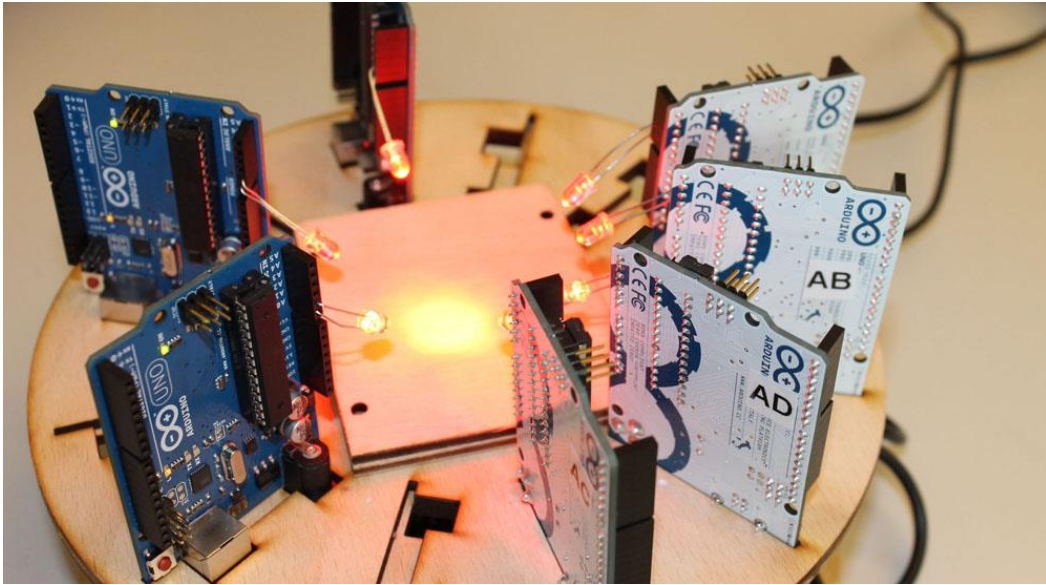


Figure 12: coloured LEDs.

In ITS, LED-based traffic light emitter is also used for signalling at the same time (Figure 13). Furthermore, it is understood that a number of LEDs are needed to offer visibility at longer distance and data transmission, to cover a larger road area along the road length.

Wide coverage of light illumination is expected to offer larger service area that is, the area in which data information is received reliably.

In the absence of LEDs road illumination lights, traffic lights VLC system's topology become dynamic and consequently characterized by the variability of the transmission channel.

Emitter-receiver distance and ambient noise can change, making the signal-to-noise ratio (SNR) vary significantly in the outdoor optical communication channel.

Shorter distances between emitter and receiver allow the use of higher transmission rates; on the other hand, an increase in the ambient noise intensity can be counterbalanced by the decrease on transmission rate.

It is known that in VLC communication, the connectivity is more important than the transmission rate, putting under an obligation that these systems must be provided with transmission rate adaptation mechanisms.

This property allows the system to respond to the network topology and channel dynamic nature, also offering the perspective of use in multiple applications and granting compatibility guaranties with other existing systems.

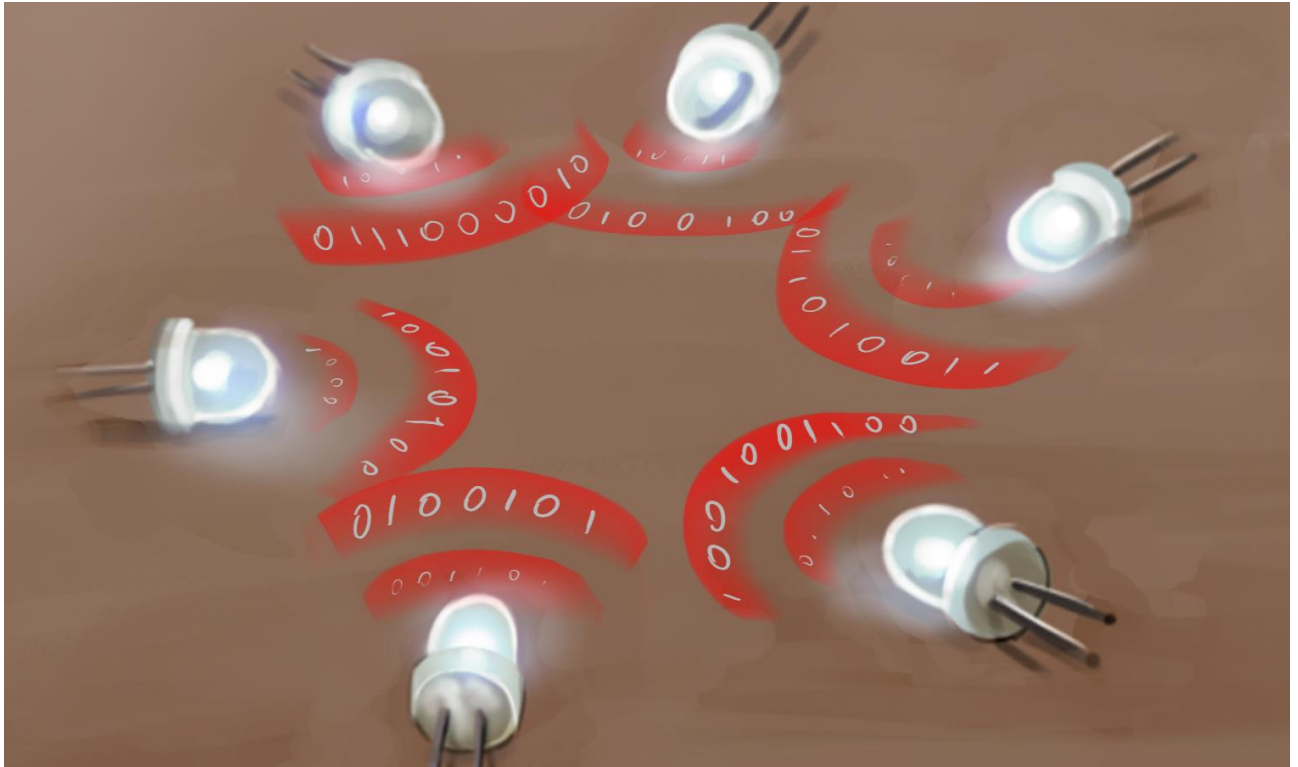


Figure 13: VLC with LEDs

LEDs have changed the concept of lighting not only in an expectation of the ultimate efficiency but also in tremendous opportunities for versatile and “smart” lighting applications.

LED-based lighting technology, solid-state lighting [61, 62, 63, 64] allows for unprecedented versatility in control over the radiation spectrum, which can be tailored for specific needs from general to many specific scenarios.

Low-voltage driver, fast switching, and compatibility with networked computer controls enable intelligent lighting systems with software-controlled stability, operating function, adaptation, and energy savings.

Such systems are expected to emerge and become disruptive and a revolutionary technology in the near future but same constraints are present. Some constraints are related to the illumination level (dimming), colour temperature and

diffusiveness related to the positioning of the LEDs; from that constraint depend the spatial distribution of the luminance and thus of the power distributions. Other constraints depend on the component that form an LED luminaire; in particular the LED source together with the driver electronics and the optical system (Figure 14) [68] are responsible for multiple functions such as dimming support, efficient power supply, temperature control of the LED source, heat sinking and realization of a light radiation pattern.

These functionalities are required to achieve the desired lighting conditions and meet the manufacturer's specifications in terms of expected lifetime and device efficiency, but they also have an impact on the performance of the LED luminaire as a VLC transmitter.

The nonlinear I-V characteristics of the source, the voltage drop across LEDs' active region is constant, while the light output is driven by the current passing through them.

This nonlinear response can in some cases severely degrade the dynamic range of useful driving currents; this is particularly relevant in multilevel modulation and OFDM schemes, where, pre-distortion of the signal may help in removing the effect of nonlinearities [69].

Three approaches are followed to produce white light efficiently in LED-based illumination; it can be multi-colour LEDs or a phosphor layer able to convert blue light into other colours, or a mixture of the two.

Most commercial luminaires make use of a phosphor layer, the phosphor layer initially absorbs blue radiation energy and then re-emits it in the form of longer wavelengths to create an optical spectrum with the desired illumination characteristics.

For inorganic phosphors, this conversion process limits their ability to respond to light brightness changes faster than a few megahertz.

Recently, there is a trend toward organic phosphor or quantum-dot approaches, which may provide faster response times.

However, the chemical stability of these materials is still limited, hindering their wide application in commercial products in the near future.

Building a receiver that only exploits photons toward the blue part of the spectrum gives a way to overcome the bandwidth limitation of the phosphor layer.

However, a significant percentage of the emitted power in other optical wavelengths is discarded.

A major challenge in joint illumination/communication systems is set by the strict requirement for power-efficient operation and relates mainly to the LED driving electronics.

Also, the driver must convert the current into light and operate between 100-500 KHz limiting the modulation systems [47].

We have seen many positive aspects and some constraints referred to LEDs, but a beautiful characteristic is given by the fact that an LED can be used both as transmitter and receiver in a simple way (Figure 15).



Figure 14: LED components.

Applied directly across an LED accurately enough to attain a desired current; some means must be used to limit the current [70]; in discrete systems, this is typically done by placing a resistor in series.

Under reverse bias conditions, a simple model for the LED is a capacitor in parallel with a current source which models the optically induced photocurrent, in which we want to measure the photocurrent.

An inexpensive way to make a photo detector out of an LED is to tie the anode to ground and connect the cathode to a CMOS I/O pin driven high; this reverse biases the diode, and charges the capacitance.

Next switch the I/O pin to input mode, which allows the photocurrent to discharge the capacitance down to the digital input threshold.

By timing how long this takes, we get a measurement of the photocurrent and thus the amount of incident light.

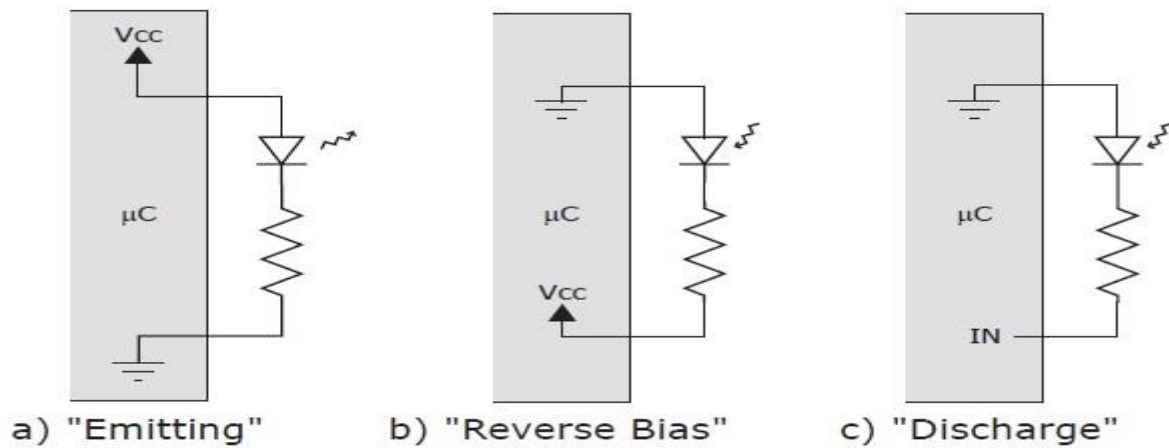


Figure 15: LEDs configurations

The finite bandwidth of front-end devices limits the speed of a communication system.

Different laboratory experiments have shown communication capability of a single link up to 3 Gb/s [71].

However, in order to go well beyond the Gb/s rate, it is likely that multiple-input multiple-output (MIMO) would need to be employed in VLC (Figure 16).

Currently, there are two possible implementations of MIMO receiver systems, one based on PDs and the other on imaging type sensors.

Utilizing PDs has the advantage that the hardware implementation is relatively simple; on the other hand, imaging sensors facilitate easy separation of MIMO channels.

However, the speed and accuracy of their present hardware implementations considerably limit their application in VLC-MIMO.

Recent studies of MIMO have shown that for a well distributed configuration of transmitters, receiver elements with angle diversity have the potential to reach very high communication capacity that scales almost linearly with the MIMO order employed [72].

The capacity is distributed quite uniformly and grows about linearly with the number of MIMO elements, this stems from the possibility to isolate information streams in space.

The concept of spatial modulation (SM) and spatial shift keying (SSK) are shown to be particularly applicable in an optical wireless system [73], where a low-complexity multiple-transmitter generalized SSK (GSSK) signaling technique for short-range indoor VLC is presented.

In a transmitter with N_t number of transmit elements, this signaling technique is capable of achieving a spectral efficiency of N_t b/s/Hz.

GSSK supplies higher spectral efficiency than the conventional OOK and PPM techniques.

Moreover, the GSSK transmitter is much simpler than that of an equivalent regular PAM system with similar spectral efficiency, avoiding challenges such as LED nonlinearity.

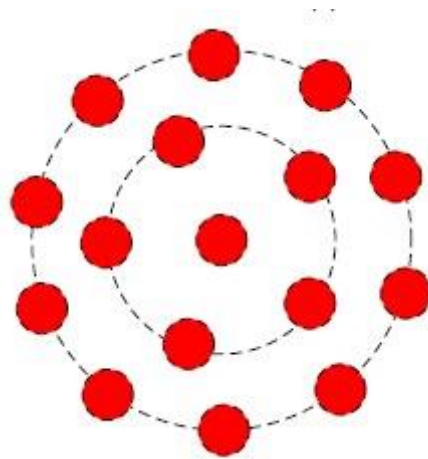


Figure 16: LEDs MIMO examples.

Also, CMOS image sensors have gained popularity in recent years because of advances in multi-functionalization, low manufacturing costs, and low power consumption.

The key element of a CMOS image sensor is the photo diode (PD), which is one component of a pixel, PDs are typically organized in an orthogonal grid. In operation, light passing through a lens strikes a PD, where it is converted into a voltage signal and then passed through an analog-to-digital converter.

The converter output is often referred to as a luminance, since a CMOS image sensor is composed of a PD array, PD outputs, specifically light intensity or luminance values, are arranged in a square matrix to form a digital electronic representation of the scene.

A CMOS image sensor can also be used as a VLC reception device (Figure 17) [74].

A particular advantage of CMOS image sensors usage is, due to the massive number of pixels available, its ability to spatially separate sources.

Here, the sources include both noise sources, such as the Sun, streetlights and other ambient lights, and LED transmission sources.

If a single-element PD is used as a VLC reception device, the VLC system cannot be used in direct sunlight, this is because direct sunlight is typically strong and can often be received at an average power that is much higher than that of the desired signal. Furthermore, it is very difficult to reduce the enormous amount of noise signals summing all background lights in the field of view (FOV) to the optical signal level, even if an optical band-pass filter (OBPF) is used.

When a single-element PD is used outdoors, directed linkage with small optical beam divergence is necessary, otherwise, the PD cannot be used in direct sunlight.

In some cases, a receiver equipped with a telephoto lens that achieves an extremely narrow FOV can be used [75, 76], but this type of receiver is unsuitable for mobile usage because it limits the angle of incidence and requires complex mechanical tracking.

In contrast, because of its ability to separate sources spatially, a VLC receiver utilizes only the pixels that it recognizes as LED transmission sources and discards all other pixels, including those detecting noise sources.

The ability to spatially separate sources also provides an additional feature to VLC, specifically, the ability to receive and process multiple transmitting sources.

As shown in Figure 17, data transmitted from an LED traffic light sign and data transmitted from LED brake lights of a vehicle ahead can be captured simultaneously.

Furthermore, if a source is composed of multiple LEDs, as in the case of LED traffic lights or brake lights, parallel data transmission can be accomplished by modulating each LED independently.

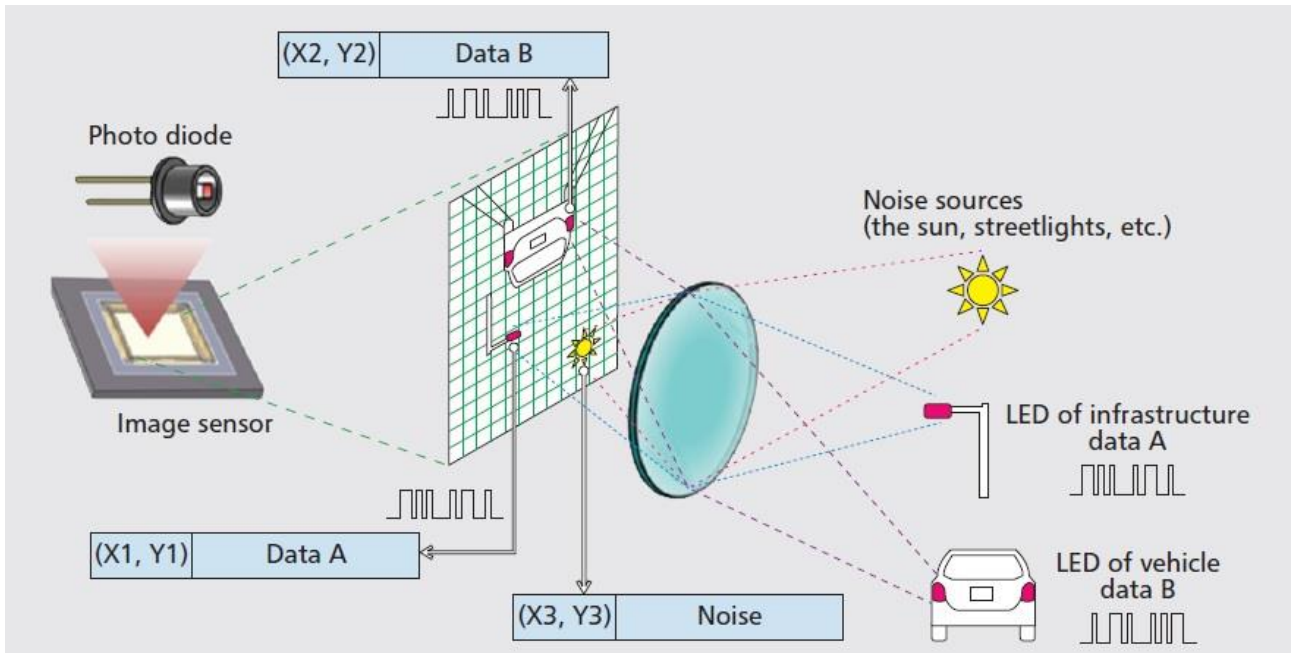


Figure 17: PDs as VLC receiver.

4.4 Dimming, flickering and eye safety

The two main challenges for communication using visible light spectrum are flicker mitigation and dimming support.

Dimming refers to the possibility of the user to change the luminance level of the light and it is important in VLC for power saving and energy efficiency.

It is desirable to maintain communication while a user arbitrary dims the light source, the human eye responds to low light levels by enlarging the pupil, which allow more lights to enter the eye.

The equation (4.4.1) shows the relation between perceived and measured light and is given by [24]:

$$perceived_{light(\%)} = 100 * \sqrt{\frac{measured_{light(\%)}}{100}} \quad (4.4.1)$$

In the following figure (Figure 18) we can see the perceived light as a function of measured light given by (4.4.1).

Communication support needs to be provided when the light source is dimmed over a large range.

It is possible to use some solutions in the modulation formats in order to mitigate the dims problem.

In On-Off Keying modulation is possible to redefine the “on” and “off” levels, gives a constant bit rate as the light dims, which means the range must decrease, but it also risk colour shift due to the LEDs being underdriven.

In Variable Pulse Position Modulation is possible varying the duty cycle, in that way the part of frame in which the information is present can be subdivide in sub-frames with the appropriate length and compensation symbols are added in the middle of the sub-frames to modify the luminosity average value.

Then, data-rate is proportional to the number of the compensation symbols but it has a constant range.

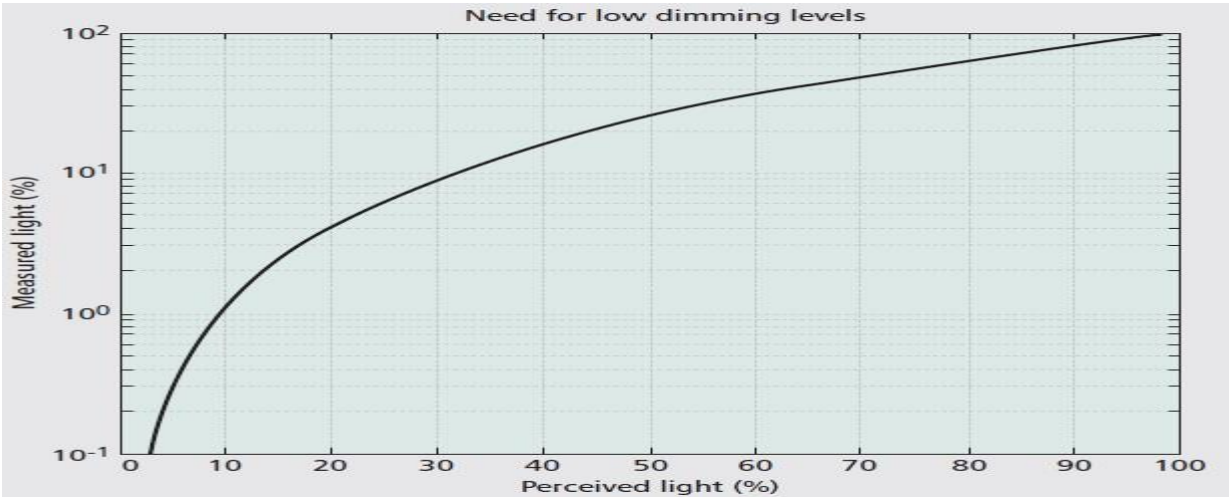


Figure 18: Measure VS Perceived light

The other main challenges for visible light communication is flicker mitigation. Flicker refers to the fluctuation of the brightness of light, any potential flicker resulting from modulating the light source s for communication must be mitigated, because flicker can cause noticeable negative physiological changes in humans. To avoid flicker, the changes in brightness must fall within the maximum flickering time period (MFTP) [70].

The MFTP is the maximum time period over which the light intensity can change without the human eye perceiving it; a frequency greater than 200 Hz or MFTP lower than 5 ms is generally considered safe. Therefore, the modulation process in VLC must not introduce any noticeable flicker either during the data frame or between data frames. The flicker in VLC can be classified in:

- Intra-frame flicker is defined as the perceived brightness fluctuation within a frame. In OOK is avoided by using the dimmed OOK mode and Run Length Limited line coding, VPPM use RLL codes and does not cause any inherent intra-frame modulation.
- Inter-frame flicker is defined as the perceived brightness fluctuation between adjacent frames and can be mitigated with idle or visibility pattern.

We have seen the two main challenges in communication in this spectrum and how is possible to mitigate flicker and support dimming, that solutions are also defined in the IEEE 802.15.7 visible light communication standard. One of the biggest concerns surrounding the use of VLC is eye safety. Well in the eye there are not blood flows that can help to relieve temperature changes, so in any IEEE specification will need to include strict eye safety regulations.

Also in the regulations of VLC are present emission limits, is normal that if we use a 100KW of light, which would result in people's eyes burning. Another potential risk from VLC is flicker.

Flicker can trigger seizures in people who suffer from a condition known as photosensitive epilepsy.

A general rule to generate flicker-free light is to use higher frequency than those we can perceive (below 150 Hz).

Energy-saving fluorescent lighting nowadays modulates in the kilohertz frequency band, so these lamps are constructed to be eye-friendly.

4.5 Luminance intensity

Obviously the two main characteristic that determine the luminance intensity are the distance from which the signal light must to be seen (d) and the background luminosity (L_B).

The relationship between background luminance and required luminance of a signal light (L_s) of a fixed size is given by [77].

$$L_s/L_B = C_1 ; C_1: constant. \quad (4.5.1)$$

Also, the optimal luminance intensity of a traffic signal light is independent of size:

$$L_s * \varphi = C_2 ; C_2: constant. \quad (4.5.2).$$

Where φ is the solid angle subtended by the signal light and is equal to:

$$\varphi = A/d^2 ; A: area of the signal. \quad (4.5.3)$$

The luminance intensity results:

$$I = L_s A \rightarrow I/d^2 = C_2 . \quad (4.5.4)$$

Therefore the luminance intensity necessary for a signal light to be seen at a certain distance is:

$$I_d = C d^2 L_B [cd] ; C = constant. \quad (4.5.5)$$

The optimum intensity depends on sky luminance and distance of the driver from the signal.

Another important parameters that determine the luminance intensity is the visibility angle (θ), the luminous intensity is related with the visibility angle by [78]:

$$I_{\theta} = \left(\frac{\theta}{3}\right)^{1.33} . \quad (4.5.6)$$

Then, the Fisher Equation [77] for the necessary luminous intensity requirements is given as:

$$I_{d,\theta} = C * \left(\frac{\theta}{3}\right)^{1.33} * d^2 * L_B. \quad (4.5.7)$$

However, for the green and yellow signal lights the luminous intensity need to be higher than that of a red signal light.

This is due to the Helmholtz-Kohlrausch effect [79].

The Helmholtz-Kohlrausch effect comes into play when a chromatic stimulus appears to have a greater brightness than a white reference stimulus of the same luminance. The ratio of the luminance of the chromatic stimulus, with equal brightness is written as B/L .

The effect varies by wavelength and saturation, with highly saturated reds and blues having a higher B/L value than yellow or greens.

In [80], final recommendation for the intensity ratio for red, yellow and green is suggested to be (1;2.5;1.3).

The Institute of Transportation Engineers “Vehicle Traffic Control Signal Heads” (ITE VTCSH) then re-evaluated the equation for minimum maintained intensity requirements for LED-based traffic lights, which is given as [80]:

$$I(\theta_{\text{horiz}}, \theta_{\text{vert}}, \text{size, colour}) = f(I_{\text{horiz}}) * f(I_{\text{vert}}) * I(-2.5,0) . \quad (4.5.8)$$

Where:

$$f(I_{\text{horiz}}) = 0.05 + \left\{ 0.95 * \exp \left[-\frac{1}{2} \left(\frac{\theta_{\text{horiz}}}{11} \right)^2 \right] \right\} ;$$

$$f(I_{\text{vert}}) = 0.05 + 0.9434 \exp \left[-\frac{\theta_{\text{vert}} + 2.5}{5.3} \right] , \theta_{\text{vert}} > -2.5^{\circ};$$

$$f(I_{\text{vert}}) = 0.26 + \frac{\theta_{\text{vert}}}{143} + 0.76 * [e^{-0.02(\theta_{\text{vert}}+2.5)^2}]^{-0.07*\theta_{\text{vert}}}, \theta_{\text{vert}} \leq -2.5^\circ;$$

and, $I(-2.5,0) =$

| | | |
|--------|----------------------|------------|
| Colour | Traffic Light(200mm) | T.L(300mm) |
| Red | 165cd | 365cd |
| Yellow | 410cd | 910cd |
| Green | 215cd | 475cd. |

In (Table 2) is shown the minimum maintained luminous intensity for different angles for red, green and yellow LED [88].

| Vertical Angle (deg) | Horizontal Angle (deg) | Luminous Intensity (candela) | | | | | |
|---|------------------------|------------------------------|--------|-------|---------------|--------|-------|
| | | 200mm (8 in) | | | 300mm (12 in) | | |
| | | Red | Yellow | Green | Red | Yellow | Green |
| 0.0 (d=50m) h _r =5m w _r =14m | 0.0 | 106 | 262 | 138 | 234 | 582 | 304 |
| | 2.5 | 102 | 254 | 133 | 226 | 564 | 295 |
| | 5.0 | 96 | 238 | 125 | 212 | 528 | 276 |
| | 7.5 | 84 | 209 | 110 | 186 | 464 | 242 |
| | 10.0 | 71 | 176 | 92 | 157 | 391 | 204 |
| | 12.5 | 58 | 144 | 75 | 128 | 319 | 166 |
| | 15.0 | 45 | 111 | 58 | 99 | 246 | 128 |
| | 17.5 | 33 | 82 | 43 | 73 | 182 | 95 |
| | 20.0 | 25 | 62 | 32 | 55 | 137 | 71 |
| 22.5 | 18 | 45 | 24 | 40 | 100 | 52 | |
| 2.5 (d=34.65m) | 0.0 | 69 | 172 | 90 | 153 | 382 | 200 |
| | 2.5 | 68 | 168 | 88 | 150 | 373 | 195 |
| | 5.0 | 63 | 156 | 82 | 139 | 346 | 181 |
| | 7.5 | 56 | 139 | 73 | 124 | 309 | 162 |
| | 10.0 | 46 | 115 | 60 | 102 | 255 | 133 |
| | 12.5 | 38 | 94 | 49 | 84 | 209 | 109 |
| | 15.0 | 30 | 74 | 39 | 66 | 164 | 86 |
| | 17.5 | 21 | 53 | 28 | 47 | 118 | 62 |
| | 20.0 | 17 | 41 | 22 | 37 | 91 | 48 |
| 22.5 | 12 | 29 | 15 | 26 | 64 | 33 | |
| 5.0 (d=26.43m) | 0.0 | 46 | 115 | 60 | 102 | 255 | 133 |
| | 2.5 | 45 | 111 | 58 | 99 | 246 | 128 |
| | 5.0 | 41 | 103 | 54 | 91 | 228 | 119 |
| | 7.5 | 36 | 90 | 47 | 80 | 200 | 105 |
| | 10.0 | 31 | 78 | 41 | 69 | 173 | 90 |
| | 12.5 | 25 | 62 | 32 | 55 | 137 | 71 |
| 7.5 (d=21.3m) | 0.0 | 31 | 78 | 41 | 69 | 173 | 90 |
| | 2.5 | 31 | 78 | 41 | 69 | 173 | 90 |
| | 5.0 | 28 | 70 | 37 | 62 | 155 | 81 |
| | 7.5 | 25 | 62 | 32 | 55 | 137 | 71 |
| | 10.0 | 21 | 53 | 28 | 47 | 118 | 62 |
| | 12.5 | 18 | 45 | 24 | 40 | 100 | 52 |
| 10.0 (d=17.7m) | 0.0 | 23 | 57 | 30 | 51 | 127 | 67 |
| | 2.5 | 23 | 57 | 30 | 51 | 127 | 67 |
| | 5.0 | 21 | 53 | 28 | 47 | 118 | 62 |
| | 7.5 | 18 | 45 | 24 | 40 | 100 | 52 |
| 12.5 (d=15.2m) | 0.0 | 18 | 45 | 24 | 40 | 100 | 52 |
| | 2.5 | 17 | 41 | 22 | 37 | 91 | 48 |
| | 5.0 | 17 | 41 | 22 | 37 | 91 | 48 |
| | 7.5 | 13 | 33 | 17 | 29 | 73 | 38 |

Table 2: minimum maintained luminous intensity.

In (Figure 19) is shown the minimum maintained red signal luminous intensity requirement on traffic light axis at 50m and 34.65m and at different horizontal angles resulting from installation of traffic light at a height of 5m, while (Figure 20) illustrates for all three colour signals at 50m distance.

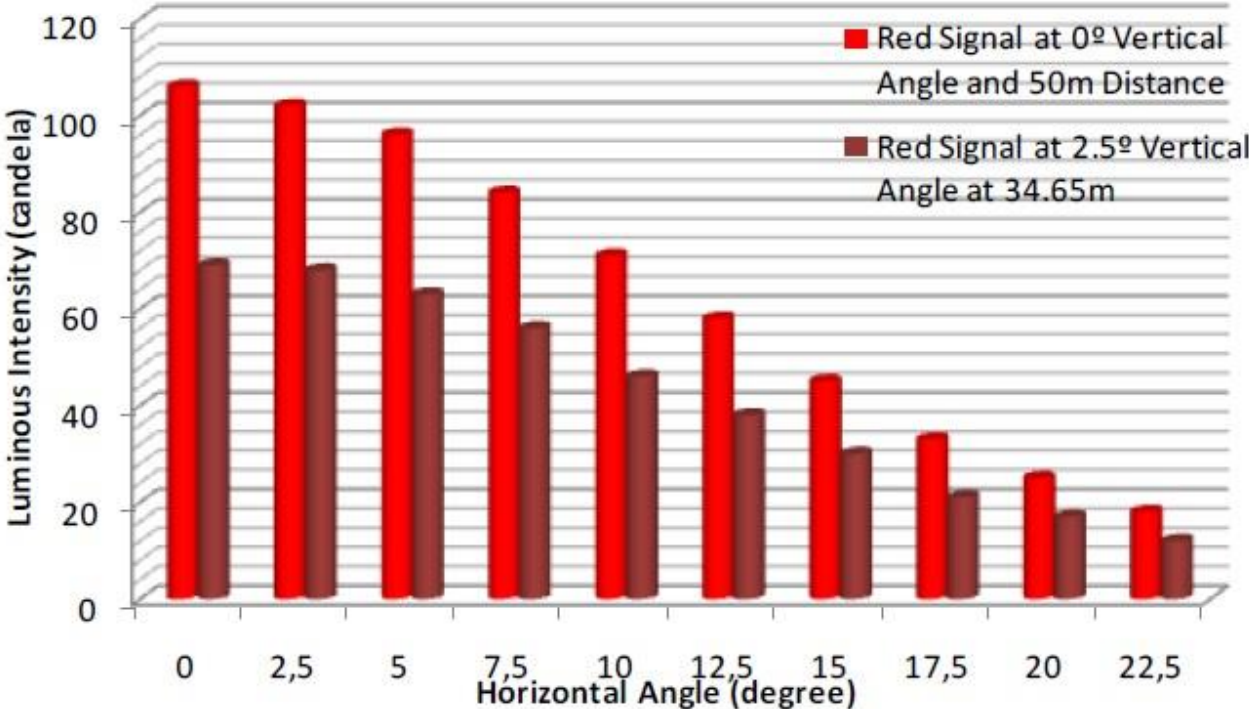


Figure 19: minimum maintained red signal luminosity.

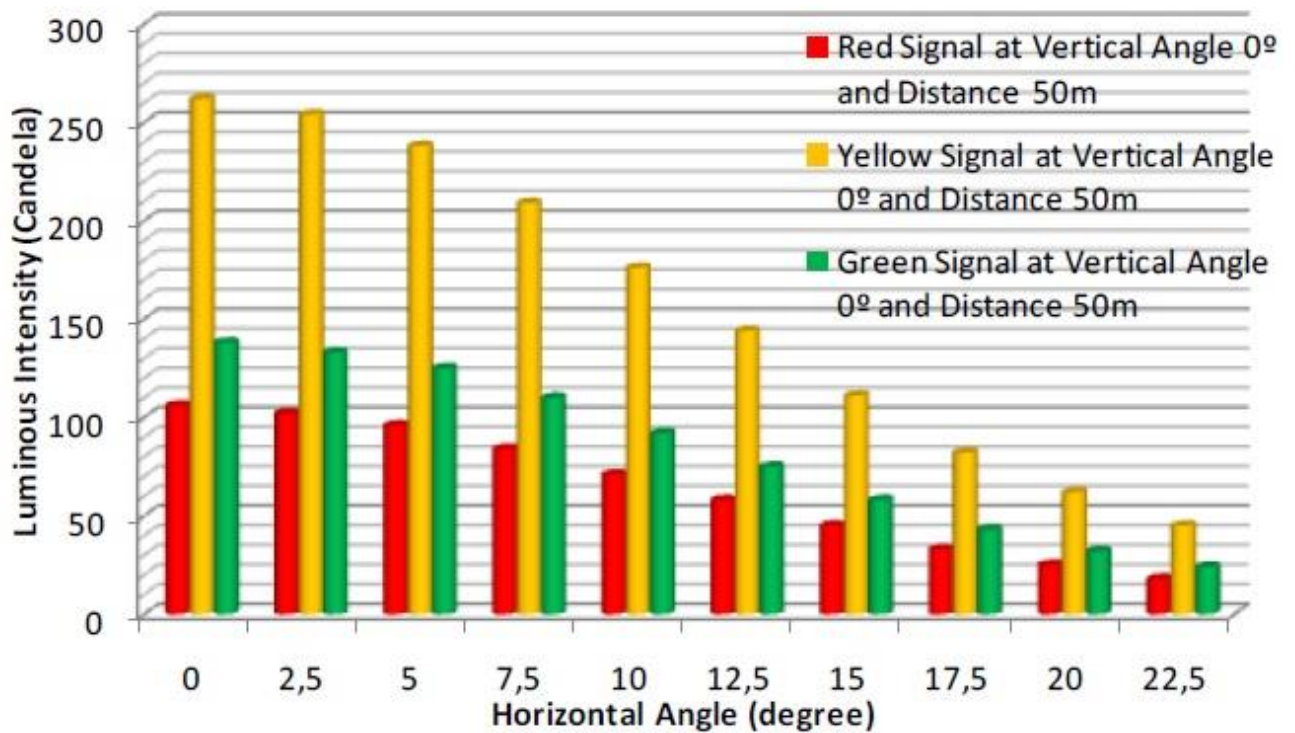


Figure 20: minimum maintained signal luminosity for red, green and yellow LEDs.

These specifications provide significant inputs for comparison and design of LED-based traffic lights which are gradually becoming popular.

However, as discussed before, they can be designed aiming for multiple functions of signaling, data transmission and illumination.

Let us now examine the LED as a points source emitter.

Ideally, a LED source is a Lambertian emitter, in which irradiance distribution is a cosine function of the viewing angle.

This dependence turns out to be a power law that primarily depends on the encapsulate and semiconductor region shapes.

In (Figure 21) [12] is shown a practical approximation of the irradiance distribution, given by:

$$E(d, \theta) = E_0(d) * \cos^m(\theta). \quad (4.5.9)$$

Where $E_0(d)$ is the irradiance on the axis at a distance d .

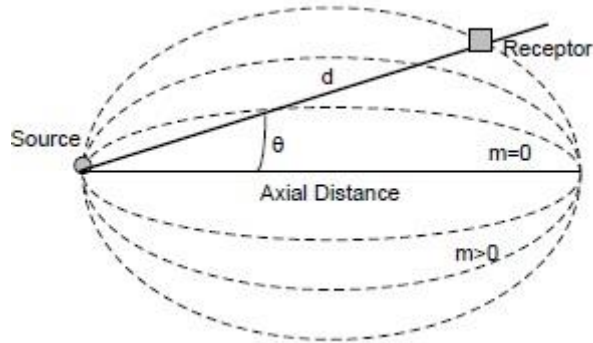


Figure 21: Lambertian emitter source

The value of m depends on the relative position of the LED emitting region from the curvature center of the spherical encapsulant.

If the chip position coincides with the curvature center, the number $m \approx 1$ and the source is nearly a perfect Lambertian.

Typical LEDs often have values of $m > 30$ and the drop of intensity with the viewing angle is pronounced.

The number m is given by the half power angle $\theta_{1/2}$ that is provided by the manufacturer.

$$m = \frac{\ln 2}{\ln(\cos \theta_{1/2})} ; 15^\circ < \theta_{1/2} < 45^\circ. \quad (4.5.10)$$

The LED emitter is modeled using a generalized Lambertian radiation pattern [82, 83], in which P_T represent the transmission power:

$$R_E(\theta, m) = \frac{m + 1}{2\pi} * P_T * \cos^m(\theta); \theta \in \left[\frac{-\pi}{2}, \frac{\pi}{2} \right]. \quad (4.5.11)$$

Fig. 3.5(a) shows the polar plot for different mode number of the radiation lobe while Fig. 3.5(b) illustrates the same for the normalized values.

It is seen that as m increases the directivity of the radiation pattern increases.

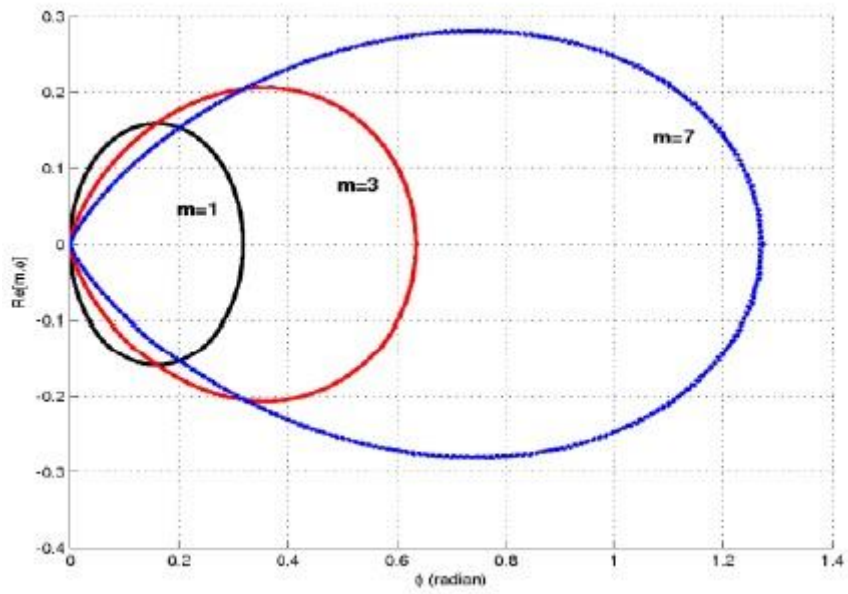


Figure 22: radiation lobe.

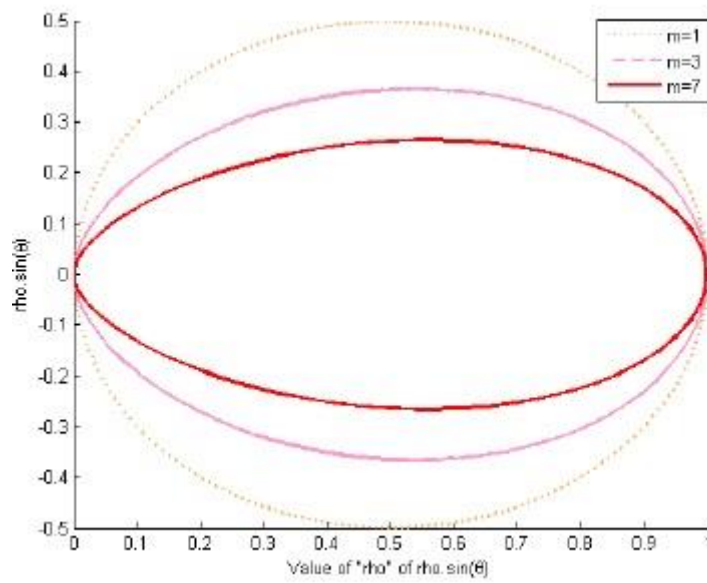


Figure 23: normalized radiation lobe.

Conventional LEDs have very small values of lumen in the order of less than unity, generally given in milli Candela (mcd).

Therefore, we would need a large number of such LEDs to get few tens of lumen in total. Also, the area of the available traffic lights is not sufficient to accommodate over thousands of LEDs, even without considering manufacturing constraints.

Hence, it is possible to use HB-LEDs able to provide few lumens of intensity but highly directive, or power LEDs which have few tens of lumen and wide viewing angles. Power LEDs normally have wide view angles and therefore, lens becomes necessary to obtain adequate radiation pattern. The lens is very costly as compared to LEDs. On the other hand, HB-LEDs come with narrow view angles which can be used without lens. Another major difference is found to be in the reliability. For example, suppose to need 1050 lm and we can use one of the two circuit that are represented in (Figure 24). Therefore, we can select the first circuit with HB-LED in which each row provide 32 lm or the second circuit in with power LEDs in which each row provide 175 lm. If we select the power LEDs circuit and a LED fails, the traffic light would lose nearly 175 lm affecting the coverage area. However, if one of the HB-LED fails, the traffic light would lose nearly 32 lm which may not affect so significantly. Hence, the usage of HB-LEDs improves the robustness of traffic light, implying less performance degradation under damaged condition.

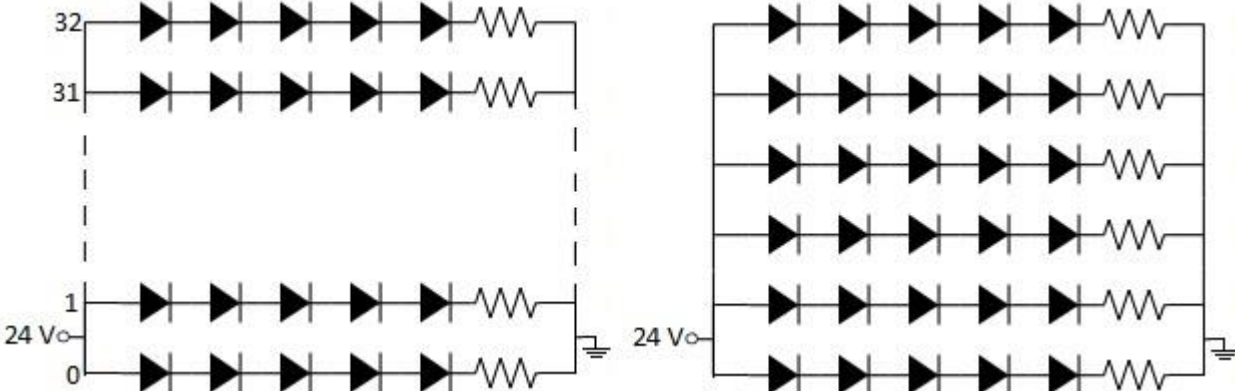


Figure 24: schematic circuit with HB-LEDs and power LEDs that provide 1050 lm.

Far field point [84] source approach is the simplest way to modelling the VLC optical system, because of discrete nature of the source this assumption may not

always hold. Considering one LED placed at $(x_0, y_0, 0)$ over a plane (Figure 25), in Cartesian coordinates (x, y, z) , the target placed at (x, y, z) , and \bar{n}_s represents the heading of the source. From geometry:

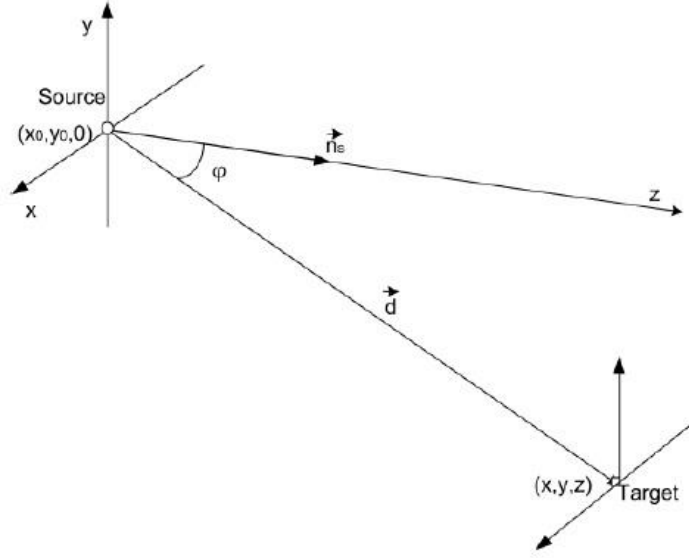


Figure 25: Cartesian representation of a source emitter

$$\begin{aligned} \cos \varphi &= \frac{\langle \bar{n}_s * \bar{d} \rangle}{\|\bar{n}_s\| * \|\bar{d}\|} ; \|\bar{n}_s\| = 1 ; \|\bar{d}\| \\ &= \sqrt{(x - x_0)^2 + (y - y_0)^2 + z^2} . \quad (4.5.12) \end{aligned}$$

We have assumed $\bar{n}_s = (0, 0, 1)$ and $\bar{d} = (x - x_0, y - y_0, z)$, so the irradiance is therefore, give as [85]:

$$\begin{aligned} E(x, y, z) &= \frac{m + 1}{2\pi} * \frac{\cos^m(\varphi)}{\|\bar{d}\|^2} * E_0 = \frac{m + 1}{2\pi} * E_0 * \frac{z^m}{\|\bar{d}\|^2 * \|\bar{d}\|^m} = \\ &= \frac{m + 1}{2\pi} * E_0 * \frac{z^m}{[(x - x_0)^2 + (y - y_0)^2 + z^2]^{\frac{m+2}{2}}} . \quad (4.5.13) \end{aligned}$$

There are many possible arrangements in which LEDs can be uniformly arranged for the signaling and lighting. Square arrays, triangular arrays and ring arrays are shown in (Figure 26), while in (Table 3) we can see a characteristics comparison.

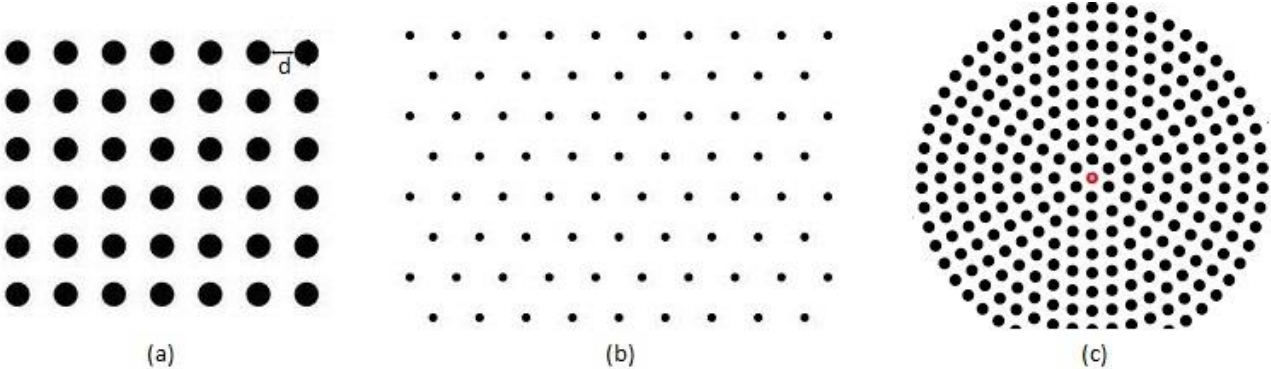


Figure 26: Array arrangement: (a) square; (b) triangular; (c) circular

| Array Traffic Light Diameter | | Maximum | | Road Widthwise Coverage (at 10m) ¹ | LED Occupancy (%) | Visibility |
|------------------------------|-------|-------------|--------------------|---|-------------------|--|
| | | No. of LEDs | Luminous Intensity | | | |
| Triangular | 200mm | 274 | 4421 cd | 2.94m | 40.72 | Light output is perceived as a high intensity source in the center with some dark area in the dome periphery |
| | 300mm | 554 | 9801 cd | 6.38m | 41.63 | |
| Square | 200mm | 361 | 5957 cd | 4.32m | 50.77 | Light output is more uniform with reduced dark areas. However creates a stripe pattern effect |
| | 300mm | 841 | 13877 cd | 7.42m | 52.56 | |
| Co-centric Rings | 200mm | 580 | 9570 cd | 6.32m | 81.56 | Produces the most uniform light perception with the LEDs covering the entire dome |
| | 300mm | 1310 | 21615 cd | 8.58m | 81.88 | |

Table 3: Standard 5mm diameter LEDs with assembly tolerance radius of 1.25mm and luminous output of 16,5 cd.

Subsequently, we will consider vehicular networks so now, let us focus on circular ring array pattern which are usually applied in the headlights. assuming that, $\|\vec{d}\| \gg rm$, where rm is the radius of outer ring, the position of each LED is $(x_i, y_i, 0)$ and the target is considered to be an ideal receiver, that is full FOV and infinitesimal detection area; the distance results:

$$d_i = (x - x_i, y - y_i, z) \quad (4.5.14)$$

and LED coordinates become:

$$x_i = r_k \cos\left(\frac{2\pi i}{N_k}\right) + x_0; y_i = r_k \sin\left(\frac{2\pi i}{N_k}\right) + y_0 \quad (4.5.15)$$

where k is the index of a ring of LEDs and N_k is the number of LEDs in ring k , as is shown in (Figure 27).

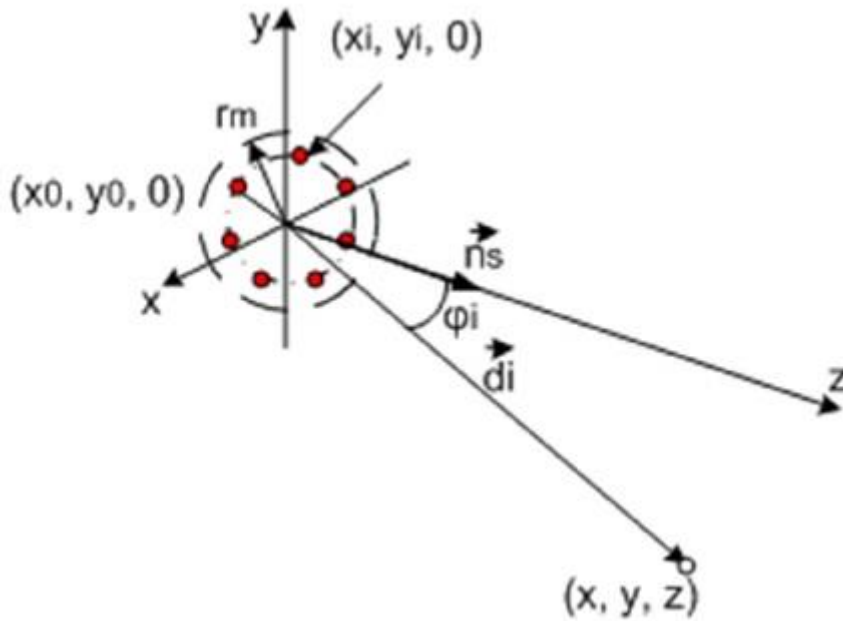


Figure 27: LEDs circular rings

Therefore for a single ring the irradiance is given as:

$$E(x, y, z) = E_0 * \frac{m + 1}{2\pi} \sum_{i=0}^{N_k-1} \frac{z^m}{[(x - x_i)^2 + (y - y_i)^2 + z^2]^{\frac{m+2}{2}}}; \quad (4.5.16)$$

and for a multiple concentric rings will become [67]:

$$E(x, y, z) = E_0 * \frac{m + 1}{2\pi} \sum_{k=0}^{M-1} \sum_{i=0}^{N_k-1} \frac{z^m}{[(x - x_i)^2 + (y - y_i)^2 + z^2]^{\frac{m+2}{2}}}. \quad (4.5.17)$$

(Table 3) is shown that is possible to cover up to 82% of the entire dome, with an optimal placement of the LEDs in a circular ring array pattern.

Now, we can try to evaluate the total irradiation for a generic multilane traffic light system.

The traffic light source (semaphore) is considered to be at the height of h from the receiver plane, so each LED on the array has coordinate $(x_i, y_i + h, z)$ while the receiver position has coordinate (x, y, z) .

Assuming receiver orientation of θ with respect the normal and σ_i is the angle of incidence while φ_i being the angle of irradiance as is shown in (Figure 28).

The optical power detected by a photo detector with active area A_d at a distance d from the single LED emitting source is given by [12]:

$$E_r(x, y, z) = A_d * E(0) * \frac{m + 1}{2} * \frac{\cos^m(\varphi)}{d^2} * \cos \sigma * \text{rect}\left(\frac{\sigma}{FOV}\right) \quad (4.5.18)$$

where the rect function defines bound on the field of view of the receiver, so its value is 0 for 0° and 1 for 90° .

The direct distance d_i between each LED in the emitter source and receiving detector if it is a circular array of LEDs is given as:

$$d_i = (x - x_i, y - y_i - h, z) \quad (4.5.19)$$

and,

$$\|d_i\| = \sqrt{[(x - x_i)^2 + (y - y_i - h)^2 + z^2]}. \quad (4.5.20)$$

the cosine terms can be found using internal product definition as:

$$\cos(\varphi_i) = \frac{z}{\sqrt{\|d_i\|}} \quad (4.5.21)$$

while

$$\cos(\sigma_i) = \frac{(y - y_i - h) * \cos \theta + z * \sin \theta}{\sqrt{\|d_i\|}}. \quad (4.5.22)$$

Therefore, the total irradiation from a traffic light consisting of an array of LEDs in a LoS link, results [55]:

$$E_T(x, y, z) = A_d * E(0) * \frac{m+1}{2} * \sum_{k=0}^{M-1} \sum_{i=0}^{N_k-1} \frac{\cos^m(\varphi_i) * \cos(\sigma_i)}{\sqrt{\|d_i\|^{m+3}}} * \text{rect}\left(\frac{\sigma_i}{FOV}\right). \quad (4.5.23)$$

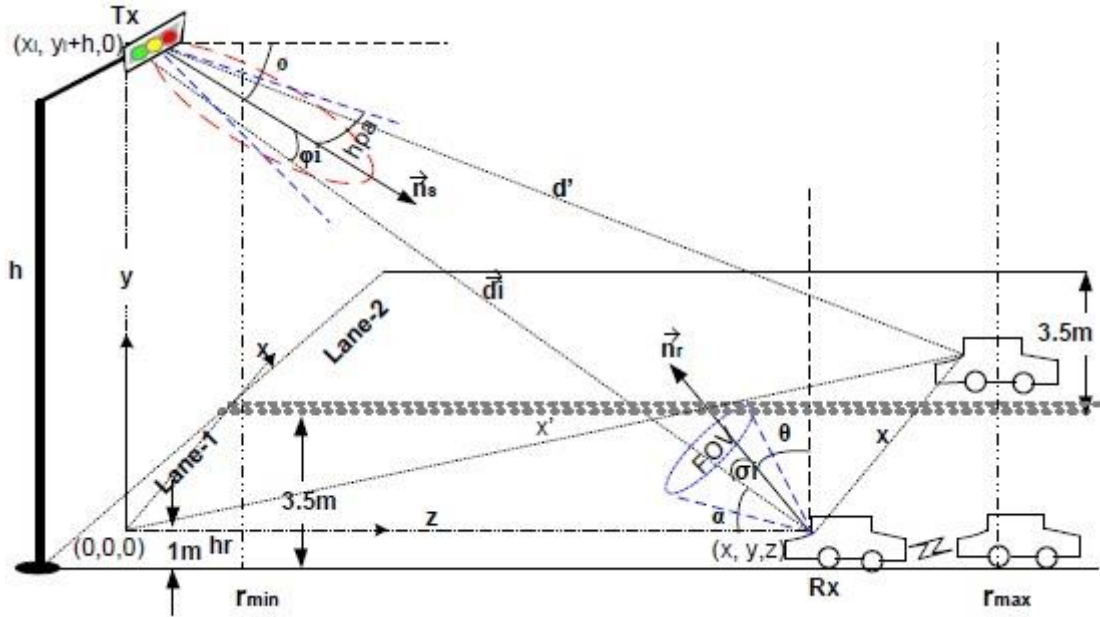


Figure 28: Multilane traffic system

4.6 VLC channel

VLC systems unavoidably suffer from limitations common in all optical wireless IM/DD systems, such as noise and interference impairments.

However, the high transmitted power in joint illumination/communication systems can lead to an uncommon SNR dependence on free-space propagation distance.

In IM/DD systems, apart from the thermal noise due to the electronics in the receiver, noise related to the nature of photon counting exists.

Photon counting is a Poisson process, which implies that the noise level depends on the average number of received photons.

While non-signal photons from sources with constant intensity create a DC offset that can easily be removed, a noise component proportional to this DC

level also emerges in addition to the anticipated signal-dependent noise component.

As shown in (Figure 29) [87], the SNR has a dependence on distance similar to wireless radio links ($1/d^2$) when signal-dependent Poisson noise is dominant, while a stronger dependence ($1/d^4$) which is usually found in the literature for IM/DD channels, occurs when thermal noise or ambient light from other sources determine the noise level in the receiver.

They do not suffer of multipath fading because their wavelength is much less respect a typical photodetector area.

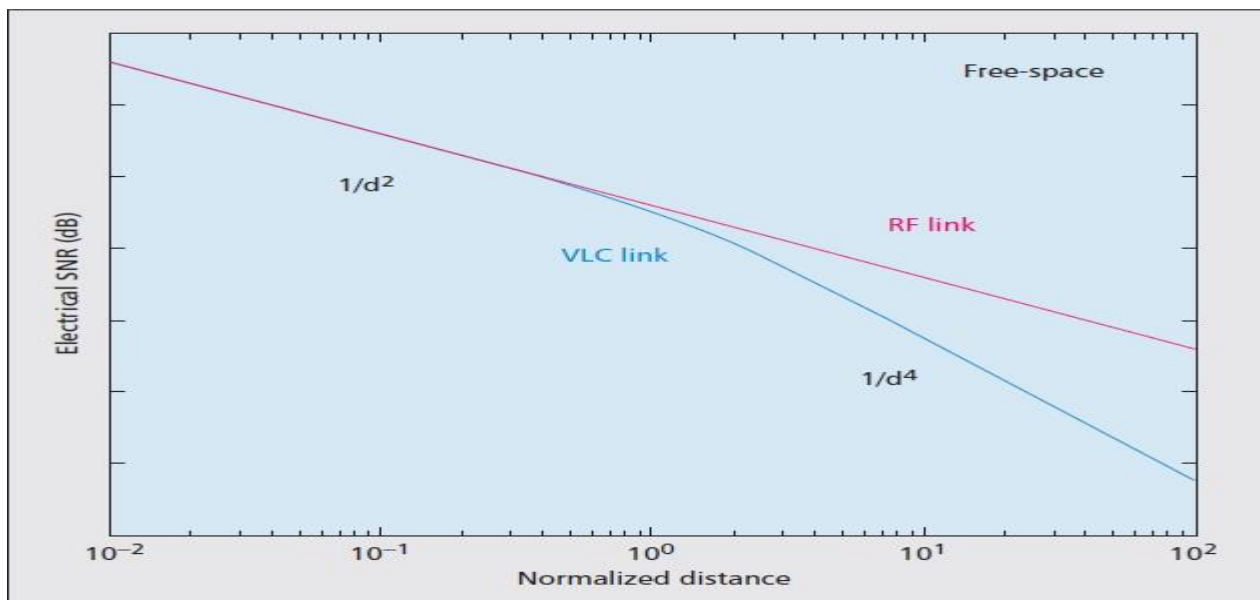


Figure 29: SNR as a function of distance

The square root (SR) channel description, introduced in [88], conveniently transforms the complex nature of VLC links into the widely understood additive white Gaussian noise (AWGN) channel description by applying Anscombe's square root transform at the output of the PD.

In the SR channel description, the only noise component is additive and Gaussian in nature with zero mean and fixed variance equal to $1/4$.

Assuming that the signal has B symbols/s (B is the double of the achievable bandwidth), the maximum data rate results:

$$C = \frac{B}{2} \log_2 \left(1 + \frac{2}{\pi e} \frac{(\sqrt{\lambda_{max}} - \lambda_0 - \sqrt{\lambda_0})^2}{B} \right) \quad (4.6.1)$$

where λ_{max} is the signal wavelength and λ_0 the ambient wavelength. (Figure 30) illustrates the capacity of the system as a function of the signaling rate B in the aforementioned scenario.

The discontinuity at 4 Msymbols/s (~ 2 MHz) and the slope change above this point are a consequence of the reduction in the number of received photons due to the optical blue filter that is used to overcome the phosphor low-pass response.

Actually, for signaling rates above 40 Msymbols/s (~ 20 MHz), the low-pass response of the LEDs will further reduce the collected number of photons.

However, the capacity estimation in this region is based on the total number of blue photons and acts as an upper bound to the achievable rates (dashed lines). In reality, OOFDM schemes could be used here to distribute the signal power in frequency in accordance to the low-pass LED response [89].

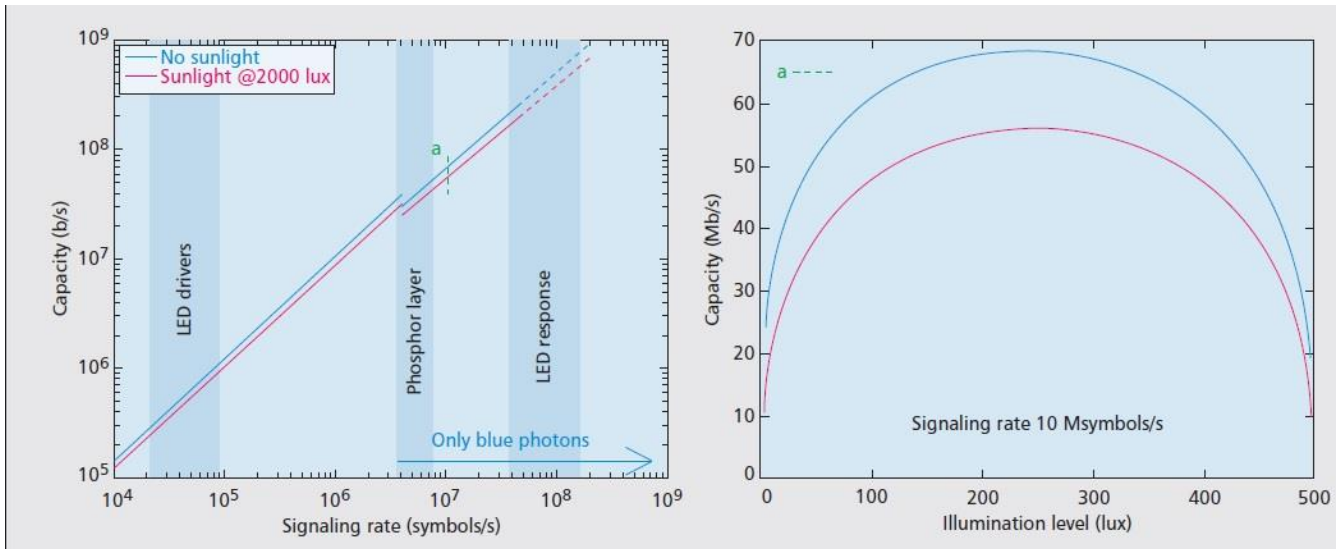


Figure 30: (a) capacity as a function of signalling rate; (b) capacity as a function of illumination level.

Interestingly, for VLC via downlighting luminaires and detectors facing downward (Figure 31(a)), there is no line of sight (NLOS).

In these links, propagation highly depends on the diffusive reflection of the illumination footprint underneath the luminaires, which in practice is a few meters wide.

Signals can only propagate and interfere over large distances, by either multiple reflections or light sources having emission angles that are not common for Lambertian- or spot-angle-limited lamps [90].

The number of useful reflections, however, is limited as a result of the diffusive and weak reflective nature of most of the common building materials used in walls, floors, and ceilings (R).

Therefore, a very steep increase of propagation loss occurs when horizontal distance grows (Figure 31(b)).

As we can see the communication between adjacent luminaries is already possible and it will increase its capacity thanks to the evolution of the studies of LEDs.

Multipath fading can be neglected in optical wireless channel.

In the channel model, the information carrier is a light wave whose frequency is about 10^{14} Hz.

Moreover, detector dimension is in the order of thousands of wavelengths, leading to efficient spatial diversity, which also prevents multipath fading.

With detector conversion efficiency R , the electrical signal is RPr . The electrical SNR is then defined as [95]:

$$\text{SNR} = \frac{\sqrt{2}RP_r}{\sqrt{N_0B}}. \quad (4.6.2)$$

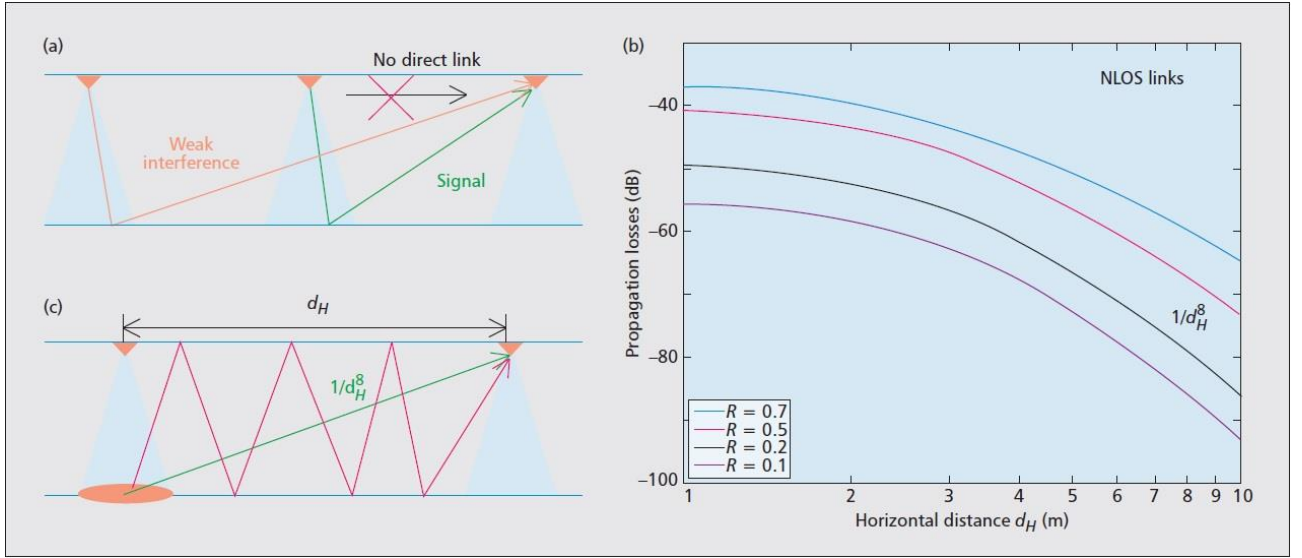


Figure 31: (a)(c) no direct link examples; (b) propagation losses as a function of horizontal distance.

VLC systems in outdoor applications require LoS propagation. Propagation characteristic drastically change due to communication environment, especially the effect of weather conditions is strong and also because of interference caused by other light source. Atmospheric obstacles such as rain, fog and so on, decrease the received signal. In addition, communication characteristics change with season, time and region [91]. The discussion here presented is restricted to the LoS case since this is the most relevant scenario for the intended application. if we consider that the transmitter emits an axial symmetric radiation pattern described by the radiant intensity ($P_T R_0(\varphi)$), a receiver located at distance (d) and angle (φ) with respect to the transmitter senses an irradiance value of:

$$I_s(d, \varphi) = \frac{P_T R_0(\varphi)}{d^2}. \quad (4.6.3)$$

The power detected and received by PD with an effective area ($A_{\text{eff}}(\sigma)$), is given as:

$$P_r = I_s(d, \varphi) * A_{\text{eff}}(\sigma); \sigma: \text{incidence angle.} \quad (4.6.4)$$

The frequency response of visible light channels are relatively flat near to DC, so commonly the channel is characterizes by its DC gain ($H(0)$), given by:

$$H(0) = \begin{cases} \frac{A_d}{d^2} * R_0(\varphi) * T_s(\lambda) * g(\lambda) * \cos \sigma, & 0 \leq \sigma \leq FOV \\ 0, & \sigma > FOV \end{cases} \quad (4.6.5)$$

where, A_d is the detector area, T_s is the optical filter gain and g is the gain of optical concentrator.

For a transmitter consisting of an array of LEDs, the LoS channel gain is given as [83, 85]:

$$\begin{aligned} H_T(x, y, z) &= A_d P(t) T_s(\lambda) g(\lambda) E_0 \frac{m+1}{2\pi} * \\ &* \sum_{k=0}^{M-1} \sum_{i=0}^{N_k-1} \frac{\cos^m(\varphi) \cos(\sigma_i)}{[(x-x_i)^2 + (y-y_i-h)^2 + z^2]^{\frac{m+3}{2}}} \text{rect}\left(\frac{\sigma_i}{FOV}\right). \end{aligned} \quad (4.6.6)$$

If the area of the detector, the total transmitted power, the gain of the filter and the gain of concentrator are all normalized to one, the loss on the channel over distance can be drawn (Figure 32).

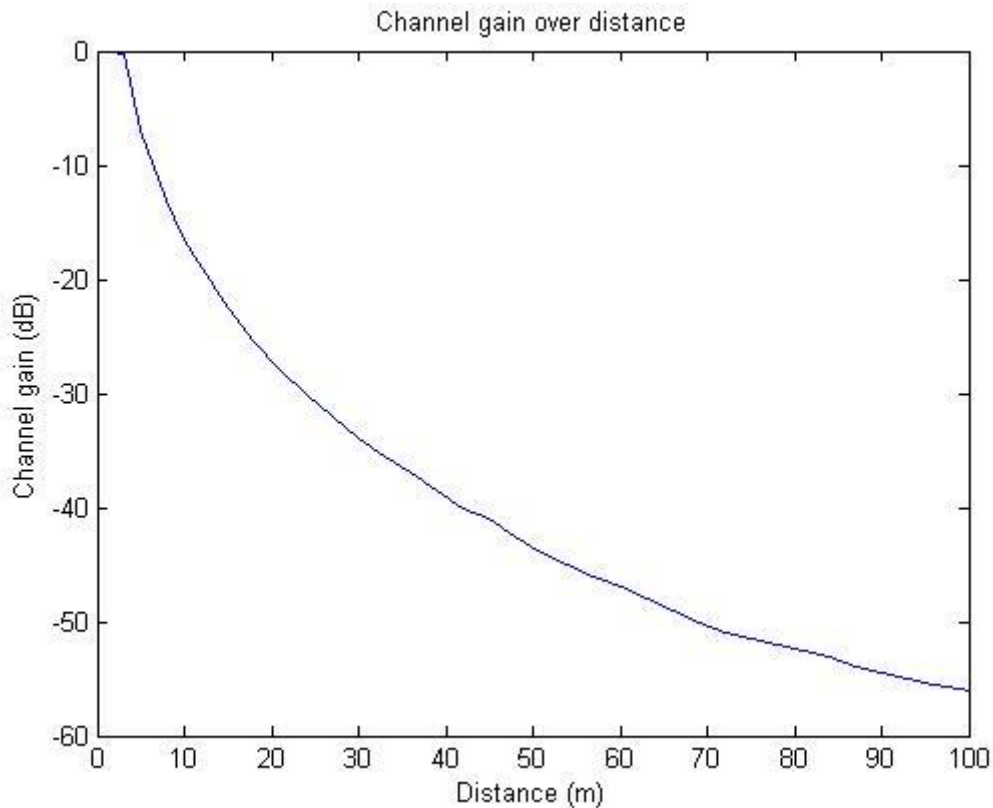


Figure 32: channel gain over the distance for a transmitter constitute by an array LEDs.

Atmospheric channel is one of the most complex channels in the communication world, fog and clouds scatter and absorb optical signals which cause transmission errors. It is possible to identify a fog condition with a visibility range and relate it to the optical attenuation by using the Kruse formula [92] and it results:

$$\Gamma(V, \lambda) = \frac{17}{V} * \frac{550}{\lambda} * 585V^{1/3} \left[\frac{\text{dB}}{\text{Km}} \right] \quad (4.6.7)$$

where, V is the visual range in km, λ is wavelength in nanometers, and Γ is the attenuation in dB/km. However, this formula is not adequate for visible light channels, because the wavelength dependence of fog is too small in the visible and infrared range. Therefore it is necessary to specify a fog condition with a parameter that is more general than its visibility range.

In one of the models analyzed [92], the parameter that indicates the thickness of fog is the optical depth. The optical depth generally indicates the average number of interactions that light will incur when propagating through a multiple-scatter channel. The optical depth (τ_0) is defined as:

$$\tau_0 = \rho * \sigma_t * L \quad (4.6.8)$$

where ρ is the density of fog particles, σ_t is the scattering cross section and L is the distance at which fog particles reside. Light transmission through dense fog can be analyzed using vector radiative transfer theory (VRTT) [93, 94]. RT theory is based on the assumption of power conservation, and it is applicable for studying multiple-scattering effects. The received signal consists of two components the coherent intensity and diffused (incoherent) intensity. The coherent intensity is the function of angular frequency (ω) and the optical depth,

$$J_{\text{coh}} = I_{\text{coh}}(\omega, \tau_0)e^{-\tau_0}, \quad (4.6.9)$$

while, the diffused intensity also depends on scatter angle (θ), and given as:

$$J_{\text{diff}} = \pi I_d(\omega, \tau_0)\theta^2. \quad (4.6.10)$$

where, the diffused intensity is considered uniform for small scattering angles ($\Delta\theta$).

Therefore, the total intensity can be given as:

$$J_t = J_{\text{coh}} + J_{\text{diff}}. \quad (4.6.11)$$

The frequency response represents the characteristics of the channel as a function of frequency shown (Figure 33). (Figure 33(a)) shows that the frequency response of the channel has the characteristics of a low pass filter, while (Figure 33(b)) shows the characteristic of the phase.

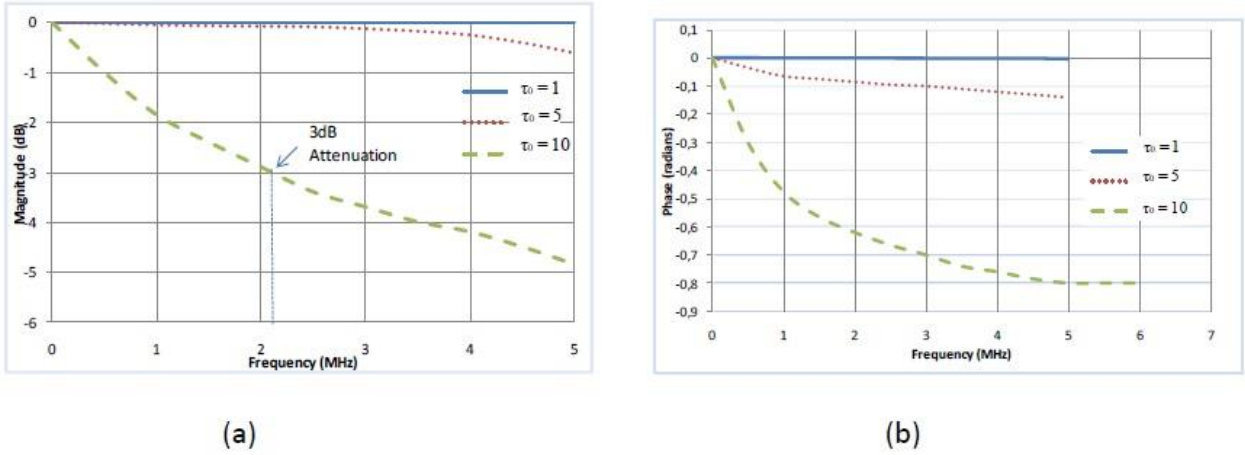


Figure 33: frequency response of the channel, varying the optical depth.

Atmospheric conditions affect channel variation, in addition, there are multiple of other interfering sources such as, artificial and natural lights. In the fog environment due to optical depth, light rays are scattered and therefore, detector's effective FOV gets slightly changed. A detector with area A_d and specified FOV will intercept the light intensity. When the FOV covers only one scatter angle θ , we can replace θ with half-angle FOV. However, when the FOV covers more than one scattering angle, the integration of incoherent intensity from all scattering angles is needed. Following this, the received power was calculated from the specific intensity by solving VRRT equation in [92] with normalized transmitted power of 1W. The received power (P_s) and the background light power (P_{bg}) are defined as:

$$P_s = I_{coh}(\omega, \tau_0)e^{-\tau_0} + \pi I_d(\omega, \tau_0)FOV^2 A_d \lambda T_f, \quad (4.6.12)$$

and

$$P_{bg} = H_{bg}FOV^2 A_d \lambda T_f, \quad (4.6.13)$$

Where, H_{bg} is the background radiance, λ is wavelength of the light wave, and T_f is the filter transmittivity. The received power when bit 1 is transmitted (ON) is always higher than the received power when bit 0 is transmitted (OFF). Since, during bit 1 transmission there will also be background power. The detector current during ON state will be:

$$I_1 = R * P_1 = R * P_s + R * P_{bg}, \quad (4.6.14)$$

while, the detector current during OFF state results:

$$I_0 = R * P_0 = R * P_{bg}. \quad (4.6.15)$$

Now knowing that the thermal noise (n_{th}), shot noise (n_{sh}) and background radiation (n_{bg}) are given by:

$$\sigma_{th}^2 = \frac{4KT_eFB}{R_L}; \quad \sigma_{sh}^2 = 2qRP_sB; \quad \sigma_{bg}^2 = 2qRP_{bg}B \quad (4.6.16)$$

where K is Boltzmann's constant ($K = 1.381E-23$), q is the electronic charge ($q = 1.6E-19$ C), T_e is the temperature (290K), F is the circuit noise figure, B is the bandwidth of the detector, R_L is load resistance (ohm), and R the responsivity of the detector (amperes per watt), defined as:

$$R = \frac{\eta * q * \lambda}{h * c}. \quad (4.6.17)$$

where, η is the quantum efficiency of the photo detector, h is Planck's constant ($h = 6.6E-34$ J/s), and c is the velocity of the light wave ($c = 3E8$ m/s). The detector noise variance during ON and OFF state is given as:

$$\sigma_1^2 = \sigma_{th}^2 + \sigma_{sh}^2 + \sigma_{bg}^2 \quad (4.6.18)$$

and

$$\sigma_0^2 = \sigma_{th}^2 + \sigma_{bg}^2. \quad (4.6.19)$$

Therefore, SNR in presence of fog results:

$$\text{SNR} = \frac{RP_s}{\sqrt{\sigma_1^2} + \sqrt{\sigma_0^2}}. \quad (4.6.20)$$

The steady background irradiance produced by natural and artificial light sources is usually characterized by the DC current it induces on the receiver PD since the resulting shot noise power is directly proportional to that current. This current is usually referred as the background current (I_{bg}) [96]. Noise variance of ambient skylight and circuit thermal noise is considered to be the same as in (4.6.16):

$$\sigma^2 = \frac{4KT_eFB}{R_L} + 2qRP_sB + 2qRP_{bg}B, \quad (4.6.21)$$

Therefore, the SNR in presence of background irradiance is given as:

$$\text{SNR} = \frac{RP_s}{\sqrt{\sigma^2}}. \quad (4.6.22)$$

4.7 Modulation system

The choice of modulation technique in the design of VLC systems remains one of the most important technical issues.

Background from IR technology suggests the use of modulation techniques such as OOK, L-pulse position modulation (L-PPM), subcarrier phase shift keying (SC-PSK) and these have been discussed and proposed [83, 97].

-On-Off-keying:

On-Off-Keying is the simplest form of amplitude-shift keying (ASK) modulation that represents digital data as the presence or absence of a carrier wave.

The compensation time is realized fully turning on or off the light source for the required duration to provide dimming and allow a DC component which determines the light intensity to be added to the waveform controlling the light source.

$$N = \frac{AT_1 + BT_2}{T_1 + T_2} \quad (4.7.1)$$

where N is the average brightness (percent), A is the brightness of data (percent) in period T_1 and B is the average brightness of the compensation symbols (percent) in period T_2 . The OOK frame's structure of IEEE 802.15.7 standard is shown in (Figure 34). It consists of a preamble for the synchronization, a PHY header that provide details on the frame and sub-frames with resynchronization in order to not lose the system's synchronization.

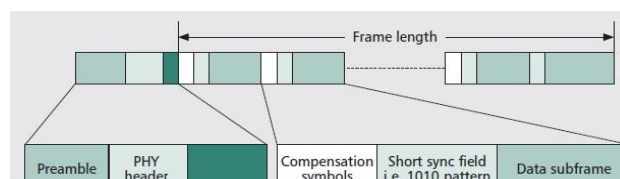


Figure 34: OOK frame's structure.

On-Off-Keying transmitter emits a rectangular pulse of duration $1/R_b$ and of intensity $2P$ to signify a one bit, and no pulse to signify a zero bit. The bandwidth required by OOK is roughly R_b [98]. BER is given in terms of minimum distance. In this type of receiver design, the receiver will choose a signal from the set of known signals which is the closest to the received signal.

Since the receiver observes which of the possible signals is closest to the received signal, it stands to reason that it is less likely to make an error due to noise.

That is, one important measure of the noise immunity of a given signal set is the minimum Euclidian distance between signals, defined as:

$$d_{\min} = \min_{i \neq j} \|x_i - x_j\|. \quad (4.7.2)$$

Knowing the energy per bit (E_b), the minimum distance in term of energy per bit, results:

$$d_{\text{OOK}}^2 = 2 * E_b. \quad (4.7.3)$$

The BER is then given in terms of minimum distance as:

$$\text{BER} = Q\left(\frac{d_{\min}}{\sqrt{2N_0}}\right) \rightarrow \text{BER}_{\text{OOK}} = Q\left(\sqrt{\frac{E_b}{N_0}}\right) = Q\left(\sqrt{\frac{2R^2P_s^2T_b}{N_0}}\right). \quad (4.7.4)$$

In terms of error function, it is given as:

$$\text{BER} = \frac{1}{2} \text{erfc}\left(\sqrt{\frac{R^2P_s^2T_b}{N_0}}\right) \quad (4.7.5)$$

and the power required by OOK to achieve a given BER results:

$$P_{OOK} = \frac{1}{R} * \sqrt{\frac{N_0 * R_b}{2}} * Q^{-1}(BER). \quad (4.7.6)$$

-Variable Pulse Position Modulation:

Pulse position modulation is an impulse modulation system in which the information is coded from the impulse position of duration τ inside the sampling period, in relation of its contents. PPM is a phase modulation that maintains constant the impulse amplitude and width. That kind of modulation subdivides the channel in τ/T temporal slots or sends a message that can be coded in 2^τ possible temporal combinations. L-PPM utilizes symbols consisting of L time slots. A constant power is transmitted during one of these chips and zero during remaining chips. Hence, encoding $\log_2 L$ bits in the position of the high chip. If the amplitude of transmitted waveform is A, the average transmitted power for L-PPM is A/L. For any L greater than 2, PPM requires less optical power than OOK. In principle, the average optical power requirement can be made arbitrarily small by making L suitably large, at the expense of increased bandwidth.

For a given bit rate, L-PPM requires more bandwidth than OOK by a factor of $L/\log_2 L$ [83, 98]. In addition to the increased bandwidth requirement, PPM needs more transmitted peak power and both slot and symbol-level synchronization.

The variable terms in VPPM represents the change in the duty cycle in response to the requested dimming level. In (Figure 35) are shown examples of PPM; in the second we can see an example of VPPM with a 75% of duty for both “0” and “1”.

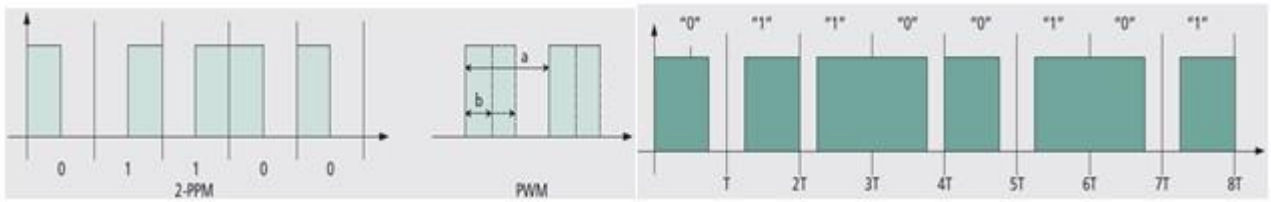


Figure 35: examples of VPPM signals

In the IEEE 802.15.7, the input of the VPPM systems is sent through a RS FEC encoder for error protection, followed by a 4B6B RLL code for DC balance and flicker mitigation. The 4B6B RLL code (Figure 36) are always 50 percent duty cycle during one encoded symbol, DC balanced run length limiting code, error detection capability, run length limited to four and reasonable clock recovery. The preamble and header is encoded using OOK, it need the N percent adjustment; while for the data with VPPM the visibility level for dimming is automatically satisfied.

| 4B (input) | 6B (output) | Hex |
|------------|-------------|-----|
| 0000 | 001110 | 0 |
| 0001 | 001101 | 1 |
| 0010 | 010011 | 2 |
| 0011 | 010110 | 3 |
| 0100 | 010101 | 4 |
| 0101 | 100011 | 5 |
| 0110 | 100110 | 6 |
| 0111 | 100101 | 7 |
| 1000 | 011001 | 8 |
| 1001 | 011010 | 9 |
| 1010 | 011100 | A |
| 1011 | 110001 | B |
| 1100 | 110010 | C |
| 1101 | 101001 | D |
| 1110 | 101010 | E |
| 1111 | 101100 | F |

Figure 36: 4B6B run length limiting code

An illustration of L-PPM and its inverted version is shown in (Figure 37). Assuming that the information is random with uniform distribution, the minimum distance is given as:

$$d_{\min}^2 = 4 * R^2 * P_s^2 * T_b * \log_2 L \quad (4.7.7)$$

So the BER results:

$$\begin{aligned} \text{BER}_{L\text{-PPM}} &= Q\left(\sqrt{\frac{E_b}{N_0}} * \sqrt{\log_2 L}\right) \\ &= Q\left(\sqrt{\frac{2 * R^2 * P_s^2 * T_b}{N_0}} * \sqrt{\log_2 L}\right). \end{aligned} \quad (4.7.8)$$

The average optical signal power required to achieve a given BER for an L-PPM system can be found by solving for P_s :

$$P_{LPPM} = \frac{1}{R} \left(\frac{N_0 * R_b}{2 * \log_2 L} \right) Q^{-1}(BER). \quad (4.7.9)$$

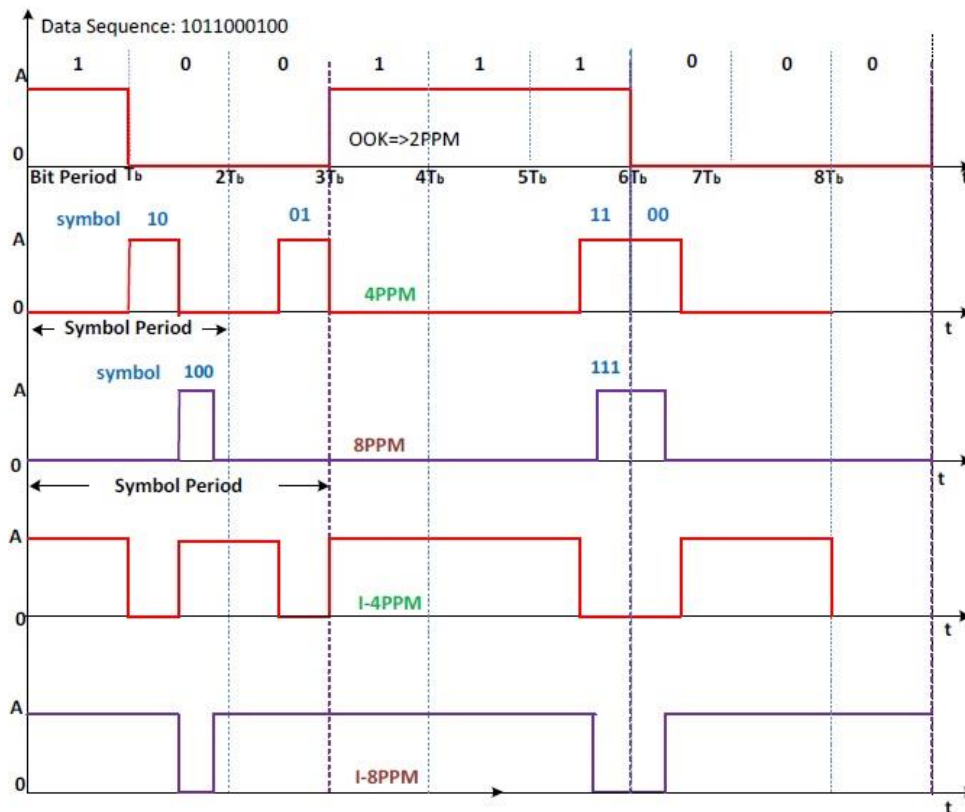


Figure 37: examples of L-PPM and I-LPPM

Also an inverted version of the PPM exists. I-PPM yields higher brightness than conventional PPM. Inverting the pulse position of conventional PPM, we obtain I-PPM.

The optical intensity is “off” during the 1-th sub-interval and “on” everywhere else.

In the case of I-LPPM, the minimum distance is given as:

$$d_{\min}^2 = \frac{2 * E_b * \log_2 L}{L - 1}. \quad (4.7.10)$$

The BER is:

$$\begin{aligned} \text{BER}_{\text{I-LPPM}} &= Q\left(\sqrt{\frac{E_b}{N_0}} * \sqrt{\frac{\log_2 L}{L-1}}\right) \\ &= Q\left(\sqrt{\frac{2 * R^2 * P_s^2 * T_b}{N_0}} * \sqrt{\frac{\log_2 L}{L-1}}\right). \quad (4.7.11) \end{aligned}$$

and the average optical signal power required, results:

$$P_{\text{I-LPPM}} = \frac{1}{R} \sqrt{\frac{N_0 * R_b}{2}} \sqrt{\frac{L-1}{\log_2 L}} Q^{-1}(\text{BER}). \quad (4.7.12)$$

-Color Shift Keying:

The use of multiple colors (RGB) to create the white light, forms the principle behind CSK modulation.

It uses faster white LEDs that can be more useful for communication can be generated by simultaneously exciting red, green and blue LEDs [99]. Color shift keying modulation is similar to frequency shift keying in that the bit patterns are encoded to color (wavelength) combinations.

For example, for 4-CSK (two bits per symbol) the light source is wavelength keyed such that one of four possible wavelengths is transmitted per bit pair combination.

In (Figure 38) we can see the division of the spectrum in 7 color bands defined by the IEEE 802.15.7 standard given by the CIE 1931 color coordinates in which the 3-bit values in figure represent each of the seven color bands.

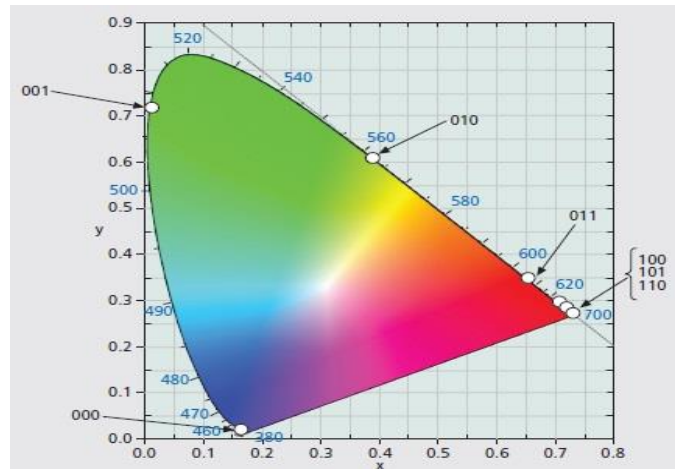


Figure 38: IEEE standard colors for CSK

The CSK signal is generated by using three color light source out of the seven, the three vertices of the CSK constellation triangle are decided by the center wavelength of the three color bands on XY color coordinates. It has the advantages that the final output color is guaranteed (white) by the color coordinates, the total average power of all CSK light source is constant although each light source power may have a different instantaneous output power. There is no flicker issue due to the amplitude variations, it support amplitude changes with digital-to-analog converters (higher complexity) and so allowing higher order modulation support to provide higher data rates at a lower optical clock frequency. An example of constellation is shown in (Figure 39) [70].

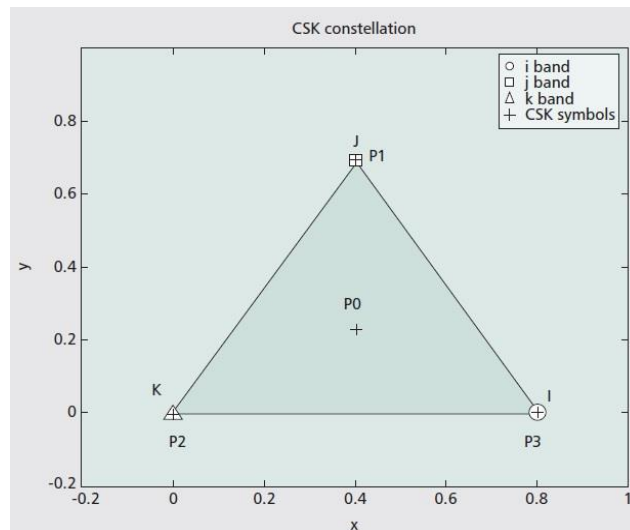


Figure 39: example of CSK constellation

-Sequence Inverse Keying Modulation:

SIKM uses the concept of Direct Sequence Spread Spectrum. Spread spectrum modulation technique can minimize the effect of interference according to the processing gain advantage.

While the additional bandwidth requirement of a spread-spectrum modulation scheme reduces the system bandwidth efficiency, the processing gain of the spread spectrum technique helps to combat artificial light interference effects and multipath dispersion without the need for extra circuitry such as equalizers. The use of DSSS in optical wireless (OW) system is based on the basic principle of unipolar-bipolar correlation .

Because in optical medium there is no negative going pulses and when there is no light pulse, the signal has to be represented by zero level.

Therefore, a technique called unipolar-bipolar sequencing, allows the same spreading codes of radio systems to be used in optical systems, is employed instead.

Unipolar-bipolar sequencing, involves transmission of a unipolar spreading sequence and correlation with a bipolar version of the same spreading sequence, preserves the correlation properties of bipolar-bipolar sequencing although with the introduction of a fixed dc offset.

At the transmitter, a unipolar spreading sequence is modulated by binary data such that the sequence is transmitted for a binary “1” while the inverse sequence is transmitted for a binary “0”. This type of modulation is called as SIK [100]. In the SIKM The modulator part basically performs digital operation of XNOR where incoming data bit is modulated by a pseudo noise random data with a bit rate higher than the data bit. Thus, the transmitted data is said to be spread. A similar operation is needed at the receiver to de-spread the incoming sequence from the channel. The spread data is then used to modulate the intensity of the LED light source. The optical signal is characterized by an average optical power P and a peak pulse power $2P$. The light propagates through free space channel, get added with noise and then, detected by photodiode (or LED). The detected photocurrent for the LoS case can be given as:

$$r_n(t) = 2RP_s b(t) \oplus s(t) + f(t) + n(t). \quad (4.7.13)$$

Where $f(t)$ is the interfering signal at the output of the photodiode due to ambient light, $n(t)$ is the channel noise process, $b(t)$ is the sequence of unit amplitude rectangular data bits each of duration T_b and $s(t)$ is the periodic pseudo noise sequence of unit amplitude rectangular chips each of duration T_c . The $f(t)$ as discussed in [100] has the DC component RP_f and AC component $RP_f f'(t)$ with P_f as the average interfering power from other sources of light. This received signal is AC coupled and so the DC term will be removed. At the receiver, this signal is multiplied by $s'(t)$ (de-spread) and then integrated over one data bit duration and zero threshold detected, so the correlator output results:

$$r_{rx}(T_b) = \int_0^{T_b} 2RP_s b(t) \oplus s(t) s'(t) dt + \frac{1}{T_b} \int_0^{T_b} RP_f f'(t) s'(t) dt + \frac{1}{T_b} \int_0^{T_b} n(t) s'(t) dt. \quad (4.7.14)$$

Since $f'(t)$ varies slowly with respect to the spreading code $s'(t)$ over the

integration period T_b , then $f'(t)$ can be approximated by $f'(T_b)$ and is constant over integration period. So, the detected signal becomes:

$$r_{rx}(T_b) = b_k R P_s + \frac{R P_f}{N} f'(T_b) + n(T_b). \quad (4.7.15)$$

The mean (μ_r) and the variance (σ_r^2) of $r_{rx}(T_b)$, can be given as:

$$\mu_r = b_k R P_s ; \sigma_r^2 = \left(\frac{\sigma_m R P_f}{N} \right)^2 + \frac{N_0}{2T_b} \quad (4.7.16)$$

where σ_m is standard deviation of $f'(T_b)$. The variance produced by light interference is reduced by processing gain N , so the SNR for the correlator output is:

$$SNR_{SIK} = \frac{\mu_r^2}{\sigma_r^2} = \frac{R^2 P_s^2}{\left(\frac{\sigma_m R P_f}{N} \right)^2 + \frac{N_0}{2T_b}} \quad (4.7.17)$$

$$\text{or } SNR_{SIK} = \frac{1}{\left(\frac{\sigma_m P_f}{N P_s} \right)^2 + \left(\frac{\sqrt{N_0 R_b}}{\sqrt{2} R P_s} \right)^2} = \frac{1}{\left(\frac{\sigma_m}{N * SINR} \right)^2 + \left(\frac{1}{SNR_{opt}} \right)^2} \quad (4.7.18)$$

where P_s is the mean optical power of the desired signal impinging the PD. The second term of the denominator can be also written as the optical signal to

noise power ratio if $\sqrt{N_0 R_b / 2} = R P_n$, where, P_n denotes a noise equivalent

optical power. The BER for the DSSS SIK system can be expressed as:

$$BER_{SIK} = Q[\sqrt{SNR_{SIK}}]. \quad (4.7.19)$$

And the average optical signal power required to achieve a given BER for a SIK system results:

$$P_{SIK} = \frac{1}{RN} \sqrt{\frac{R^2 \sigma_m^2 P_f^2 + N^2 R_b N_0}{2}} * Q^{-1}(BER_{SIK}). \quad (4.7.20)$$

Another way to transmit an unipolar signal, results that to use Direct Current biased Optical-OFDM in which a bias current is added to the bipolar signal to create the unipolar signal. It is possible also to use a ACO-OFDM or Unipolar-OFDM to not wasted the energy for the bias current. OFDM systems are very sensible to the non-linearity at the output of the LEDs (Figure 40). It is possible work in a small region in which the response is linear but the luminance dispersion requires to work in a larger region.

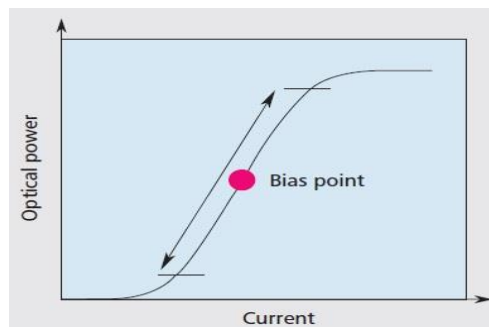


Figure 40: optical power of LEDs.

It is possible also to pre-distort the signal to create a linear output but it depends by the DAC accuracy and the inconcistency of the non-linearity output of the LED.

(Figure 41) is shown a comparison between VLC and RF cells depending on the number of APs and the size of the room[101].

A Li-Fi system can achieve over 900 times of a corresponding femtocell network, seeing the available wide bandwidth.

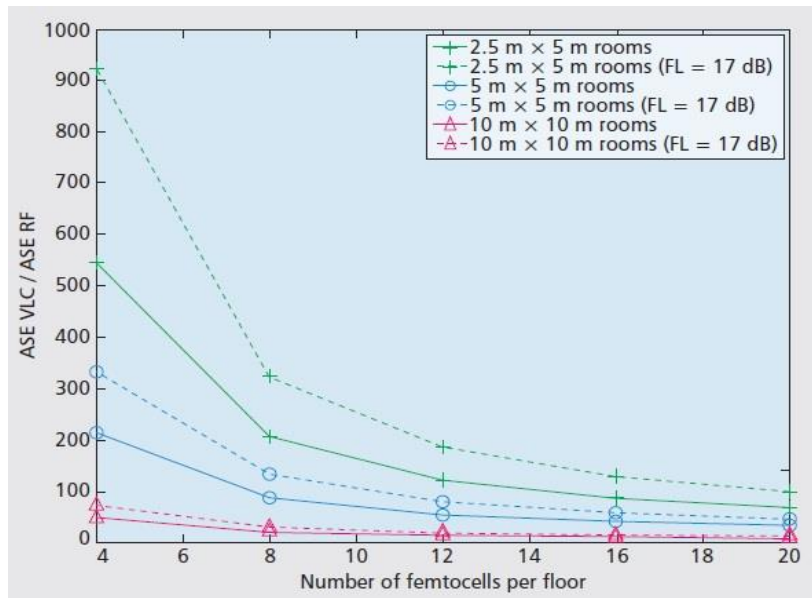


Figure 41: VLC and RF systems cells comparison.

Results from modulation analysis described previously will be presented now, considering AWGN channel and a BER of 10^{-6} acceptable for reliable data transmission.

(Figure 42) shows the require average power respect the data rate. it is possible to see that If data rate increases, the power requirement also increases. It is also observed that power requirement increases when L increases for I-LPPM, while it decreases for L-PPM. Power efficiency however, remains the same in both DSSS SIK and OOK. That is, unlike L-PPM or coded schemes which increase their power efficiency over OOK with the introduction of redundancy; DSSS has the same power efficiency as OOK. This property originates from the fact that in DSSS a single codeword is used and hence it is not possible to exploit the minimum Hamming distances between each codeword.

Instead, the redundancy or bandwidth expansion in DSSS is used to mitigate multipath ISI and narrowband light interference.

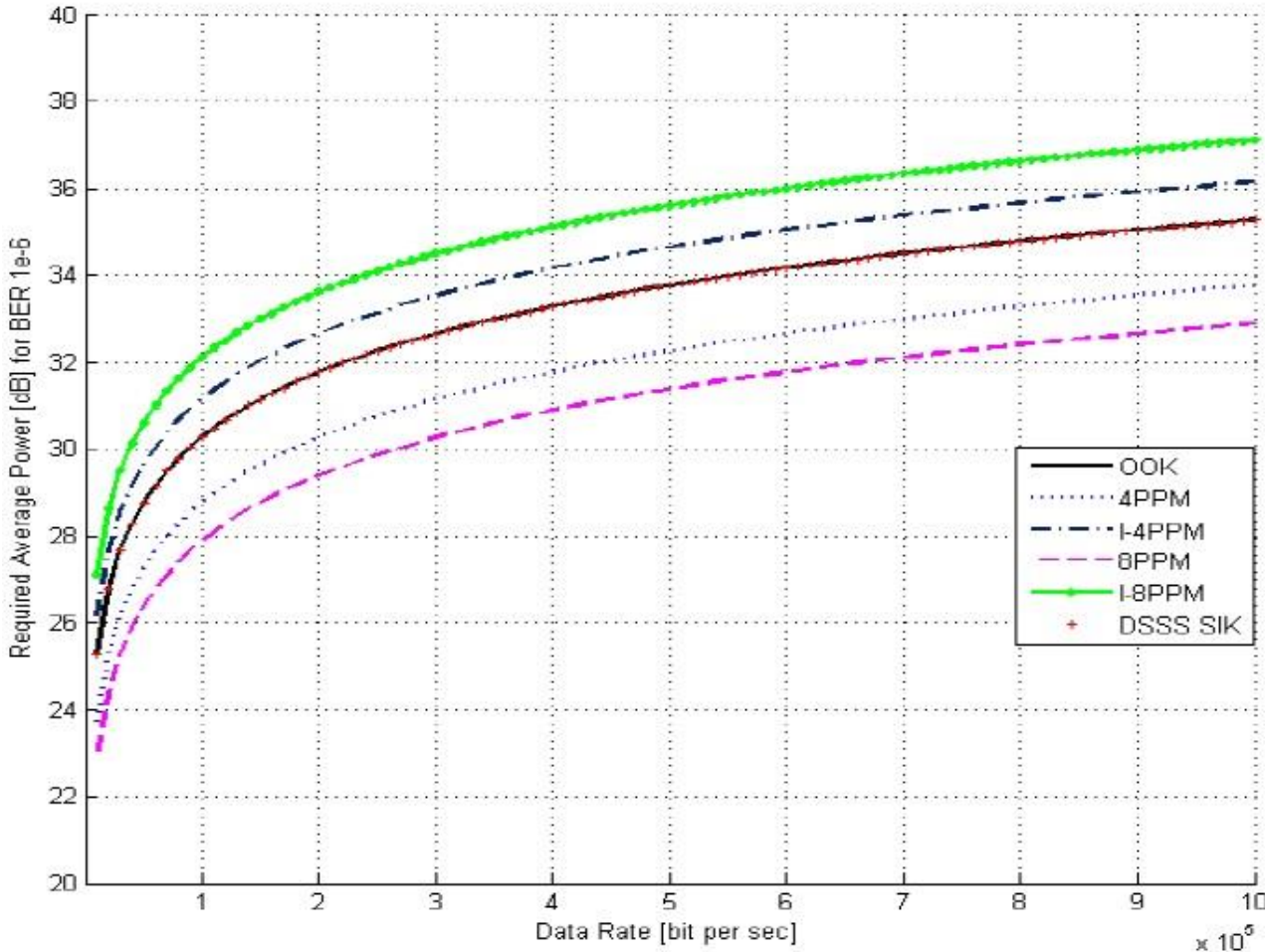


Figure 42: required average power for BER 10⁻⁶ with different data rate.

(Figure 43 (a)) and (Figure 43 (b)) show BER versus SNR curves for all modulation schemes. For these results data rate is fixed at 1MHz for all the modulation techniques. It can be seen that SIK performs better even with small interference (Figure 43 (b)). Comparing between L-PPM and I-LPPM, L-PPM performance is better. However, applications where average power is not a constraint and light remains ON for most of the pulse duration, I-PPM can offer

high data rate transmission as lights remain ON for most of the pulse duration. (Figure 44) show the BER performance with external interference, taking into account all the characteristic treated before [12]. Different modulation techniques which can be used in VLC systems have been discussed and analyzed in this chapter. BER and SNR performance parameters were evaluated and compared. Differently from the IR system in which L-PPM modulations offers very good performance, in VLCs do not offers significant improvement. Therefore, a better system based on DSSS results better in order to mitigate the effect of noise.

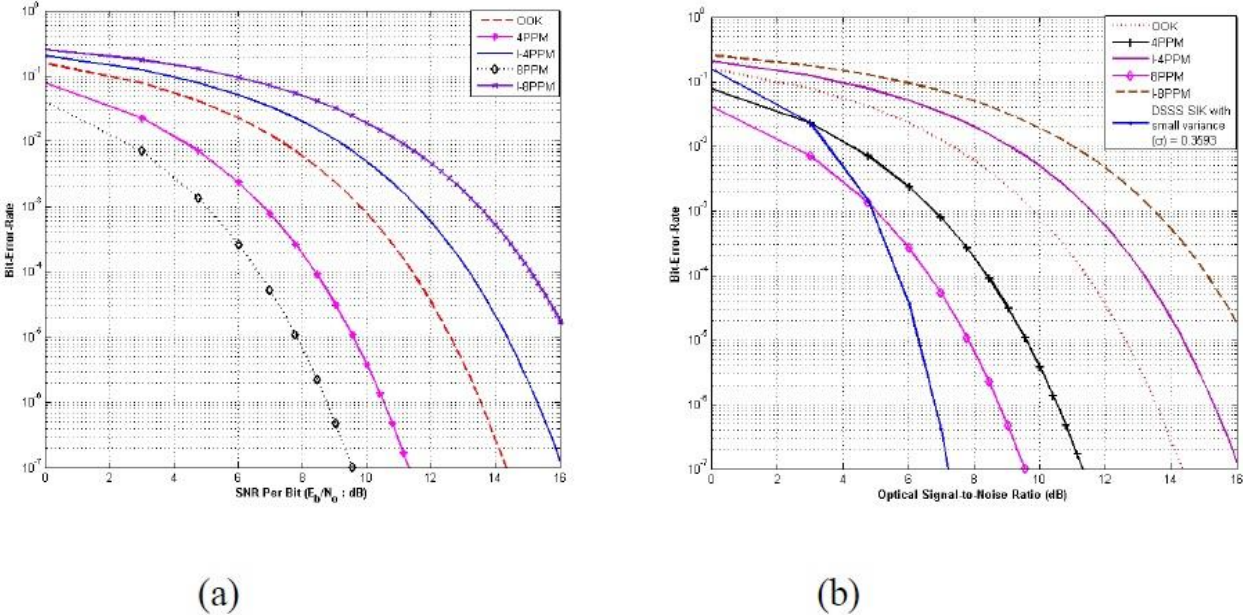


Figure 43: bit error rate over (a) SNR and (b) optical signal to noise ration.

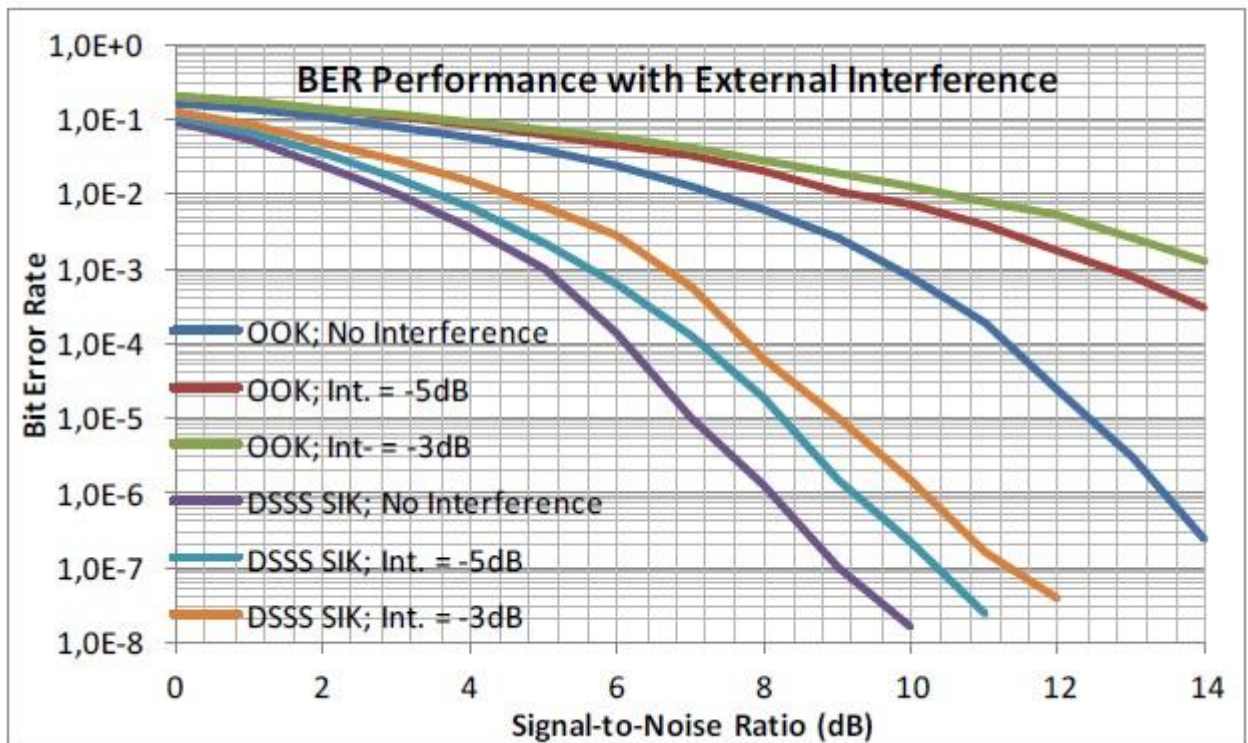


Figure 44: bit error rate over signal-to-noise ratio in presence of external interference.

4.8 Future trends

VLC systems are new attractive and futuristic systems. Their capacity to forward data and their incredible characteristic, opens the door to many possible applications and future trends. In this paragraph a list of possible future trends is presented.

Optical Femtocells: the efficiency of large networks highly depends on the ability to spatially reuse the same spectral resources, which is subject to the propagation of interference. Most popular propagation models for radio describe the propagation over a distance d by a path loss exponent β , typically ranging from 2 in free space to values larger than 4 in more complex terrains.

Interestingly, for VLC via downlighting luminaires and detectors facing downward, there is no line of sight (NLOS).

We can experience this effect when we look at a lamp from a large distance and see only an illuminated spot underneath it.

Due to the steep decline in received power, the creation of small optical cells is favourable (Figure 45).

Within each cell a luminaire acts as a base station and transmits signals to the neighbouring luminaires. Similar systems have been examined for lamp-to-user communications.

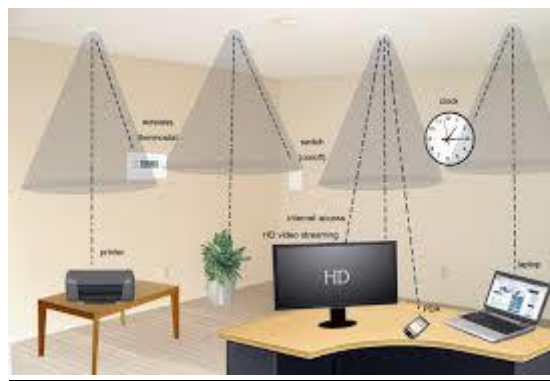


Figure 45:example of optical Femtocells

Toys communication: there is a growing interest in toys that are wirelessly connected with each other, and to computers or smartphones.

Many toy applications require only a moderate bit rate (1000 b/s) at short communication ranges (3 m), which can be reached with LED-to-LED networking, or by means of VLC in general. Therefore, it results very simple connect a toy with smartphone or PC or many other things, to improve the enjoy of users(Figure 46).



Figure 46: application of toys communication

Locating people: VLC can improve the actual system and can be used to localize people without using internet or GPRS systems. Because of the growing use of LEDs, it is also possible create new application that can help the people. For example can help to localize older people or people that have problems of Alzheimer to be found by children. It can also useful, to find lost propriety or many other thinks.

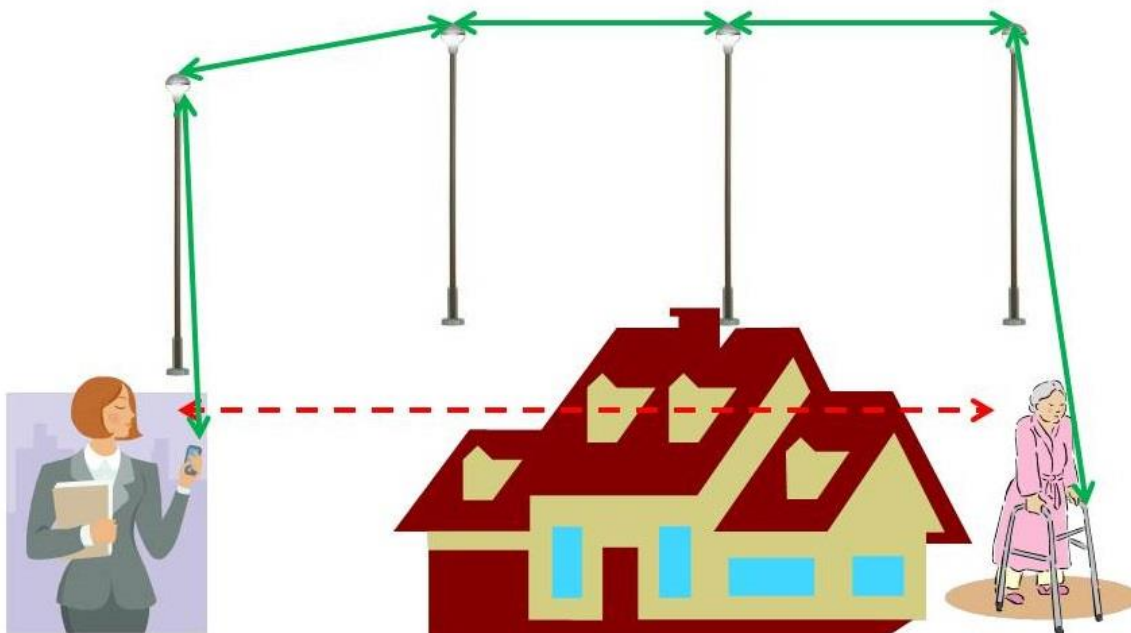


Figure 47: application of people locating.

Hurricanes' warning signals: during hurricanes, all the connections are interrupted but if the road side units are very close to the street and built to withstand hurricanes, it is possible to see where and if there are survivors.

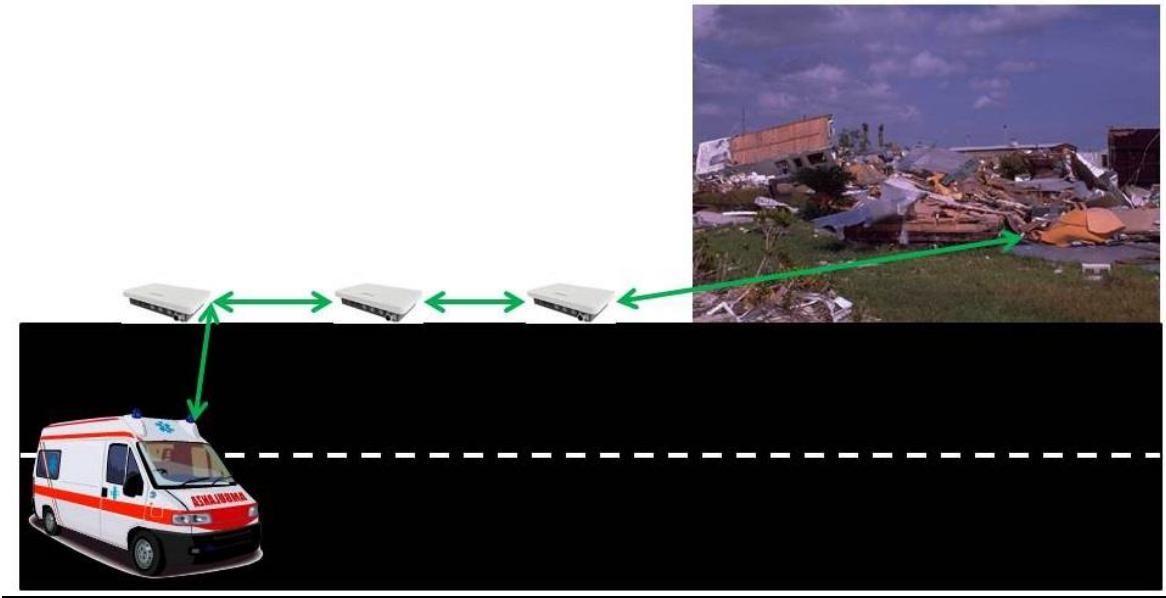


Figure 48: application of hurricane's warning signal.

Emergency signals: gas meter warning, water meter warning, electrical leakage alarm, men at work and many other signaling warning, improving the new concept of smart cities (Figure 49).

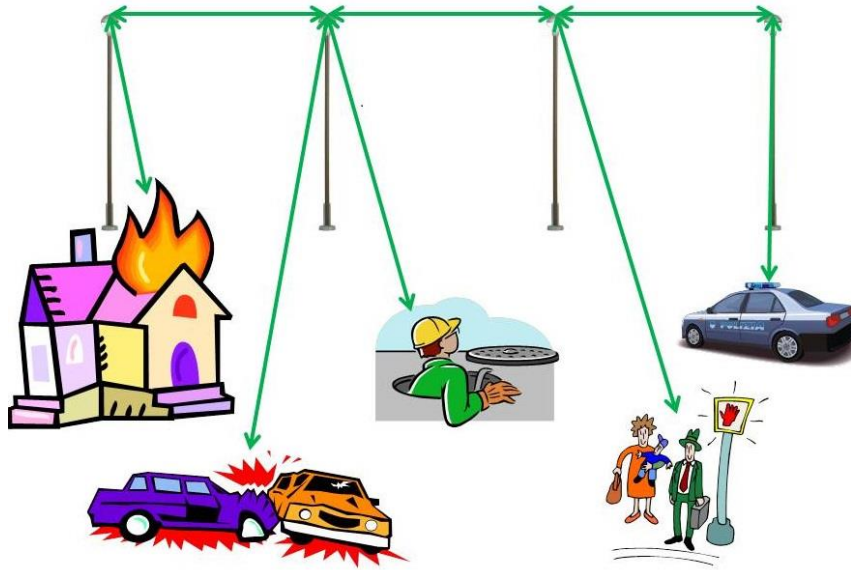


Figure 49: smart cities application.

Aps services: it can be used as access point for other systems (3G,WIFI, LTE) where they cannot arrived (hidden places) (Figure 50).



Figure 50: VLC as AP in a tunnel.

Exchange files with neighbour: VLC can be used to exchange files with near people or systems without overloading other wireless systems (Figure 51).



Figure 51: example of cellular offloading with VLC Aps

Underwater communication: create a wireless signal that can pass through the water is very difficult, with VLC system if the two devices are in LoS it is possible to communicate also underwater.

Many applications can be born as communication between subs, submarines alert messages, danger messages and so on (Figure 52).

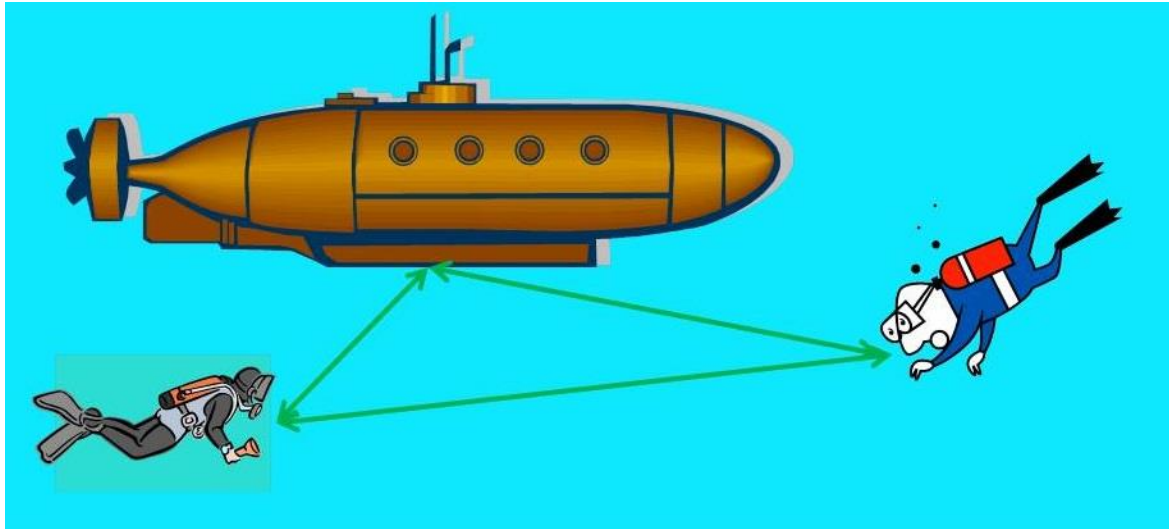


Figure 52: submarine VLC application.

Vehicular networks: many applications can improve the vehicular systems like busy intersection scheduling traffic light (Figure 51(a)), parking availability (Figure 51(b)), curve speed warning (Figure 51(c)), pedestrians and vehicles localization (Figure 51(d)), stop signal movement, collision warning (Figure 51(e)), pre-cash sensing (Figure 51(e)), emergency electronic brake light, vehicular lane change (Figure 51(f)) and so on.

helping blind people: there is the possibility to help the walking of blind people, that is something that I would like to create in order to create a more possibility also for people with view problems. Inserting a photo detector (or LEDs) in the stick blind that can communicate with semaphore or every kind of LEDs that contain information about the surrounding environment to help the walk (Figure 54). I think that this will be the right system in to create a very complete system communication and do not overload the cellular one.

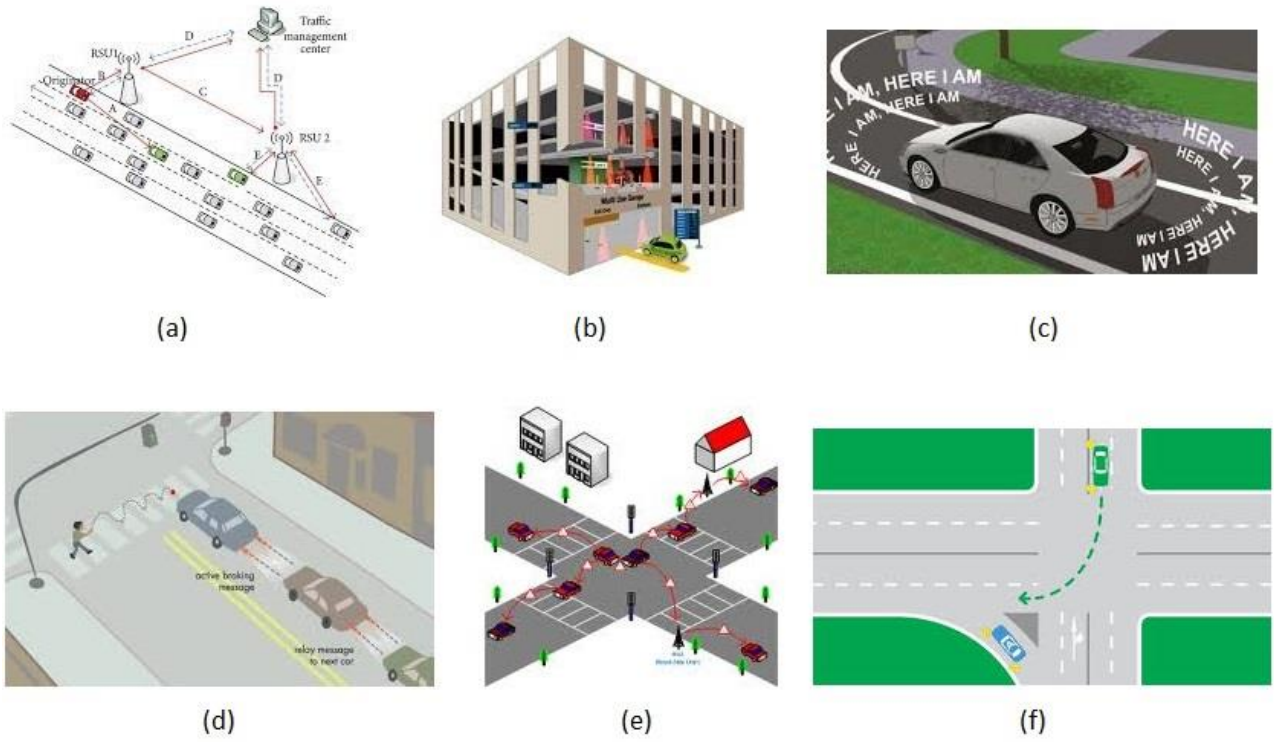


Figure 53: examples of vehicular networks with VLC

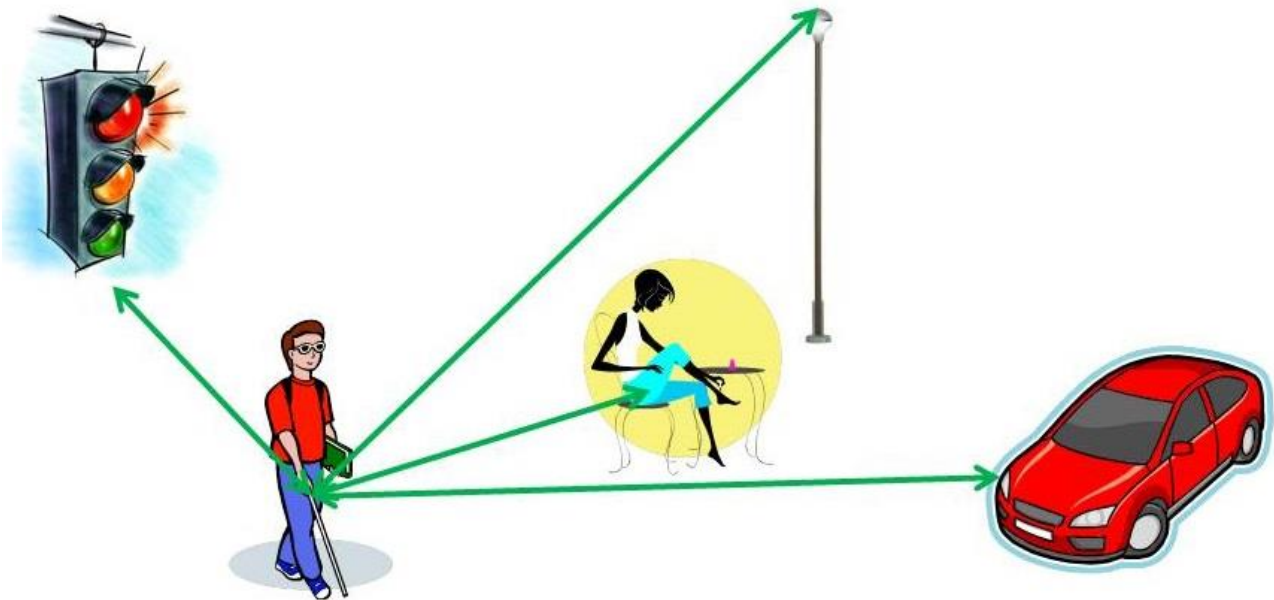


Figure 54: VLC system application to help the walk of blind people.

CHAPTER 5: VEHICULAR NETWORKS

5.1 VLC in ITS

While previous studies have documented the effectiveness of V2I and V2V communication using radio technology in terms of improving automotive safety, we can identify characteristics unique to image-sensor-based VLC as compared to radio wave technology.

V2I-VLC involves the wireless exchange of critical safety and operational data between moving vehicles and roadway infrastructure, and is identical in concept to V2I using radio wave technology, except that it uses light transmission instead of radio wave technology.

This is also true for V2V-VLC, which involves wireless exchanges of data between moving vehicles traveling in the same area.

The two primary advantages of a VLC system are its line-of-sight feature and an image sensor that not only provides VLC functions, but also the potential vehicle safety applications made possible by image and video processing.

In V2I and V2V systems, VLC offers several advantages.

Since VLC links are visible, installation of roadside equipment is much easier. Additionally, previously installed facilities, such as LED traffic lights or LED sign boards, can be used.

VLC provides an additional feature if the receiver incorporates an image sensor or a camera.

Specifically, by using image or video processing to detect and recognize moving vehicles, safety applications can be integrated [102].

For example, as methods of enhancing driving safety, adaptive cruise control, collision warning, pedestrian detection, and providing range estimations for nearby vehicles are potential candidates for incorporation into VLC systems.

It is generally accepted that VLC links depend on the existence of an uninterrupted line of sight (LOS) path between the transmitter and the receiver. In contrast, radio links are typically susceptible to large fluctuations in received signal amplitude and phase.

Unlike radio waves, VLC does not suffer from multipath fading, which significantly simplifies the design of VLC links. Because VLC signals travel in a straight line between a transmitter and a receiver, they can easily be blocked by vehicles, walls or other opaque barriers. This signal confinement makes it easy to limit transmissions to vehicles nearby.

It should be noted, however, that VLC has several potential drawbacks. First, since visible light cannot penetrate walls or buildings, VLC coverage is restricted to small areas, and some applications, such as blind spot warning, will require installation of access points that must be interconnected via a wired backbone. Furthermore, in addition to outright physical blocks, thick fog or smoke can blur visible light links and decrease system performance as we have seen before.

VLC is not only suitable for a broadcast system as road-to-vehicle or I2V communication systems but it can be equally effective in V2V and V2I communication systems. In case of V2V scenario, a vehicle in the front of traffic lights receives the traffic safety information and passes it using the brake lights to the vehicle running behind.

They can even form a vehicle ad-hoc network and share information among themselves.

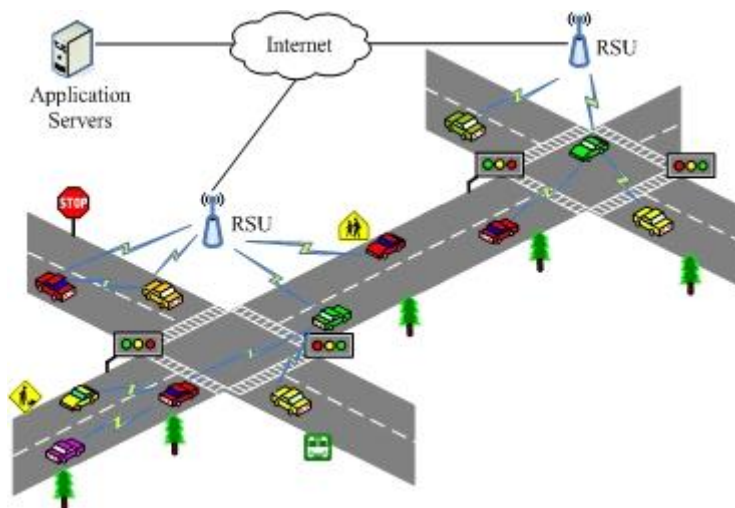


Figure 55: example of vehicular networks with VLC systems.

(Figure 55) shown an example of vehicular networks with visible light communication systems.

RSUs such as, LED-based traffic lights are well suited for broadcast communication in I2V mode [61] of vehicular communication systems. Traffic safety related information can be continuously broadcasted without extra power usage enhancing smooth traffic flow as well as reducing accident fatality. The light emitted from a traffic is modulated at a given frequency and then is detected by a photodetector (or LED) receiver on the vehicle, providing useful safety information to the driver in advance.

Hence, LED-based traffic light offers a very suitable option to be included as RSU and integrated with ITS architecture [103].

One of the suitable scenarios of interaction and communication from RSU to vehicle communication is presented in (Figure 56).

Even vehicles are now equipped with LEDs brake and head lights. They are environment friendly and have better visibility. Therefore, VLC can be considered as a supplementary communication systems not only for broadcast but also uplink communication connectivity and V2V communication facility. Along with many access technologies, LED-based VLC can be used. An additional traffic control and monitor unit is included which can provide additional support information in conjunction with other RSUs. In this systems therefore, integrating LED-based traffic light unit for broadcasting safety related information offer a cost effective method of implementation.

Since, replacement of conventional traffic light with LED-based traffic light is getting momentum, it is highly desirable to use the dual function of LED; in this case signaling and traffic broadcast unit.

The integration of traffic light VLC systems will also minimize the use of IR and short range based costly communication infrastructures.

Furthermore, in the long run it will support the ubiquitous road communication throughout the travel using LEDs road illumination systems [61].

It is possible to use ubiquitous communication infrastructures, such as, wireless access point routers, variable message sign and gateways for offering information data connectivity between mobile units and Internet. But this solution is not cost effective and it is very difficult to use wireless based access point all along the road at small intervals.

For VLC to be used, no major changes in the infrastructure are needed from the emitter side.

On the other hand, receivers are very low cost, and so no embryonic light receivers are required as automatic light sensors are common components in cars.

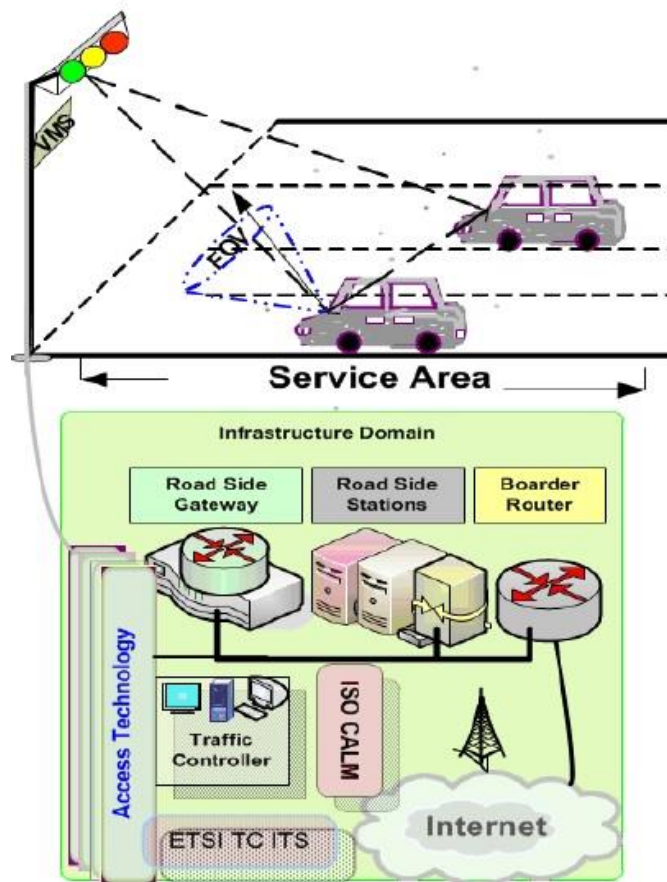


Figure 56: vehicular scenario of visible light communication integrated with ITS

Many applications are possible with VLC in vehicular networks such as:

- I2V one-hop broadcasting: required by traffic signal violation and curve speed warning applications. It can provide service for the left turn assistant and stop sign movement assistant applications where bi-directional information exchange between the vehicles and infrastructure nodes required.
- V2I one-hop anycasting: on receipt of information, infrastructure node processes through backbone network. This service, can be combined with multi-hop inter-vehicle forwarding. The combination maximizes the utilization of the backbone infrastructure network and vehicular as relays and the chance to reach every node.

- V2I unicasting: the vehicle-to/from-infrastructure unicasting network service takes place in the V2I and I2V network scenarios. This service works over single hops and multiple hops to/from a gateway infrastructure node. By using routing protocols, vehicles first find routes to a gateway infrastructure node and then start transmission to that gateway, which may use other vehicles as relays. This service requires routing protocols to discover routes and other services find paths to vehicles and infrastructure nodes via single hop transmission and multihop broadcasting.
- Limited neighbour broadcasting: this service also operates in the V2V scenario but over single hop. Each vehicle broadcasting information from all of its transmitters to its neighbouring vehicles, limited to one hop and the neighbouring vehicles do not forward the information that receive. This network service only provides vehicles with information in close vicinity, it prevents network performance degradation due to the high volume flooding.
- Multihop inter-vehicle forwarding: each vehicle acts as a relay and forwards data packets following a set of rules to prevent unnecessary broadcast flooding. This network maximizes the possibility that information is disseminated quickly and reliability among a large number of vehicles. Therefore, it is suitable for providing service such as urgent message delivery, cooperative forwarding collision warning and emergency electronic brake lights.

5.2 IEEE 802.15.7

An IEEE standard already exist, the IEEE 802.15.7. It specify the physical and medium access control parameters allow the user to specify any other parameters as in WIFI standard systems. It offers three different physical (PHY) types for VLC.

- PHY I: operates from 11.67 to 266.6 Kb/s with OOK or VPMM modulation to support the dimming. It is optimal for low bit-rate and long

distance in outdoor like in vehicular systems so it is possible to implement on vehicles, lampposts or road signs.

For outdoor applications, stronger codes using concatenated Reed-Solomon and convolutional codes are developed to overcome the additional path loss due to longer distance and potential interference introduced by optical noise sources such as daylight and fluorescent lighting.

RLL line codes are used to avoid long runs of 1s and 0s that could potentially cause flicker and clock and data recovery (CDR) detection problems.

RLL line codes take in random data symbols at input and guarantee DC balance with equal 1s and 0s at the output for every symbol. Various RLL line codes such as Manchester, 4B6B, and 8B10B are defined in the standard and provide trade-offs between coding overhead and ease of implementation. The optical clock rate for PHY I is chosen to be less than 400 kHz to account for the fact that LEDs used in applications such as traffic lights require high currents to drive the LEDs and therefore switch slowly. In (Table 4) is shown the operating mode of PHY I.

- PHY II: operates from 1.25 to 96 Mb/s with OOK or VPPM modulation to support the dimming.

It is optimal for point-to-point indoor applications with high data-rate. Also in PHY II Reed-Solomon codes as a forward error correction with a run length limiting (RLL) in order to prevent problems on clock or long runs of 1s and 0s detection.

For PHY II, the optical clock rate is chosen to be less than 120 MHz to accommodate fast LEDs used in mobile and portable devices for communication.

In (Table 5) the operating mode of PHY II is shown.

- PHY III: operates between 12 and 96 Mb/s with multiple optical sources with different frequencies (colors) and uses a particular modulation format called color shift keying (CSK). (Figure 57) shows the CSK system configuration for PHY III with three color (bands i , j and k) light sources

where after the scrambling and channel encoding the logical value (0,1) are transformed into xy values according to a mapping rules.

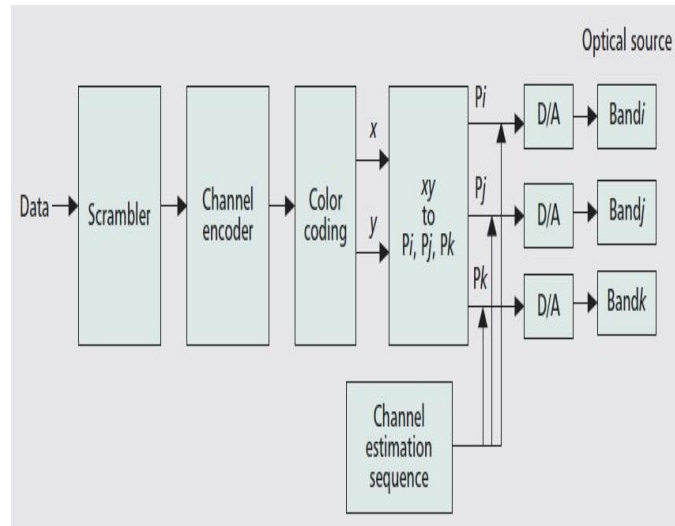


Figure 57: CSK system diagram for PHY III

The scrambler is necessary to create pseudo-random data and prevent data pattern dependent color shift and also subject of a FEC block for error protection. These xy values are transformed into intensity (P) in order to satisfy the following equations [104]:

$$\begin{aligned}
 x_p &= P_i x_i + P_j x_j + P_k x_k; \\
 y_p &= P_i y_i + P_j y_j + P_k y_k; \\
 P_i + P_j + P_k &= 1.
 \end{aligned}$$

The idle pattern helps to maintain visibility and flicker-free operation, it should have the same duty cycle to minimize flicker.

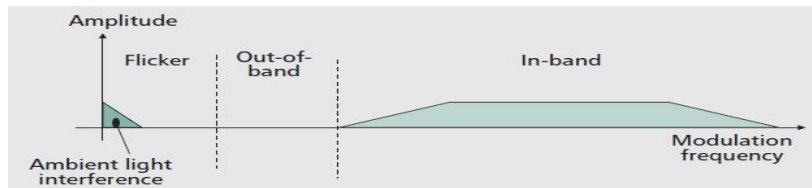


Figure 58: Modulation domain spectrum for visible light communication

In (Figure 58) is shown all the characteristic views so far, the flicker region must be less than 200 Hz where eye safety may be of concern, behind the 60 Hz we have the ambient light interference, in the end we have also a part out of band that is needed for multiple PHYs to coexist the idle pattern can either be here. To support continuous illuminations from infrastructures, the standard provide support for frames that contain only idle patterns to maintain continuous visibility, the visibility pattern is similar to idle pattern except that the patterns are used inside the payload of a visibility frame. The visibility patterns are not encoded in the PHY layer and do not have a FCS associated with them and support features such as flicker mitigation, continuous visibility, device discovery and color stabilization. The number of transition between 0s and 1s can be maximized to provide high frequency switching to avoid flicker and help the CDR circuit at the receiver for synchronization purpose, a simple approach should be used for visibility pattern generation in order to not makes visibility pattern generation and use very complex and it need to avoid pattern that conflict with existing RLL code word. The low resolution patterns can be used to develop high resolution visibility patterns by averaging them across time to generate the required high resolution pattern. For example, if visibility patterns are available at 10 (percent) resolution, a 25 (percent) visibility pattern can be attained by alternately sending a 20 (percent) visibility pattern followed by a 30 percent visibility pattern. This method guarantees that all visibility patterns will retain the same properties as the base low resolution visibility patterns. The high resolution visibility pattern generation can be generalized by using the low resolution patterns according to the algorithm specified in [70], the high resolution dimming algorithm provides two patterns “*sel1pat*” and “*sel2pat*” out

of the set of “ $K+1$ ” available patterns with number of repetitions as “*reppat1*” and “*reppat2*” respectively. These two patterns are the closest available patterns on both sides of the precision requirement. For example, if visibility patterns are at 10 percent resolution, there are 11 patterns ($K = 10$) and any requirement between 20.01 and 29.99 percent will time-multiplex the 20 and 30 percent visibility patterns as shown in (Figure 59), and then adjust the repetition ratio of 20 and 30 percent patterns to get the required precision with the minimum number of repetitions. The operating modes of PHY III is shown in (Table 6).

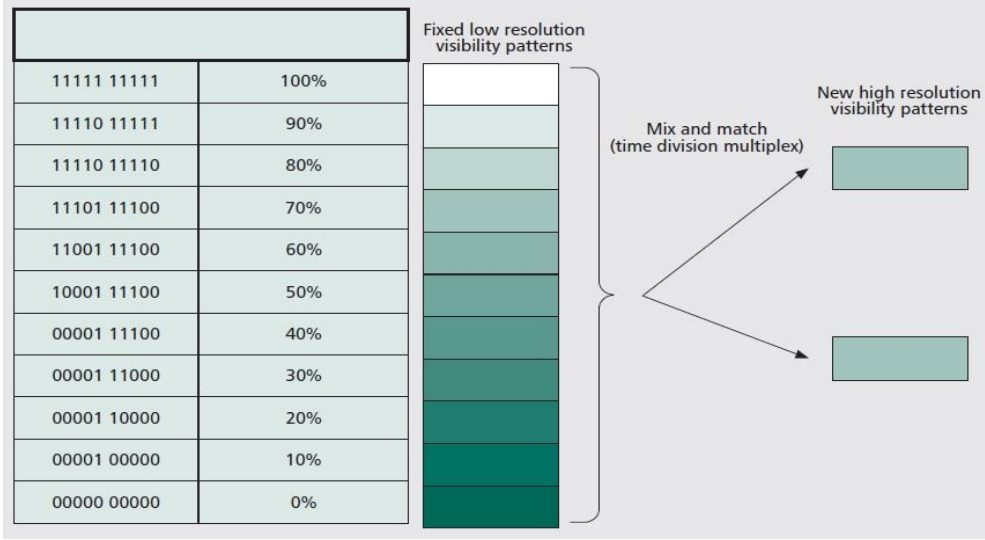


Figure 59: high resolution dimming with visibility pattern.

| Modulation | RLL code | Optical clock rate | FEC | | Data rate |
|------------|------------|--------------------|-----------------|-----------------|------------|
| | | | Outer code (RS) | Inner code (CC) | |
| OOK | Manchester | 200 kHz | (15,7) | 1/4 | 11.67 kb/s |
| | | | (15,11) | 1/3 | 24.44 kb/s |
| | | | (15,11) | 2/3 | 48.89 kb/s |
| | | | (15,11) | None | 73.3 kb/s |
| | | | None | None | 100 kb/s |
| VPPM | 4B6B | 400 kHz | (15,2) | None | 35.56 kb/s |
| | | | (15,4) | None | 71.11 kb/s |
| | | | (15,7) | None | 124.4 kb/s |
| | | | None | None | 266.6 kb/s |

Table 4: PHY I operating modes.

| Modulation | RLL code | Optical clock rate | FEC | Data rate |
|------------|----------|--------------------|-------------|-----------|
| VPPM | 4B6B | 3.75 MHz | RS(64,32) | 1.25 Mb/s |
| | | | RS(160,128) | 2 Mb/s |
| | | 7.5 MHz | RS(64,32) | 2.5 Mb/s |
| | | | RS(160,128) | 4 Mb/s |
| | | | None | 5 Mb/s |
| OOK | 8B10B | 15 MHz | RS(64,32) | 6 Mb/s |
| | | | RS(160,128) | 9.6 Mb/s |
| | | 30 MHz | RS(64,32) | 12 Mb/s |
| | | | RS(160,128) | 19.2 Mb/s |
| | | 60 MHz | RS(64,32) | 24 Mb/s |
| | | | RS(160,128) | 38.4 Mb/s |
| | | 120 MHz | RS(64,32) | 48 Mb/s |
| | | | RS(160,128) | 76.8 Mb/s |
| | | | None | 96 Mb/s |

Table 5: PHY II operating modes.

| Modulation | Optical clock rate | FEC | Data rate |
|------------|--------------------|-----------|-----------|
| 4-CSK | 12 MHz | RS(64,32) | 12 Mb/s |
| 8-CSK | | RS(64,32) | 18 Mb/s |
| 4-CSK | 24 MHz | RS(64,32) | 24 Mb/s |
| 8-CSK | | RS(64,32) | 36 Mb/s |
| 16-CSK | | RS(64,32) | 48 Mb/s |
| 8-CSK | | None | 72 Mb/s |
| 16-CSK | | None | 96 Mb/s |

Table 6: PHY III operating modes.

The data frame of the IEEE 802.15.7, consist of three elements:

- Synchronization header (SHR) that contain the fast locking pattern (FLP) and the topology-dependent pattern (TDP), which are useful to synchronize and block the clock and the data recovery (CDR);
- Physical header (PHR) which the information about data like length, modulation and FEC;
- Physical service data unit (PSDU) that contain the MAC header (MHR).

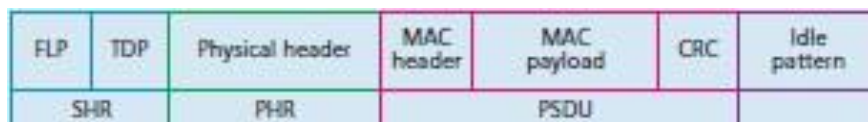


Figure 60: IEEE 802.15.7 data frame.

(Figure 60) shows the data frame just described with its characteristic. In this chapter we have seen how many possible trends and evolution can create

the VLC in the vehicular systems. To support that, the IEEE 802.15.7 is described with its characteristic.

CHAPTER 6: SIMULATION OF VLC IN VEHICULAR NETWORKS AND COMPARISON WITH IEEE802.11p

6.1 IEEE 802.11p

Until now, the IEEE 802.11 p is the most studied and deepened standard. IEEE 802.11 p provides a communication standard for Wireless Access in Vehicular Environment (WAVE), including both safety and non-safety communications, operating in the 5GHz frequency band standard. Due to the high velocity of vehicles, wireless channels change rapidly with time, providing much greater challenges for vehicular networks than other commercial communication systems (e.g., WLANs).

IEEE 802.11p has been released in recent years, which has the same PHY-layer frame structure as the IEEE 802.11a/g standard.

However, it uses a bandwidth of 10 MHz and operates at the 5.9-GHz band. The narrower bandwidth and the higher carrier frequency make vehicular networks even more vulnerable to fast-fading channels.

Pilot sub-carriers in each OFDM symbol could provide some information for timevarying channels. Nevertheless, in a multi-path channel with large delay spread, the number of pilots in IEEE 802.11p standard is too small to achieve an accurate channel estimate for each sub-carrier in the OFDM symbols.

Decision-aided channel tracking techniques have been proposed to estimate the channel on each sub-carrier, which works well in high signal-to-noise ratio (SNR) scenarios.

Correspondingly, the decision become erroneous when the SNR is low, leading to poor performance of the channel estimation.

Leveraging the decoded information to track the fast-fading channels has been shown to achieve more robustness due to the error correction gains from the decoder, which is the state-of-the-art method via simulation.

However, the decoder delay introduced by the buffer time in convolutional decoders usually makes the channel estimate stale.

As a result, there is usually residual phase error for the OFDM symbols due to the residual carrier frequency offset, oscillator phase error, and channel variations. This residual phase error usually degrades the system performance significantly. Thus, leveraging the small number of pilots to recover the phase error usually performs poorly and it needs the help of phase tracking systems.

The amendment respect to IEEE 802.11a defines a new operational model, wireless access in the vehicular environment (WAVE), which is dedicated for vehicular communications.

The basic MAC and MAC extension layers of WAVE are standardized in IEEE 802.11p and IEEE P1609.4, respectively.

The basic MAC is the same as IEEE 802.11 Distributed Coordination Function (DCF), which is based on the Carrier Sense Multiple Access with Collision Avoidance (CSMA/CA) scheme and the MAC extension layer adopts concepts from Enhanced Distributed Channel Access (EDCA) of IEEE 802.11e, like virtual station, Access Category (AC) and Arbitrary Inter-Frame Space (AIFS), in order to support traffic prioritization.

WAVE is a multi-channel system with one Coordinator Channel and multiple Service Channels.

In order to coordinate the access to CCH and SCHs, IEEE P1609.4 specifies a globally synchronized channel coordination scheme based on the Coordinated Universal Time.

Meanwhile, IEEE 1609 standard family cooperates with IEEE 802.11p to support resource management, security, network service, and multi channel operations.

The IEEE 1609.3 standard defines a WSMP (WAVE Short Message Protocol) for the delivery of the event-driven or periodic-driven packets.

In the standard, WSMP only verify the packet size on receipt of packets, but does not deal with congestion control.

In general, periodic-driven traffic is heavier than event-driven traffic. Without congestion control, when the number of periodic-driven packets increases, the queue within the RSU would be overwhelmed by the periodic driven packets, and the even-driven packets would be dropped consequently. The event-driven packet loss could result in unsafe driving environment, so if the size of the memory is smaller than the number of packets the devices may drop periodic-driven packets and loss information.

An example of IEEE 802.11p systems is shows in (Figure 61) and (Figure 62), in which vehicles generate a constant bit rate traffic with a fixed packet size in a channel data rate at 3 Mbps.

The transmission range is 80 meters, in (Figure 61) and (Figure 62) [105] we can see how the performance decrease increasing the number of vehicles. This is because with more nodes transmitting, the chance of collision increases therefore vehicles will spend more time backing off.

Moreover, (Figure 62) also verifies the fact that choosing the correct backoff window size can significantly increase network throughput. The above observations indicate that it is necessary to design an algorithms to adjust the backoff window size for each vehicle ‘on the fly’ in order to be adaptive to the environmental changes and achieve better throughput performance.

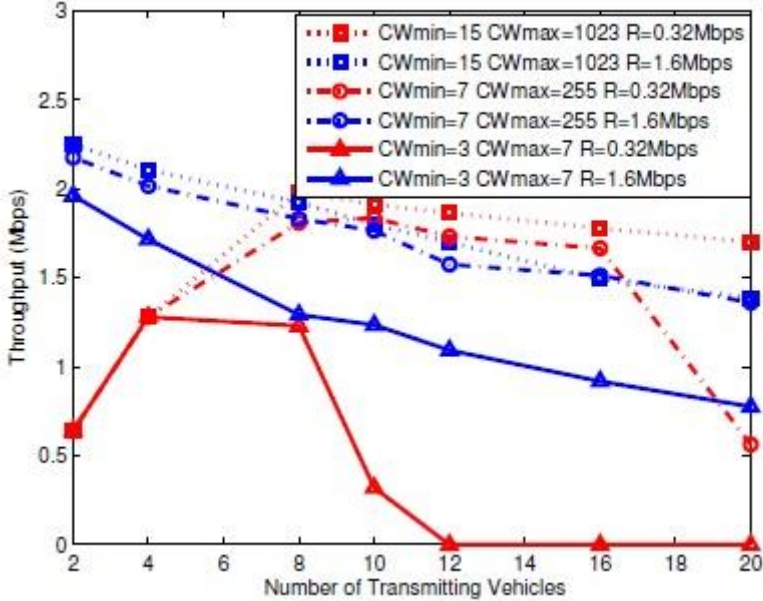


Figure 61: Saturation and non-saturation throughput for different window size.

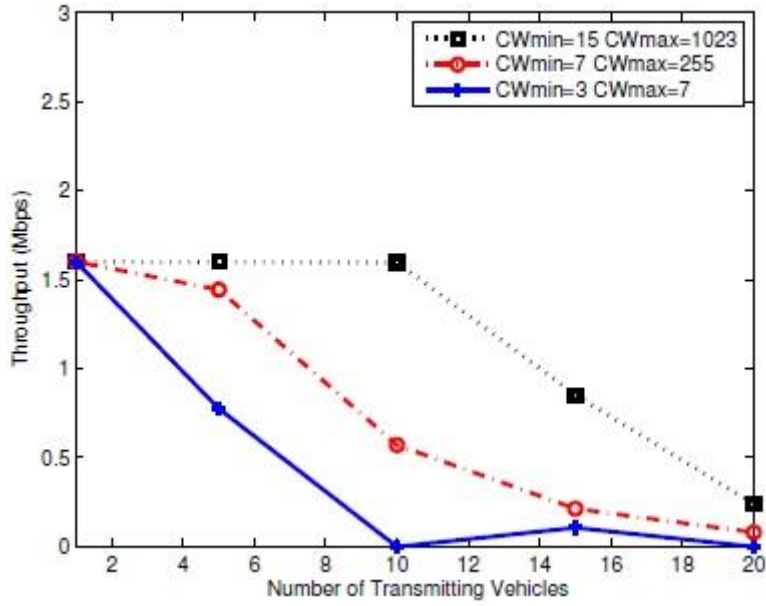


Figure 62: Average throughput for different window size.

It is important observe how the data-rate is different from the nominal one and it reach at maximum 1-1.6 Mbps that the vehicles have to share. The main problem of that system is the congestion of caused by the heavy traffic load in the channel, seeing that all vehicles share the same channel. In order to estimate the path loss exponent and the standard deviation, the linear regression is use. As a result of the linear regression, the path loss exponent ranged from 2.32 to 2.75 and the standard deviation from 5.5 to 7.1 dB. However, a dual-slope piecewise-linear model is able to represent the measurements more accurately. In [107], the path loss is characterize by a path loss exponent γ_1 and a standard deviation σ_1 within a critical distance d_c . Beyond this critical distance, the signal strength falls off with another path loss exponent γ_2 with a standard deviation σ_2 .

The formulation of the model is given as:

$$P(d) = P(d_0) - 10\gamma_1 \log_{10} \left(\frac{d}{d_0} \right) + X_{\sigma_1}, \quad d_0 < d < d_c \quad (6.1.1)$$

$$P(d) = P(d_0) - 10y_1 \log_{10} \left(\frac{d}{d_0} \right) - 10y_2 \log_{10} \left(\frac{d}{d_0} \right) + X_{\sigma_2}, \quad d > d_c$$

where $P(d)$ is received signal strength at distance d , $P(d_0)$ is its counterpart at reference distance. In the conventional flat earth model, d_c is taken to be the distance where the first Fresnel zone touches the ground and is referred to as the Fresnel distance. The distance for the first Fresnel zone can be calculated as:

$$d_F = \frac{4h_T h_R}{\lambda} \quad (6.1.2)$$

where h_T and h_R are antenna heights of the transmitter and the receiver, respectively, while λ is the wavelength of the electromagnetic wave at 5.9 GHz. The heights of the antennas can be set at a usually vehicle height between 1.50 to 2 meters, giving a Fresnel distance of 225 m. The results of a piecewise linear fit the measurement as is possible to see in(Figure 74). As indicated by the standard deviations, the dual-slope models generally fit the data more accurately. We found that placing the breakpoint at the theoretical Fresnel distance of 225 m results in larger standard deviation values than those obtained with a critical distance of 100 m, implying a poorer fit. A critical distance less than the Fresnel distance may be caused by the presence of vehicles, pedestrians and other objects on the road creating reflections from points higher than the ground. In this case the houses and buildings between the vehicles increased the attenuation and intermittently obstructed the line-of-sight. This observation suggests the desirability of a multi-state model, with different states being applicable when a line-of-sight does and does not exist between the vehicles. In classical propagation models, the log-normal model is a statistical description of random variations in signal strength that are observed over distances large compared to a wavelength and are the result of scattering by and transmission through multiple objects and obstructions. This large-scale fading, referred to as shadowing, is distinct from the small-scale fading that occurs on the scale of a wavelength and results from interference between multipath components.

The total fading observed is generally a combination of these two effects. Due to the small distance scales and dominance of the line-of-sight component in V2V channels, it is likely that the fading is dominated by small-scale fading with very little shadowing. In this case X_σ is actually not a Gaussian random variable, but rather has statistics determined by the small-scale fading.

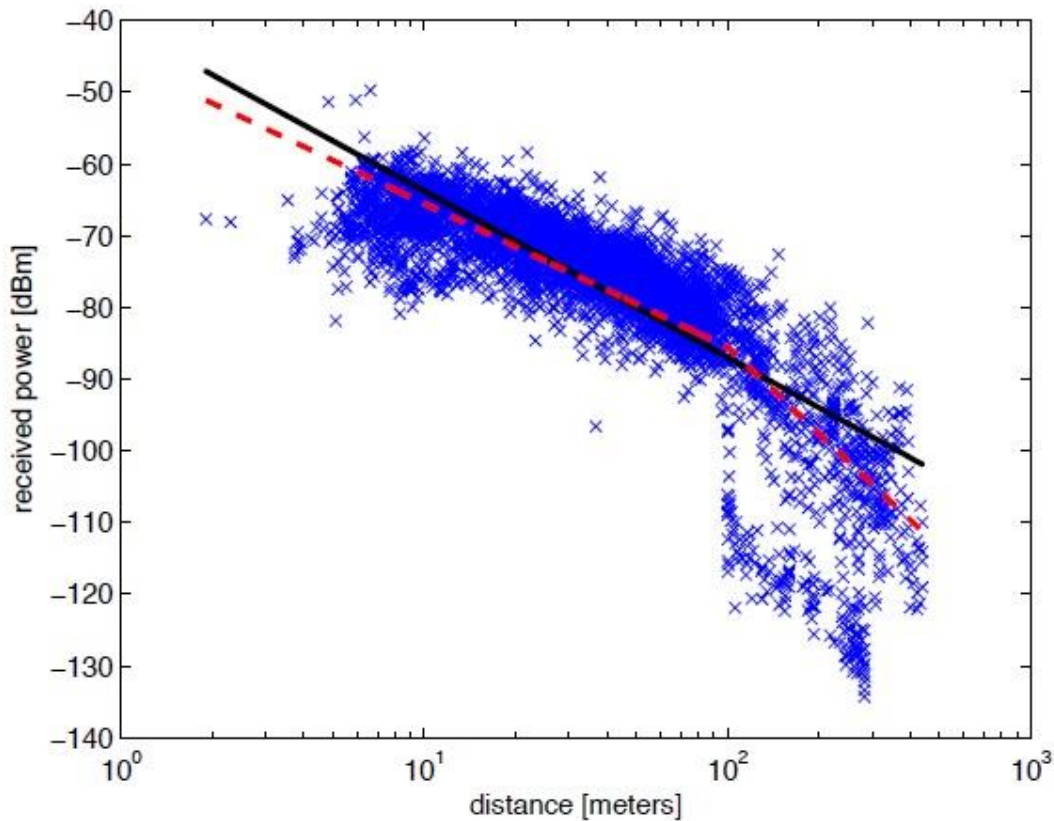


Figure 63: receiver power as a function of the distance in IEEE 802.11p system

6.2 Ns-3 simulator

The ns-3 simulator is a discrete-event network simulator targeted primarily for research and educational use. The project, started in 2006, is an open-source project developing ns-3. Ns-3 is open-source so all the project still maintain an open environment for researchers to contribute and share their software.

It is a new simulator written in C++ and it is not an extension of ns-2. Ns-3 has been developed to provide an open, extensible network simulation platform, for networking research and education. It provides models of how packet data networks work and perform and provide a simulation engine for users to conduct simulation experiments. Many simulation tools exist for network simulation studies ns-3 is designed as a set of libraries that can be combined together and also with other external software libraries. While some simulation platforms provide users with a single, integrated graphical user interface environment in which all tasks are carried out, ns-3 is more modular in this regard. Several external animators, data analysis and visualization tools can be used with ns-3. However, users should expect to work at the command line and with C++ and/or Python software development tools. Complex software systems need some way to manage the organization and changes to the underlying code and documentation. The ns-3 project uses Mercurial as its source code management system. Once you have source code downloaded to your local system, you will need to compile that source to produce usable programs.

Recently these systems have been developed using the Python language. The build system Waf is used on the ns-3 project, in (Figure 64) is shown how is simple to compile an example. With a simple code line, the Waf system build the project. It is one of the new generation of Python-based build systems. In (Figure 65) [106] is shows the software organization of ns-3. ns-3 is built as a library which may be statically or dynamically linked to a C++ main program that defines the simulation topology and starts the simulator. ns-3 also exports nearly all of its API to Python, allowing Python programs to import an “ns3” module in much the same way as the ns-3 library is linked by executable in C++.

```
cdj@cdj-VirtualBox: ~/workspace/ns-3-dev/ns-allinone-3.19/ns-3.19
cdj@cdj-VirtualBox:~$ cd workspace/
cdj@cdj-VirtualBox:~/workspace$ cd ns-3-dev/
cdj@cdj-VirtualBox:~/workspace/ns-3-dev$ cd ns-allinone-3.19/
cdj@cdj-VirtualBox:~/workspace/ns-3-dev/ns-allinone-3.19$ cd ns-3.19/
cdj@cdj-VirtualBox:~/workspace/ns-3-dev/ns-allinone-3.19/ns-3.19$ ./waf --run vl
cmtx
Waf: Entering directory `/home/cdj/workspace/ns-3-dev/ns-allinone-3.19/ns-3.19/b
uild'
Waf: Leaving directory `/home/cdj/workspace/ns-3-dev/ns-allinone-3.19/ns-3.19/bu
ild'
'build' finished successfully (4.527s)
```

Figure 64: building example with the build system Waf.

The source code for ns-3 is mostly organized in the src directory and can be described by the diagram in Software organization of ns-3. We will work our way from the bottom up. The simulation core is implemented in src/core. Packets are fundamental objects in a network simulator and are implemented in src/network. These two simulation modules by themselves are intended to comprise a generic simulation core that can be used by different kinds of networks.

The above modules of ns-3 are independent of specific network and device models.

Ns-3 programs may access all of the API directly or may make use of a so-called helper API that provides convenient wrappers or encapsulation of low-level API calls. The fact that ns-3 programs can be written to a combination of APIs is a fundamental aspect of the simulator.

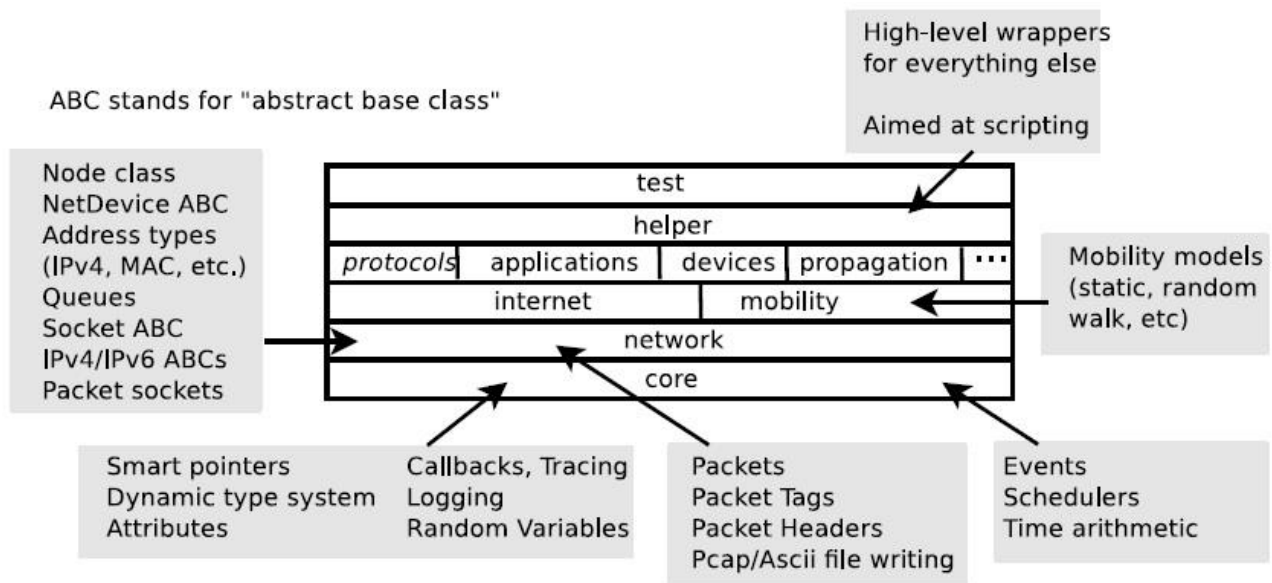


Figure 65: ns-3 software organization

Conceptually, the simulator keeps track of a number of events that are scheduled to execute at a specified simulation time.

The job of the simulator is to execute the events in sequential time order. Once the completion of an event occurs, the simulator will move to the next event.

To make this all happen, the simulator needs a few things:

- a simulator object that can access an event queue where events are stored and that can manage the execution of events;
- a scheduler responsible for inserting and removing events from the queue;
- a way to represent simulation time;
- the events themselves.

The Simulator class is the public entry point to access event scheduling facilities. Once a couple of events have been scheduled to start the simulation, the user can start to execute them by entering the simulator main loop (call Simulator::Run).

Once the main loop starts running, it will sequentially execute all scheduled events in order from oldest to most recent until there are either no more events left in the event queue or `Simulator::Stop` has been called.

To schedule events for execution by the simulator main loop, the `Simulator` class provides the `Simulator::Schedule*` family of functions.

The `Simulator` API was designed to make it really simple to schedule most events.

It provides three variants to do so:

- `Schedule` methods which allow you to schedule an event in the future by providing the delay between the current simulation time and the expiration date of the target event;
- `ScheduleNow` methods which allow you to schedule an event for the current simulation time: they will execute `_after_` the current event is finished executing but `_before_` the simulation time is changed for the next event;
- `ScheduleDestroy` methods which allow you to hook in the shutdown process of the `Simulator` to cleanup simulation resources: every ‘destroy’ event is executed when the user calls the `Simulator::Destroy` method;

There are two basic ways to schedule events, with and without context. Readers who invest time and effort in developing or using a non-trivial simulation model will know the value of the ns-3 logging framework to debug simple and complex simulations alike.

One of the important features that is provided by this logging framework is the automatic display of the network node id associated with the ‘currently’ running event.

The node id of the currently executing network node is in fact tracked by the `Simulator` class.

In some cases, most notably when simulating the transmission of a packet from a node to another, this behaviour is undesirable since the expected context of the reception event is that of the receiving node, not the sending node. It is possible also to visualize the result graphically with `NetAnim`. `NetAnim` support ns-3 and help the user to visualize the creating network, it is an offline animator based on the Qt 4 toolkit.

It currently animates the simulation using an XML trace file collected during simulation.

To create the xml file three simple step must be performed:

- Ensure that your wscript includes the "netanim" module;
- include the header [#include "ns3/netanim-module.h"] in your test program;
- Add the statement "AnimationInterface anim ("animation.xml");" before Simulator::Run().

It is possible to launch NetAnim from the command prompt, as is shown in (Figure 66).

```
91cdj@cdj-VirtualBox:~/workspace/ns-3-dev/ns-allinone-3.19/ns-3.19$ cd ..  
cdj@cdj-VirtualBox:~/workspace/ns-3-dev/ns-allinone-3.19$ cd netanim-3.104/  
cdj@cdj-VirtualBox:~/workspace/ns-3-dev/ns-allinone-3.19/netanim-3.104$ ./NetAnim  
m
```

Figure 66: launch NetAnim from the command prompt.

When NetAnim starts, it is possible to open the xml file and visualize your network implementation.

As you can see in (Figure 67), NetAnim shows the nodes in a grid in order to know the node's positions and it is possible to know also other parameters related to the nodes simply by clicking on stats as is shows in (Figure 68). From this panel is possible to:

- Set the position of the node;
- Set the color of the node;
- Enable the display of the node-trajectory;
- Set the list of IP address and Mac address combinations;

- Set any unit32 or double counters associated with the node;
- Set a custom icon for the node;
- Set the size of the node;
- Set a custom background;
- Reload the trace file;
- Tracking the route table;
- Parsing the flow-monitor xml output;
- Tracking node counter;
- View packet timeline;
- Visualize the battery level of the nodes.

Pressing the start button it is possible to launch the visualization of the application.

The message that are sent over the channel are visualize as blue lines, as (Figure 69) shows. The choice of using a simulator is given by the fact that with simulator is possible to create any environment and reproduce any possible scenario thanking into account any possible variation of that. We can use any kind of distribution to set the movement of the vehicles, we can take into account rain or fog or any environment circumstances, we can see the difference between the LoS system or the presence of a obstruction such as (objects, houses, cars, skyscraper). ns-3 has been chosen because it is a very important and widely used open software. Its widespread use can help the introduction and the sharing of the VLC systems to many users. The VLC is not implemented in ns-3, opening the possibility to publish and distribute this module.

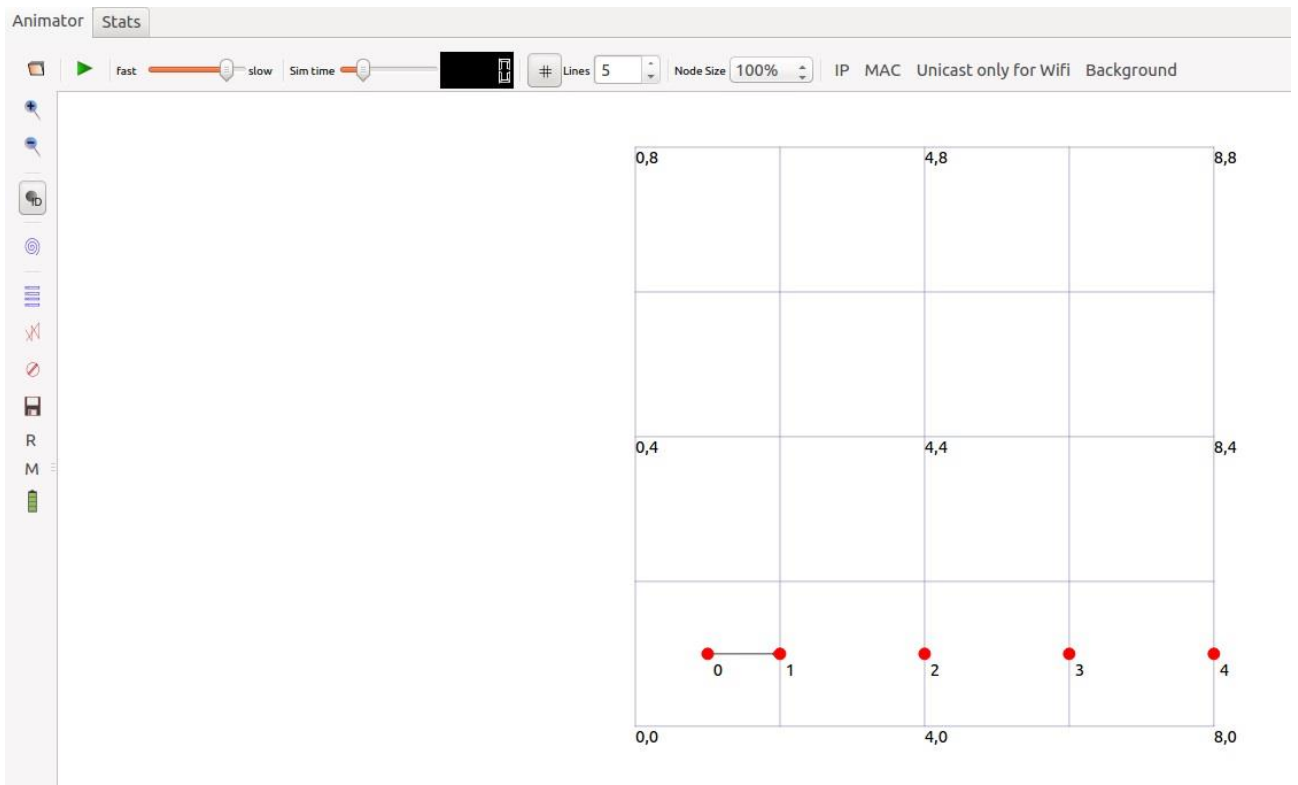


Figure 67: NetAnim panel

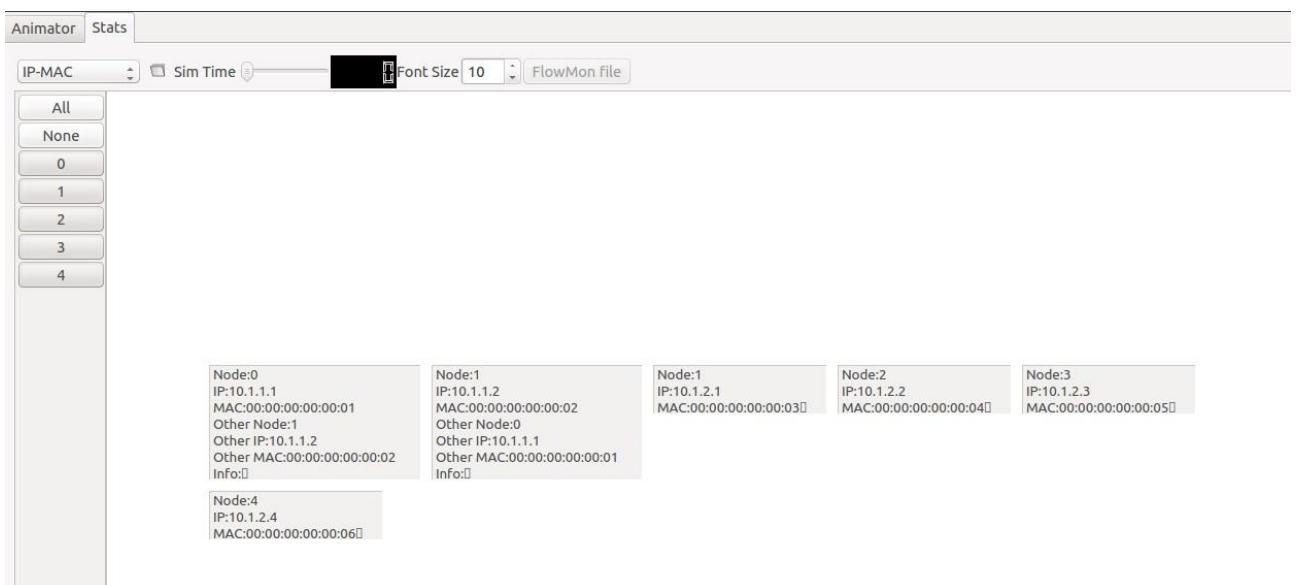


Figure 68: visualization of nodes' characteristic in NetAnim

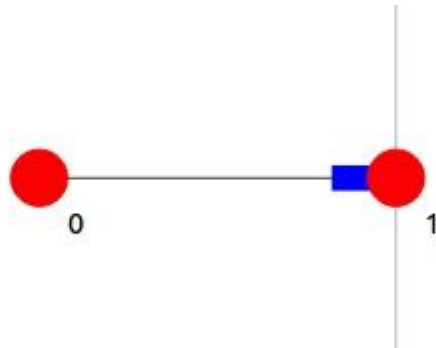


Figure 69: “blue” representation of a packet in NetAnim

6.3 Implementation of VLC in ns-3

In this chapter, the implementation of the VLC module in NS-3 is described. It reproduces a vehicular network scenario and uses the VLC communication in order to change the messages. Let's see how it is implemented. In order to create a realistic scenario, the program can take in input a digital map of the environment.

in (Figure 70) is possible to see a bitmap of the city of Bologna, while (Figure 71) shows digital representation of the top of the map (use in my example), in which “1s” represent road and “0s” represent building.



Figure 70: map of Bologna.

8500, 10300, 8000, 9600, 5

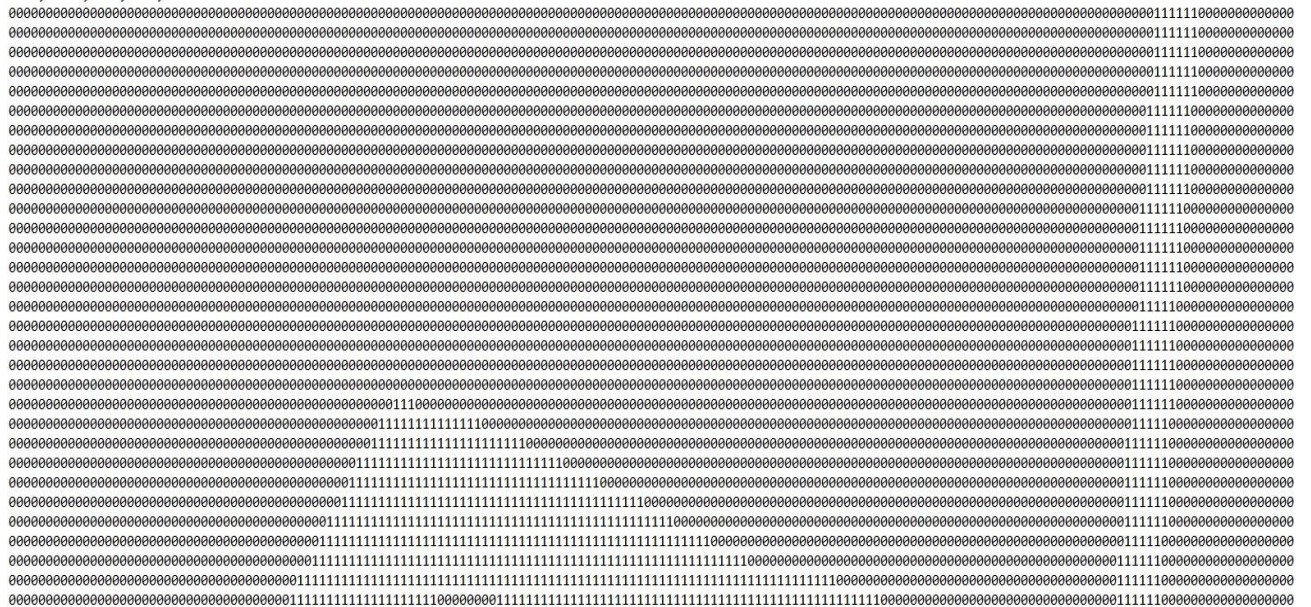


Figure 71: digital map of Bologna.

In the first row of (Figure 71) is possible to see that some values are present. These values indicate, respectively, the minimum and the maximum values of the x coordinate, the minimum and maximum values of y coordinate and the square size of the land represented from one bit. In this way, the function that read the file has a starting point to know how to create the map. To set the position of the vehicles the “SetPositionAllocator” module is used, but instead to use a mobility model, the variation of the cars’ positions is taken by an input text file. The input text file is created by the WiLAB group and reproduce realistic movement of the vehicles in the city of Bologna. as shown in (Figure 72) the text input file contain the time instant that change every second, the vehicle identification and its Cartesian coordinate at that relative instant of time. With that file we can reproduce a usually change of traffic in our environment. The vehicle are insert as a rectangle of a certain length and width; because of this parameters it is possible to set in front and back a visibility angle that can be modified depending on the transceiver structure to be simulated. The program take into account also the last position before the actual one in order to know the direction of vehicles. In this way it can know if the two vehicles are in visibility or not. In (Figure 73) are shown two examples apparently identical in which red points represent vehicles, while in (Figure 74) is shown how is important to know the vehicles’ direction.

| | | | |
|----|-----|-------|------|
| 17 | 545 | 10254 | 8009 |
| 17 | 417 | 9833 | 9102 |
| 17 | 157 | 9344 | 8938 |
| 17 | 33 | 9260 | 8966 |
| 17 | 251 | 9992 | 9067 |
| 17 | 205 | 9932 | 9096 |
| 17 | 153 | 9907 | 9108 |
| 17 | 252 | 9958 | 9087 |
| 17 | 154 | 9936 | 9098 |
| 17 | 278 | 9883 | 9124 |
| 18 | 321 | 8555 | 9288 |
| 18 | 350 | 8611 | 8371 |
| 18 | 332 | 8630 | 8433 |
| 18 | 282 | 8624 | 9083 |
| 18 | 478 | 8627 | 9386 |
| 18 | 165 | 8674 | 8732 |
| 18 | 151 | 8718 | 8722 |

Time instant

Vehicle id

(x, y) coordinate

Figure 72: vehicles input file



Figure 73: two equal example of vehicular networks

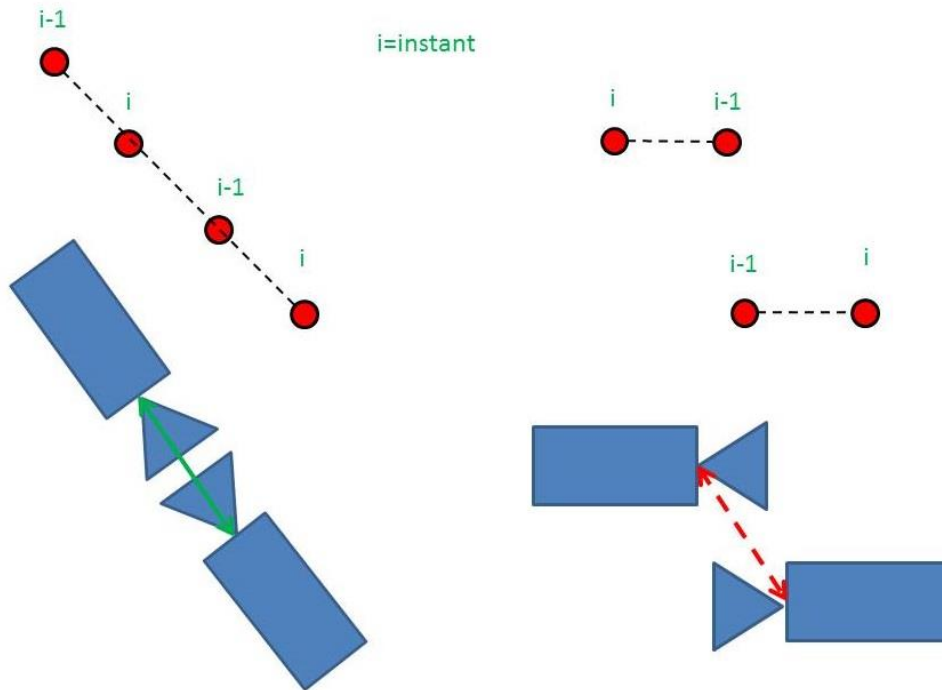


Figure 74: two examples of vehicular systems with VLC.

As we can see, in the first example of (Figure 74) the two vehicles are in communication, while in the second one no because of its directivity. In the program, it is used an optimal placement of LEDs in a circular ring array pattern, so the channel is realized taking into account the channel gain that we have seen in (Figure 32) that it is discrete as is shown in (Figure 75). The continuous line represent the theoretical characterization of the channel, while the dotted line represent the implementation of the theoretical curve in the simulator.

As we can see the two curves are very close one with the other. Setting the transmission power and the receiver sensitivity, the program can evaluate if the two nodes can see one with the other. In this example the transmission gain is set at 0 dBm and the receiver sensitivity at -30 dBm, in order to create a realistic representation and have distance range of 20 meters. With that kind of structure that we use in the example, a range of 20 meters result optimal in order to maintain a BER less than 10^{-4} also with direct

sun light, have a percentage of received packets close to 100 percent, without synchronization losses as shown in (Figure 76) [12].

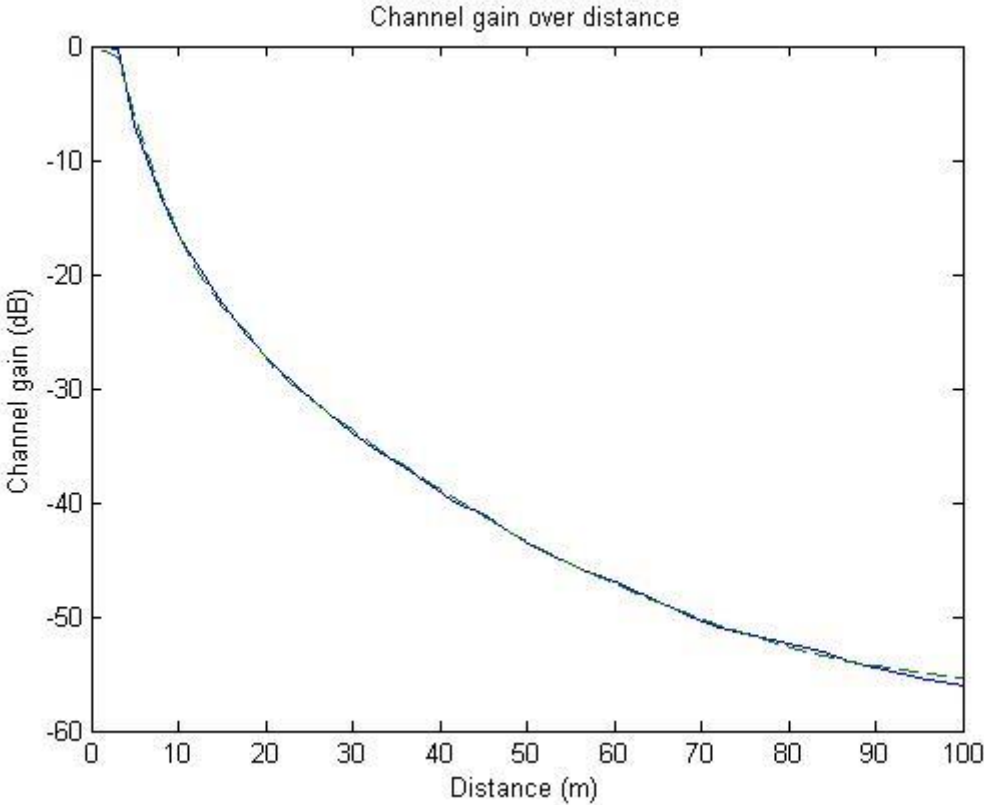


Figure 75: channel gain of the VLC simulation system.

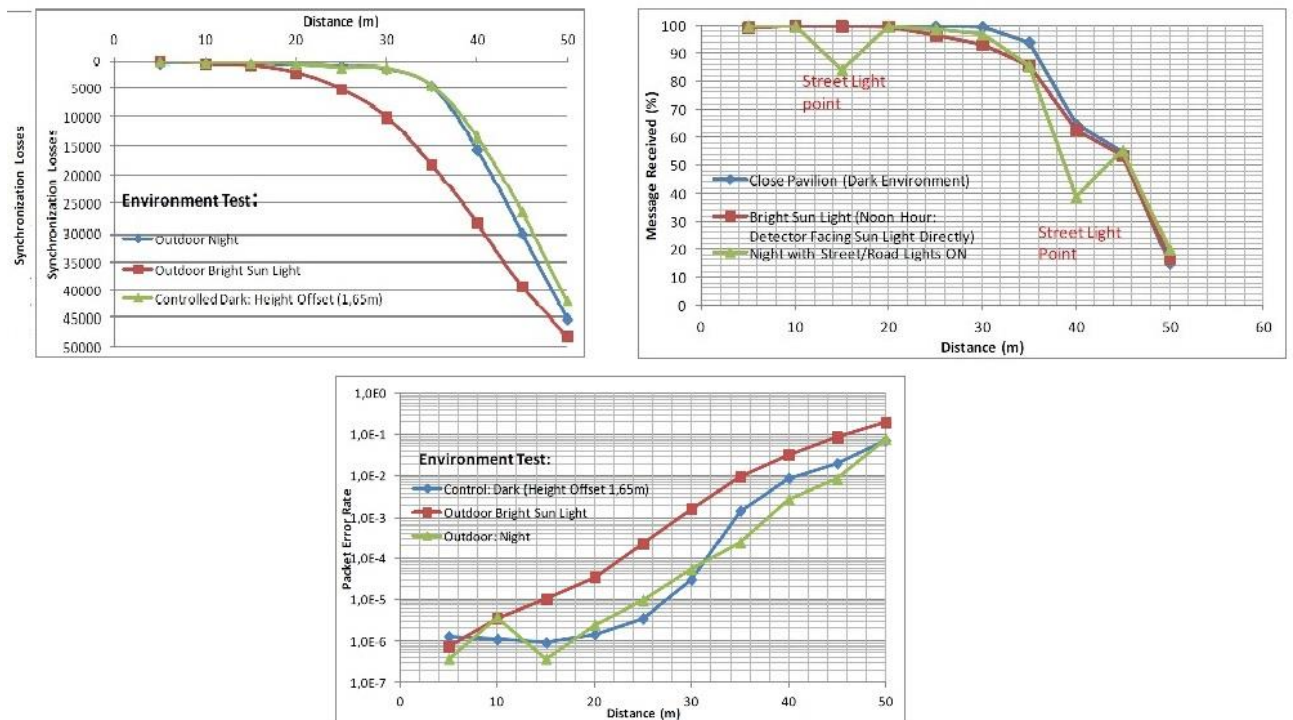


Figure 76: characteristic of our example.

Each node is virtually connected with the other nodes that can be in visibility, using the well know Cartesian equation of the straight line in explicit form:

$$y = mx + q \quad (6.3.1)$$

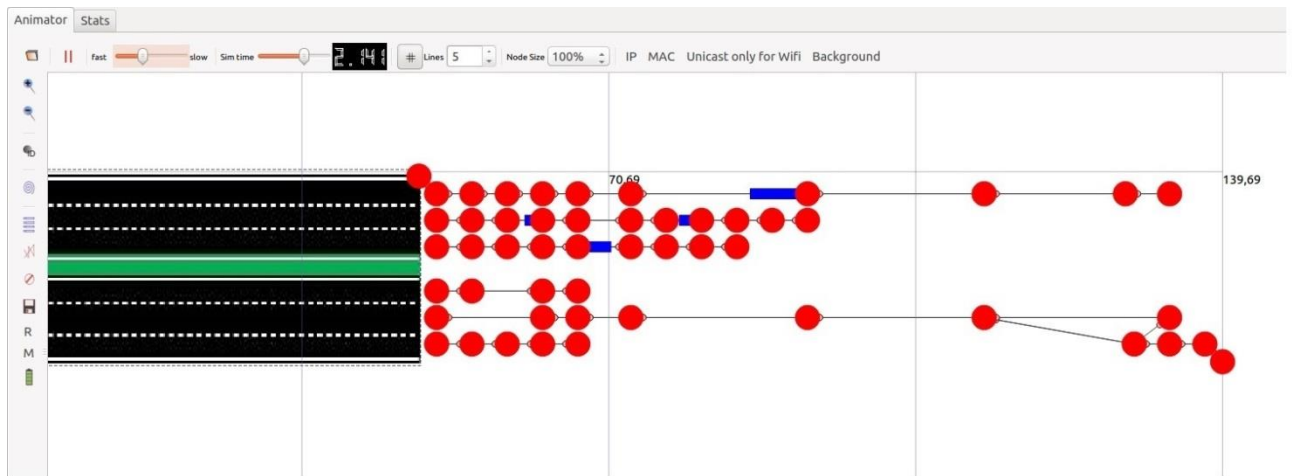
$$\text{angular coefficient: } m = \frac{y_2 - y_1}{x_2 - x_1} \quad (6.3.2)$$

$$\text{known term: } q = \frac{x_2 y_1 - x_1 y_2}{x_2 - x_1} \quad (6.3.3)$$

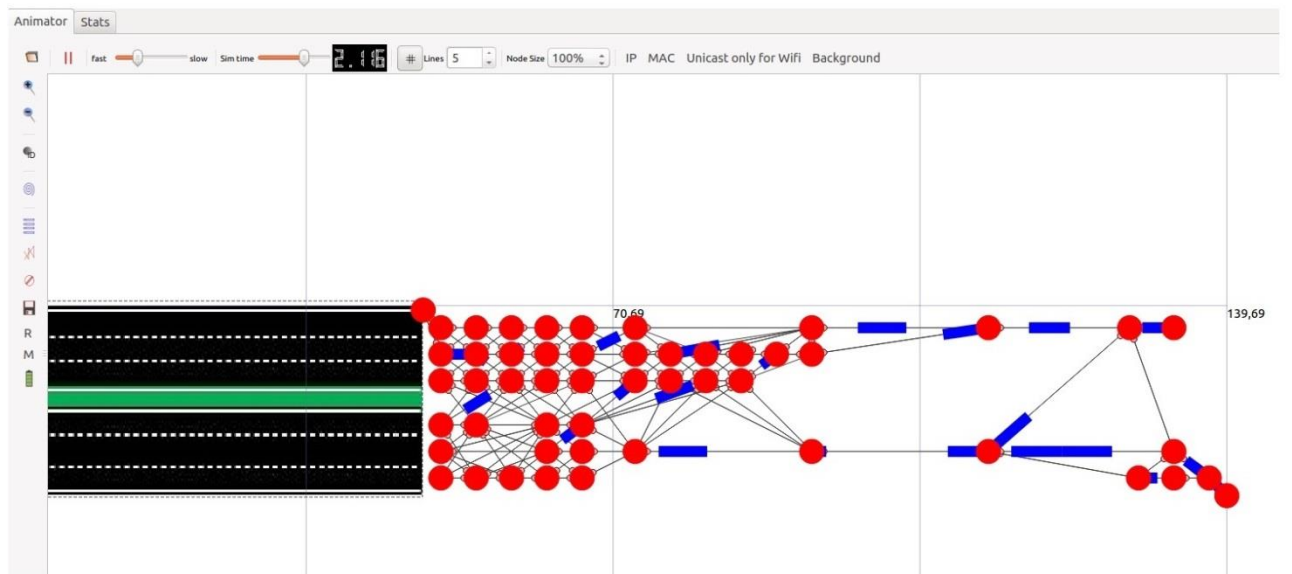
where x_1 and y_1 are respectively the x and y coordinate of a generic node, and x_2 and y_2 are respectively the x and y coordinate of another node that is in

visibility with the first. If $x_2 = x_1$ the virtual connection will be created on the vertical direction. Moving iteratively on this virtual connection and using the map of the city, in which is present if there is a road or a building, and knowing the position of the other vehicles using the position allocator, the simulator can also evaluate if the nodes remain in visibility or if there is a vehicle or a building in between. The study of the VLC in vehicular system with that program was performed with a realistic motion of 670 vehicles on average per instant. Before to show the result of the simulation in order to better see the potential of ns-3, a simple example with 51 vehicles was performed. As we have seen before, NetAnim support ns-3 for the visualization of the created network system.

With the simple example of 51 vehicles we can have a better visualization of the actual program, instead to have 670 vehicles deployed over Bologna's map, and seeing in a simple way how it work. The simulation was performed varying the visibility angle of the transceiver and some measurement are taken for 30° , 60° , 90° , 120° and 150° . (Figure 77) is possible to see the visualization of the networks with a visibility angle of 30° (Figure 77(a)) and 150° (Figure 77(b)). The street on the left can help to understand our environment without create an overlapping with the connection. As we can see, the number of connection with visibility angle of 30° are more less than the number of connection with a visibility angle of 150° . In both examples all devices are connected, so they can exchange information without use other networks. In this way it is possible to offload the cellular network, without send other information in a network already overload.



(a)



(b)

Figure 77: example of VLC in vehicular networks implemented in ns-3 with (a) visible angle equal to 30° , (b) visible angle equal to 150° .

The two snapshots are taken at a certain instant of time in which some packets were transmitted. In (Figure 78) is shown the number of connection between the nodes as a function of the visibility angle. As it is supposed the number of connection increase, increasing the visibility angle. In the graph is possible to

see how the curve increase rapidly until 90° while next increase very slowly. This is given by the fact that in the example we have an urban environment in with two tail are formed. When two vehicles are very close with other, the vertical and the horizontal distance are similar respect a vehicles in the near lane.

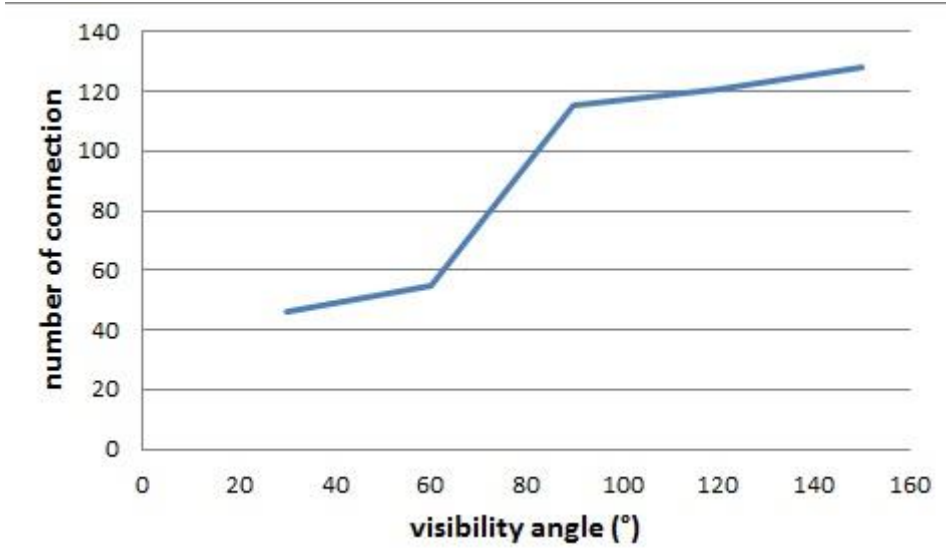


Figure 78: number of connection as a function of visibility angle.

As we can see in (Figure 79), that implies that the angle in between is equal to 45° that is the half of 90° of our consideration case, when the vehicles are in movement the horizontal distance increase respect the vertical one and so the angle decrease. Therefore, with a visibility angle of 90° we can cover all the neighbour vehicles in a very huge environment, while in other cases the angle in between cars' headlight are smaller. In (Figure 80), is shows the average number of neighbour as a function of the visibility angle, while in (Figure 81) is shown the cumulative distribution function (cdf) for different values of the visibility angle.

As we can see, the cumulative distribution function reach the one very fast for small values of visible angle respect the cumulative distribution function created with 150° of visibility angle that reach it at 12.

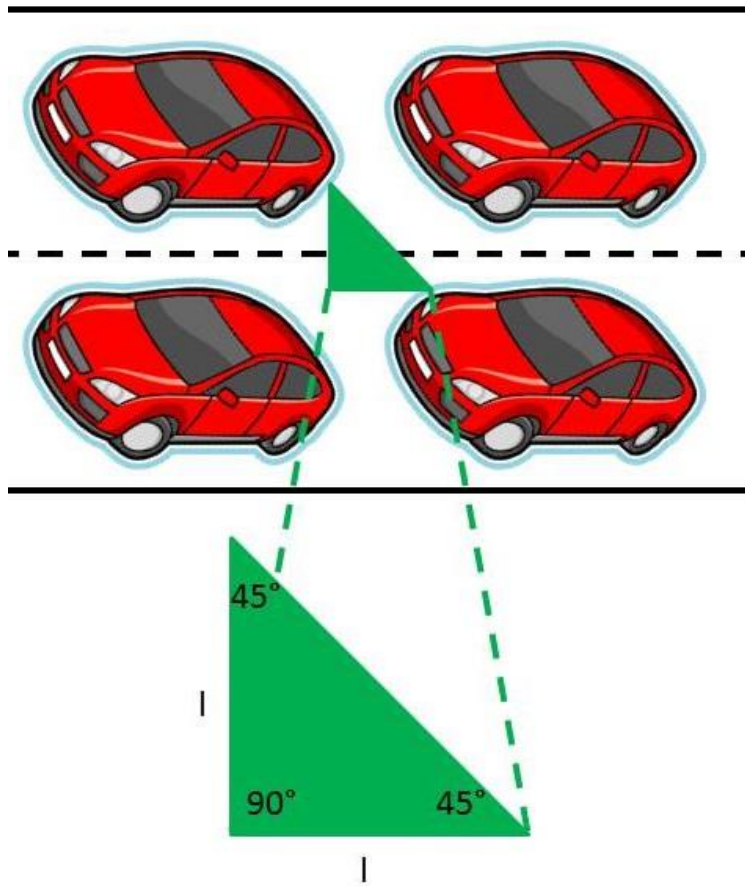


Figure 79: angle in between two near vehicles.

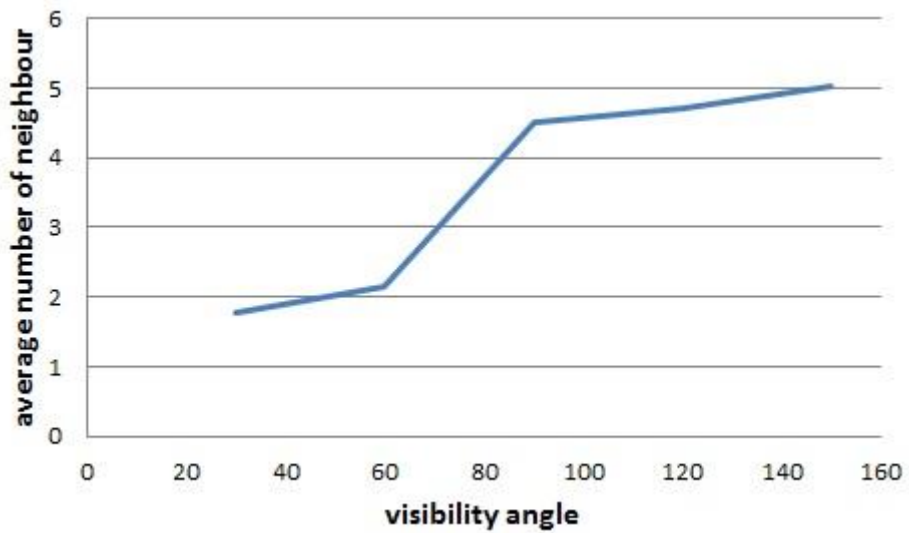


Figure 80: average number of neighbour as a function of visibility angle for 51 vehicles.

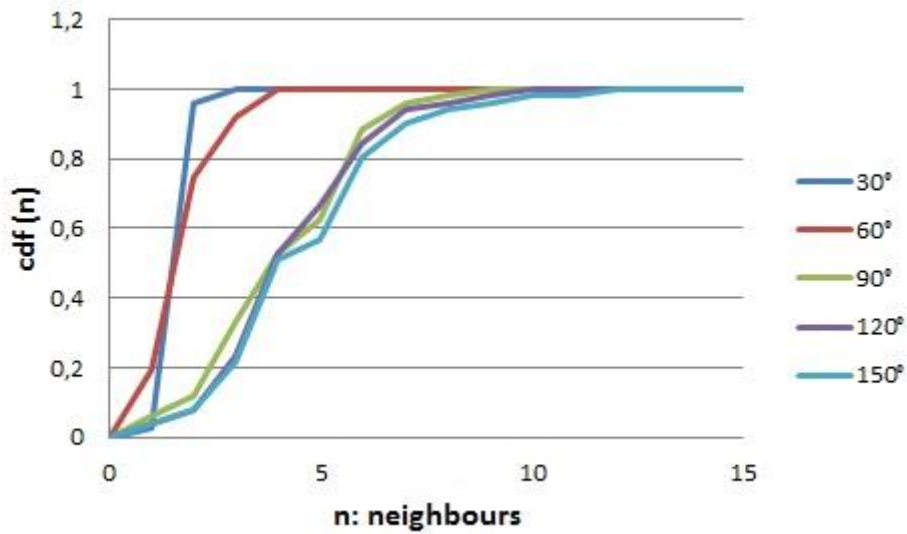


Figure 81: cumulative distribute function for different values of visibility angle with 51 vehicles.

The second example was performed with 670 vehicular in average distributed on the city of Bologna. The number of connection and the average number of neighbours are shown respectively in (Figure 82) and (Figure 83), while (Figure 84) shows the cdf in that particular case. Similar consideration respect the simple case can be done also in these graphs, but it better to shows some comparison in order to better understand the differences in a more complete scenario respect the simpler one.

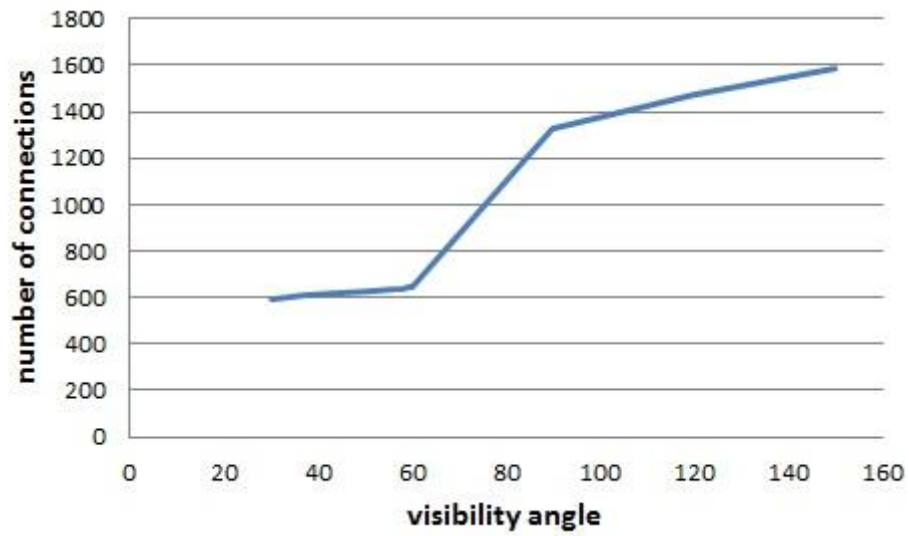


Figure 82: number of connection as a function of visibility angle.

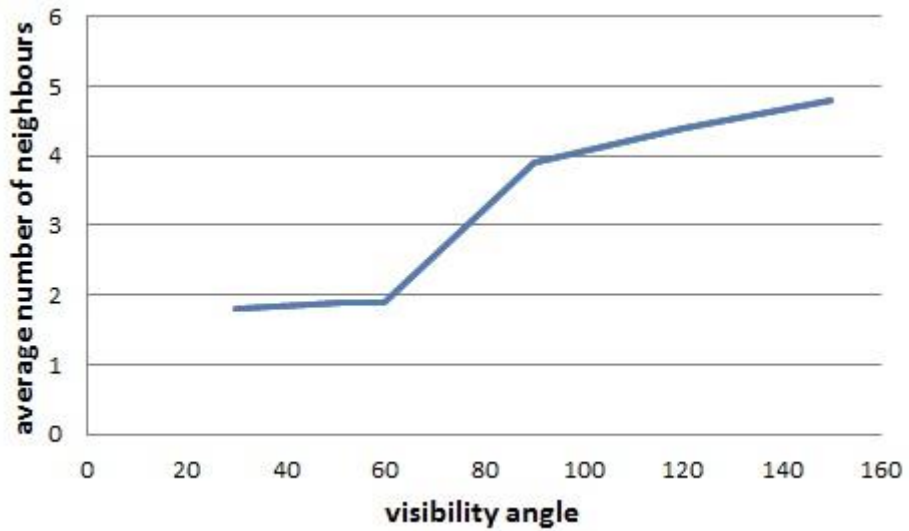


Figure 83: average number of neighbours as a function of visibility angle.

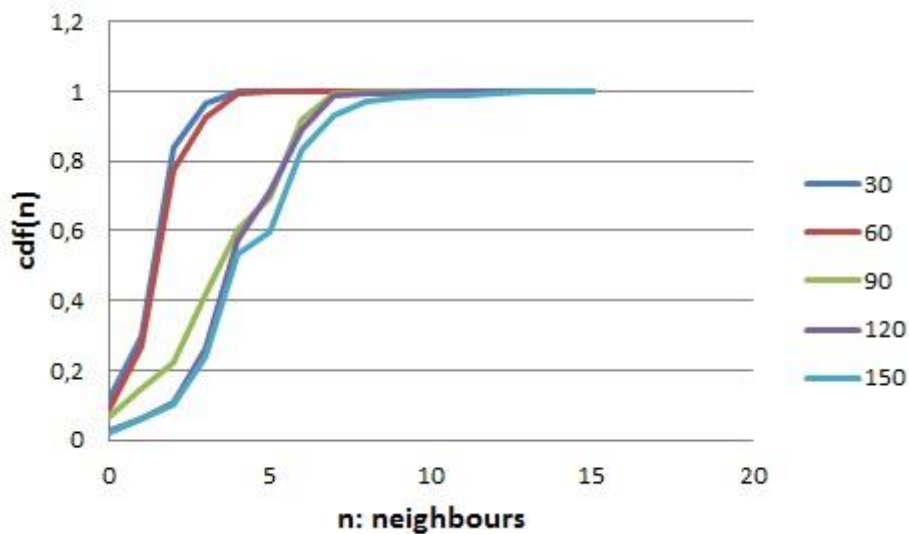


Figure 84 cumulative distribute function for different values of visibility angle with 670 vehicles.

As was expected the average number of neighbour is slightly greater as is shows in (Figure 85); because of its simple and better environment in which many nodes are near and no one has not connection with nearby vehicles. The difference between the two envelopes are not so wide, in fact the two curves are very close one with the other. The average number of neighbours result less than a typical IEEE 802.11p system. We must not forget that this neighbour are really neighbour because with the characteristic of this system, as we have seen before, we have no packet loss. In addition, using VLC there are not collision and the packet can be forwarding in a multi-hopping topology. To confirm the similarities of the two system, also the cumulative distribution functions are very close (Figure 86). The biggest difference is given by the starting points, because in the simple example of 51 vehicles all the vehicles can communicate with at least another, while in the real environment some communication cannot exist.

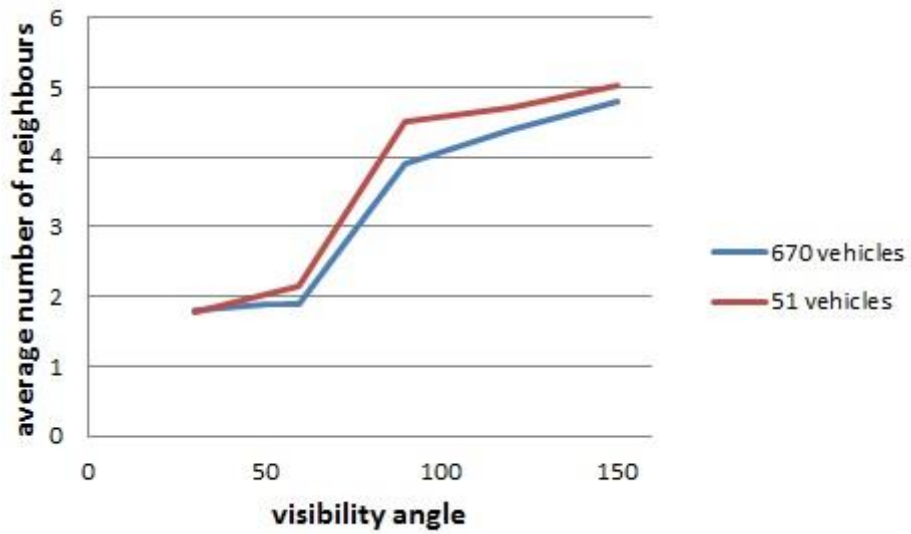


Figure 85: average number of neighbour comparison between the two applications.

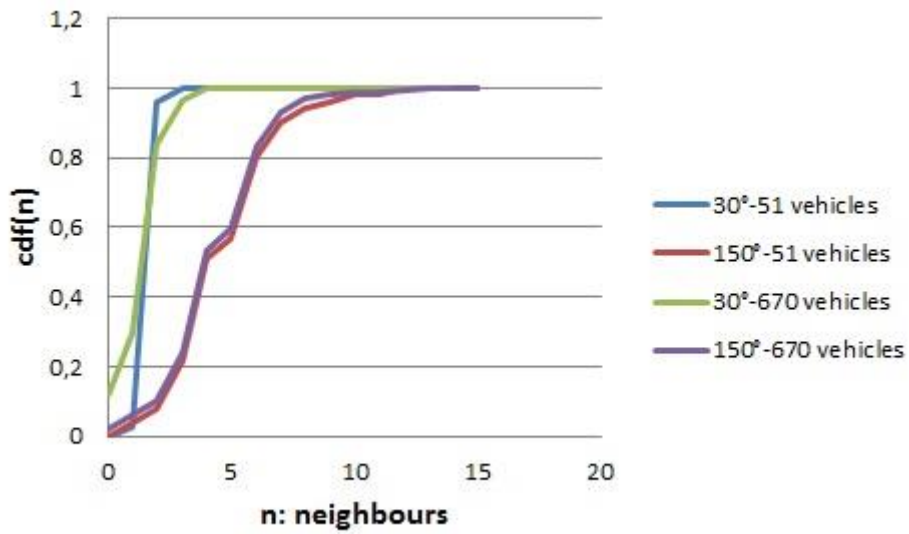


Figure 86: comparison of the cdf between the two applications.

6.4 Comparison between VLC in vehicular networks and IEEE 802.11p systems

A simulation of IEEE 802.11p system was performed in WiLab laboratory with SHINE. SHINE stands for simulation platform for heterogeneous interworking networks and allows to simulate different technology considering all the network characteristics and access technology peculiarity. Taking into account all the consideration about IEEE 802.11p seen in previous section, it was set a receiver power equal to -70dB and -85dB in order to obtain a transmission range respectively of 50 and 200 meters. The same application of Bologna was performed and the cumulative distribution function of this application is shown in (Figure 87). Also, with the IEEE 802.11p is possible to see how the cumulative distribution function reach the one much earlier respect the transmission range.

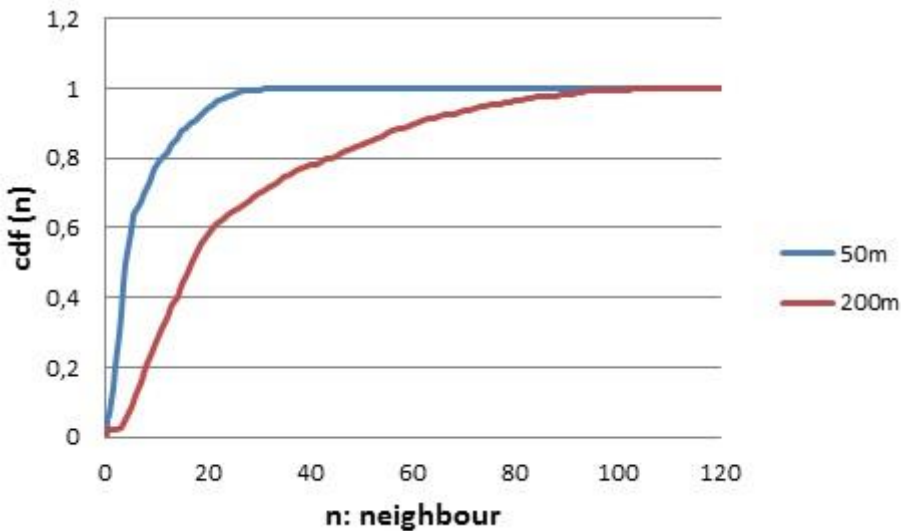


Figure 87: cumulative distribution function given by the Shine’s simulation.

A comparison between the IEEE802.11p and the VLC communication is shown in (Figure 88). The figure shows that the IEEE 802.11p performs a little better respect the VLC systems in term of cdf, but the VLC are not so far respect this standard. The factor that penalizes the VLCs in this graph is given by the fact

that they need the visibility in order to communicate. Anyway, seeing that the cdf of the VLC is not far to the one of the more focalised standard in vehicular system, the visible light communication systems can be considered as an optimal solution in vehicular systems. As mentioned before, the VLC communications do not suffer of collision situation and do not overload other wireless systems (as WiFi or LTE) that are already overloaded. However a combination of the two systems can be used, in order to do not overload the system (using as VLC as a primary solution) and do not having reception problems in hidden places.

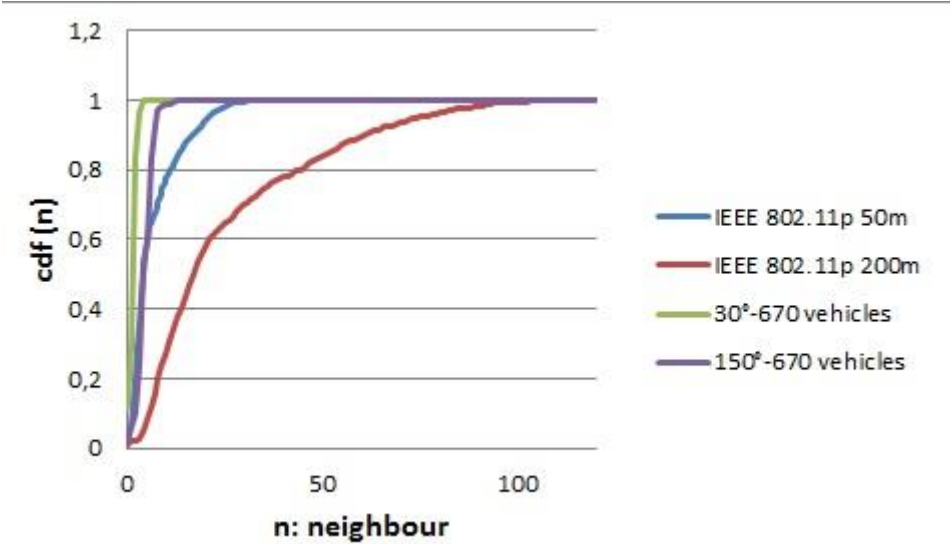


Figure 88: comparison of cdf between IEEE 802.11p and VLC communication system.

CHAPTER 7: CONCLUSION

The great importance of vehicular networks and the increasing of connected devices on board, allows new applications, but also foresees a huge use of connections, typically via cellular networks. This causes high loads and costs, opening new questions on the feasibility of short range communications in the short term to offload the cellular network.

WAVE/IEEE 802.11p is seen as the new standard for VANETs, but its development on board could be available only in the medium long term.

A new technology, based on light, can so be exploited as an alternative or an integration to 802.11p.

Thanks to high performance led development in cars' lights, VLC can be recognized as an important technology also for vehicular communications. In this thesis, after a brief introduction of ITS and vehicular networks, VLC technology in vehicular scenarios has been investigated. Its performance for short range communications among vehicles has been derived and compared with that of IEEE 802.11p in Bologna realistic scenario. Simulations have been performed through SHINE and NS3. Numerical results are encouraging, showing the high number of VLC connections that can be enabled in urban scenarios.

That system has not collision problems, allows to offload the cellular system and ensures the bit-rate in each connection instead to share the 3Mbps with all the vehicles in each group. Therefore, the designed VLC system can be effectively deployed and used in ITS to assist driver for safe driving on the road. Furthermore, with enhanced design as discussed before, the service area can be increased. Therefore, VLC systems are not only suitable for the novel applications of road traffic safety but also identify itself to be an integral part of ITS. In fact, VLC is a new emerging technology and has huge applications in the outdoor as well as indoor. The area needs to be explored to take full advantage of its unprecedented bandwidth and ubiquitous availability. It should take full advantage of advancement of LED technology.

TABLE OF FIGURES

- Figure 1: ITS architecture.11
- Figure 2: ITS communication architecture12
- Figure 3: V2V communication16
- Figure 4: C2C communication with wired backbone.16
- Figure 5:V2I communication17
- Figure 6: C2C-CC architecture18
- Figure 7: VLC application26
- Figure 8: VLC applications27
- Figure 9: VLC wavelength29
- Figure 10: VLC system architecture.....32
- Figure 11: Receiver proprieties.35
- Figure 12: coloured LEDs.....37
- Figure 13: VLC with LEDs38
- Figure 14: LED components.....40
- Figure 15: LEDs configurations41
- Figure 16: LEDs MIMO examples.....42
- Figure 17: PDs as VLC receiver.....44
- Figure 18: Measure VS Perceived light.....45
- Figure 19: minimum maintained red signal luminosity.....50
- Figure 20: minimum maintained signal luminosity for red, green and yellow LEDs.....51
- Figure 21: Lambertian emitter source.....52
- Figure 22: radiation lobe.53
- Figure 23: normalized radiation lobe.53
- Figure 24: schematic circuit with HB-LEDs and power LEDs that provide 1050 lm.54
- Figure 25: Cartesian representation of a source emitter55
- Figure 26: Array arrangement: (a) square; (b) triangular; (c) circular.....56
- Figure 27: LEDs circular rings.....58
- Figure 28: Multilane traffic system60
- Figure 29: SNR as a function of distance61
- Figure 30: (a) capacity as a function of signalling rate; (b) capacity as a function of illumination level.....62
- Figure 31: (a)(c) no direct link examples; (b) propagation losses as a function of horizontal distance.....64
- Figure 32: channel gain over the distance for a transmitter constitute by an array LEDs.....66
- Figure 33: frequency response of the channel, varying the optical depth.68
- Figure 34: OOK frame’s structure.....71
- Figure 35: examples of VPPM signals.....74
- Figure 36: 4B6B run length limiting code74
- Figure 37: examples of L-PPM and I-LPPM.....76

| | |
|---|-----|
| Figure 38: IEEE standard colors for CSK | 78 |
| Figure 39: example of CSK constellation | 79 |
| Figure 40: optical power of LEDs..... | 82 |
| Figure 41: VLC and RF systems cells comparison. | 83 |
| Figure 42: required average power for BER 10⁻⁶ with different data rate. | 84 |
| Figure 43: bit error rate over (a) SNR and (b) optical signal to noise ration. | 85 |
| Figure 44: bit error rate over signal-to-noise ratio in presence of external interference. | 86 |
| Figure 45:example of optical Femtocells | 87 |
| Figure 46: application of toys communication..... | 88 |
| Figure 47: application of people locating..... | 88 |
| Figure 48: application of hurricane’s warning signal. | 89 |
| Figure 49: smart cities application. | 90 |
| Figure 50: VLC as AP in a tunnel. | 90 |
| Figure 51: example of cellular offloading with VLC APs..... | 91 |
| Figure 52: submarine VLC application..... | 92 |
| Figure 53: examples of vehicular networks with VLC | 93 |
| Figure 54: VLC system application to help the walk of blind people. | 93 |
| Figure 55: example of vehicular networks with VLC systems. | 95 |
| Figure 56: vehicular scenario of visible light communication integrated with ITS | 97 |
| Figure 57: CSK system diagram for PHY III | 100 |
| Figure 58: Modulation domain spectrum for visible light communication..... | 101 |
| Figure 59: high resolution dimming with visibility pattern. | 102 |
| Figure 60: IEEE 802.15.7 data frame. | 105 |
| Figure 61: Saturation and non-saturation throughput for different window size..... | 109 |
| Figure 62: Average throughput for different window size..... | 110 |
| Figure 63: receiver power as a function of the distance in IEEE 802.11p system..... | 112 |
| Figure 64: building example with the build system Waf..... | 114 |
| Figure 65: ns-3 software organization..... | 115 |
| Figure 66: launch NetAnim from the command prompt. | 117 |
| Figure 67: NetAnim panel..... | 119 |
| Figure 68:visualization of nodes’ charachteristic in NetAnim..... | 119 |
| Figure 69: “blue” representation of a packet in NetAnim | 120 |
| Figure 70: map of Bologna. | 121 |
| Figure 71: digital map of Bologna | 121 |
| Figure 72: vehicles input file..... | 123 |
| Figure 73: two equal example of vehicular networks | 123 |
| Figure 74: two examples of vehicular systems with VLC. | 124 |
| Figure 75: channel gain of the VLC simulation system..... | 125 |
| Figure 76: characteristic of our example..... | 126 |

Figure 77: example of VLC in vehicular networks implemented in ns-3 with (a) visible angle equal to 30°, (b) visible angle equal to 150°.....128

Figure 78: number of connection as a function of visibility angle.129

Figure 79: angle in between two near vehicles.....130

Figure 80: average number of neighbour as a function of visibility angle for 51 vehicles.....130

Figure 81: cumulative distribute function for different values of visibility angle with 51 vehicles.131

Figure 82: number of connection as a function of visibility angle.132

Figure 83: average number of neighbours as a function of visibility angle.132

Figure 84 cumulative distribute function for different values of visibility angle with 670 vehicles.133

Figure 85: average number of neighbour comparison between the two applications.134

Figure 86: comparison of the cdf between the two applications.134

Figure 87: cumulative distribution function given by the Shine’s simulation.....135

Figure 88: comparison of cdf between IEEE 802.11p and VLC communication system.136

REFERENCES

- [1] The METIS project: “Mobile and wireless communications Enablers for the Twenty- twenty Information Society,” www.metis2020.com.
- [2] P. Demestichas, A. Georgakopoulos, D. Karvounas, K. Tsagkaris, V. Stavroulaki, Lu Jianmin, Chunshan Xiong and Jing Yao, "5G on the Horizon: Key Challenges for the Radio- Access Network," *Vehicular Technology Magazine, IEEE* , vol.8, no.3, pp.47,53, September 2013.
- [3] Cisco,“Whitepaper: Cisco visual networking index: Global mobile data traffic forecast update,” Cisco, Tech. Rep., February 2014.
- [4] D. Lopez-Perez *et al.*, “Enhanced Intercell Interference Coordination Challenges in Heterogeneous Networks,” *IEEE Wireless Commun.*, vol. 18, no. 3, pp. 22–30, June 2011.
- [5] World Health Organization, “Ten Causes of Death”, WHO, 2008.
- [6] ITS, “Intelligent Transportation Systems,” <http://www.its.dot.gov/research.htm>, 2010.
- [7] Y. Tanaka, S. Haruyama and M. Nakagawa, "Wireless optical transmissions with white coloured LED for wireless home links," in *PIMRC, The 11th IEEE International Symposium on Personal, Indoor and Mobile Radio Communications* , pp. 1325 – 1329, 2000.
- [8] M. S. Shur and R. Zukauskas, "Solid-State Lighting: Toward Superior Illumination," *Proceedings of the IEEE*, vol. 93, pp. 1691-1703, 2005.
- [9] IEEE 802.11p,“Wireless Access in Vehicular Environment (WAVE)”, IEEE, 2010.
- [10] S. Eichler, "Performance Evaluation of the IEEE 802.11p WAVE Communication Standard," in *Vehicular Technology Conference, VTC-2007 Fall, IEEE 66th*, pp. 2199-2203, 2007.

- [11] C2C, "Car 2 Car Communication Consortium." <http://www.car2car.org>, Car2X Communication System, 2008.
- [12] N. Kumar, "VISIBLE LIGHT COMMUNICATION VISIBLE LIGHT COMMUNICATION SYSTEMS FOR ROAD SAFETY APPLICATIONS," universidade de Aveiro, 2011.
- [13] CALM, "Communication Access for Land Mobile," <http://www.isotc204wg16.org/concept>, 2010.
- [14] COMeSafety, "Communication for eSafety," <http://www.comesafety.org/>, 2010.
- [15] K. Evensen, "Intelligent Transport Systems, European Standardization for ITS: WG2 Architecture," in *ETSI TC ITS Workshop*, Sophia Antipolis, 5 February 2009.
- [16] International Agency for Research on Cancer, World Health Organization, "IARC Classifies Radio Frequency Electromagnetic Fields as Possible Carcinogenic to Humans", Press Release No. 208, 31 May 2011.
- [17] S. Yousefi, E. Altman, R. El-Azouzi and M. Fathy, "Analytical Model for Connectivity in Vehicular Ad Hoc Networks," *IEEE Transactions on Vehicular Technology*, vol. 57, pp. 3341-3356, 2008.
- [18] P. Cencioni and R. Di Pietro, "VIPER: A vehicle-to-infrastructure communication privacy enforcement protocol," in *Mobile Adhoc and Sensor Systems, MASS'2007. IEEE International Conference*, pp. 1-6, 2007.
- [19] IETF, "Mobile AdHoc Networks (MANET)." <http://datatracker.ietf.org/wg/manet/>, 2011.
- [20] M. Raya and J.P. Hubaux, "Securing Vehicular Ad Hoc Networks," *Journal of Computer Security*, vol. 15, pp. 39-68, 2007.
- [21] Research and innovative technology administration (RITA), "DSRC: The Future of Safer Driving," http://www.its.dot.gov/factsheets/dsrc_factsheet.htm, 26 June 2014.

- [22] Car-to-Car communication consortium, <http://www.car-to-car.org>.
- [23] V. Vijayenthiran, “GM Participating In U.S. Car-To-Car Communications Trial,” 21 August 2012.
- [24] M. Rea, “*Illumination Engineering Society of North America (IESNA) Lighting Handbook*,” 9th ed., July 2000.
- [25] Car2Car Communication Consortium Manifesto, work in progress, May 2007.
- [26] H. Moustafa, S.M. Senouci and M. Jerby, “Vehicular Networks,” 10 November 2008.
- [27] M. Nekovee, “Sensor networks on the road: the promises and challenges of vehicular ad hoc networks and vehicular grids,” *In Proc. of the Workshop on Ubiquitous Computing and e-Research*, Edinburgh, U.K., May 2005.
- [28] J. Blum, A. Eskandarian and L. Hoffmman, “Challenges of intervehicle ad hoc networks,” *IEEE Trans. Intelligent Transportation Systems*, 4 December 2004.
- [29] Vehicle Safety Communications – Applications (VSC-A) Project, Final Report, DOT HS 811 073, January 2009.
- [30] O. K. Tonguz and G. Ferrari, “*Ad Hoc Wireless Networks: A Communication-Theoretic Perspective*”, John Wiley & Sons, 2006.
- [31] N. Wisitpongphan, O. Tonguz, J. Parikh, F. Bai, P. Mudalige and V. Sadekar, “*On the Broadcast Storm Problem in Ad hoc Wireless Network*”, IEEE Wireless Communications, 2007.

- [32] M. Torrent-Moreno, D. Jiang, and H. Hartenstein, “Broadcast reception rates and effects of priority access in 802.11-based vehicular ad-hoc networks,” *In Proc. of ACM International Workshop on Vehicular Ad hoc Networks*, Philadelphia, U.S., October 2004.
- [33] G. Karagiannis, O. Altintas, E. Ekici, G. Heijenk, B. Jarupan, K. Lin and T. Weil, “Vehicular networking: A survey and tutorial on requirements, architectures, challenges, standards and solutions,”.
- [34] M. L. Sichitiu and M. Kihl, “Inter-Vehicle Communication Systems: A Survey”, in *IEEE Communications Surveys & Tutorials*, Vol. 10, Issue 2, 2nd Quarter, pp. 88 – 105, 2008.
- [35] Car to Car Communication Consortium, “Car to Car Communication Consortium Manifesto: Overview of the C2C-CC System”, C2C-CC, version 1.1, 2007.
- [36] ETSI TR 102 638, “Intelligent Transport System (ITS); Vehicular Communications; Basic Set of Applications; Definition,” ETSI specification TR 102 638, v.1.1.1, June 2009.
- [37] Intellidrive project, “Vehicle safety applications”, ITS Joint program Office, USDOT, pp. 1-15, 2008.
- [38] IST Safespot project, “Use cases, functional specifications and safety margin applications for the SAFESPOT Project”, Safespot IST-4-026963-IP deliverable D8.4.4, pp 1 – 54, 2008.
- [39] IST PreDrive C2X project, “Detailed description of selected use cases and corresponding technical requirements”, PreDrive C2X deliverable 4.1.
- [40] IST CVIS project, “Use cases and system requirements”, CVIS IST-4-027293-IP deliverable 2.2, v. 1.0, pp 1- 256, 2006.
- [41] C. G. Gavrinca, J. Baranda and P. Henarejos, “Rapid Prototyping of Standard-Compliant Visible Light Communications System,” *IEEE Communications Magazine* , July 2014.

- [42] McKinsey & Company, “Lighting the Way: Perspectives on the Global Lighting Market,” July 2011.
- [43] T. Komine *et al.*, “Basic Study on Visible-Light Communication Using Light Emitting Diode Illumination,” *Proc. 8th Int’l. Symp. Microwave and Optical Technology*, pp. 45–48, 2001.
- [44] T. Komine and M. Nakagawa, “Fundamental Analysis for Visible-Light Communication System Using LED Lights,” *IEEE Trans. Consumer Electronics*, vol. 50, no. 1, pp 100–07, 1 February 2001.
- [45] O. Kampinga and W. Alberda, “Visible Light Communication,” http://www.wikid.eu/index.php/Visible_Light_Communication.
- [46] Renesas, “Renesas Solutions for Wireless Sensor Networks-part 1”.
- [47] H. Elgala, R. Mesleh and H. Haas, “Indoor Optical Wireless Communication: Potential and State-of-the-art,” *IEEE communication magazine*, vol. 49, no.9, pp. 56-62, September 2011.
- [48] D. O’Brien *et al.*, “Home Access Networks Using Optical Wireless Transmission,” *IEEE PIMRC*, pp. 1-5, September 2008.
- [49] N. Fujimoto and H. Mochizuki, “477 Mbit/s Visible Light Transmission Based on OOK-NRZ Modulation Using A Single Commercially Available Visible LED and a Practical LED Driver with a Pre-Emphasis Circuit,” *proc. OFC/NFOEC*, pp. 1-3, 2013.
- [50] S. Dimitrov and H. Haas, “Information Rate of OFDM Based Optical Wireless Communication Systems with Nonlinear Distortion,” *J. Lightwave Tech.*, vol. 31, no. 6, Mar. 2013, pp. 918–29.
- [51] SOCRATIC, “What on the electromagnetic spectrum has the longest wavelength?”.

[52] M. Nakagawa, "Visible Light Communications," Keio University, 25 October 2007.

[53] N. Kumar, "Visible Light Communication: Concept, Technology, Challenges and Possibilities," WCNC 2013, 25 March 2013.

[54] N. Kumar, N. Lourenço, M. Spiez and R.L. Aguiar, "Visible Light Communication Systems Conception and VIDAS," IETE Technical Review, vol. 25, no. 6, pp. 359-367, Nov-Dec 2008.

[55] N. Kumar, L.N. Alves and R.L. Aguiar, "Visible Light Communication for Advanced Driver Assistant Systems," 7th International Conference on Telecommunication, February 2009.

[56] Samsung Electronics, "Visible Light Communication Tutorial", IEEE P802.15 Working Group for Wireless Personal Area Networks (WPANs), March 2008.

[57] R. Ramirez-Iniguez, S.M. Idrus, Z. Sun, "*Optical Wireless Communications : IR for wireless connectivity*," CRC Press, 978-0-8493-7209-4, USA, 2008.

[58] J. M. Kahn and J.R. Barry, "Wireless Infrared Communications," *Proceedings of the IEEE*, Vol. 85, No. 2, February 1997.

[59] R. L. Aguiar, A. Tavares, J. L. Cura, E. De Vaaconcelos, L. N. Alves, R. Valadas and D. M. Santos, "Considerations on the design of transceivers for wireless optical LANs," in *Optical Wireless Communications (Ref. No. 1999/128)*, IEE Colloquium, pp. 2/1-231, 1999.

[60] Disney research, "Visible Light Communication," <http://www.disneyresearch.com/project/visible-light-communication/>.

- [61] S. Kitano, S. Haruyama and M. Nakagawa, "LED road illumination communications system," in *IEEE 58th Vehicular Technology Conference*, pp. 3346-3350, 2003.
- [62] A. Zukauskas, M. S. Shur and R. Gaska, "Introduction to Solid-State Lighting," Wiley's General Components and Devices, New York, Wiley, April 2002.
- [63] M. R. Krames, O. B. Shchekin, R. Mueller-Mach, G. O. Mueller, Z. Ling, G. Harbers and M. G. Craford, "Status and Future of High-Power Light-Emitting Diodes for Solid-State Lighting," *Journal of Display Technology*, vol. 3, pp. 160-175, 2007.
- [64] J. O'Connell, "The Philadelphia story," Traffic Technology International, New York, 1997.
- [65] S. Arnon, "The effect of clock jitter in visible light communication applications," *Journal of Lightwave Technology*, 2012.
- [66] S. Schmid, G. Corbellini, S. Mangold and T. Gross, "An LED-to-LED Visible Light Communication system with software-based synchronization In Optical Wireless Communication," *Globecom Workshops, 2012 IEEE*, pages 1264-1268, December 2012.
- [67] D. Giustiniano, N. Tippenhauer and S. Mangold, "Low-Complexity Visible Light Networking with LED-to-LED Communication," *IFIP Wireless Days 2012*, November 2012.
- [68] A. Tsiatmas, P. M. J. Baggen, F.M. J. Willems, J.M. G. Linnartz, and Jan W. M. Bergmans, "An Illumination Perspective on Visible Light Communications," *IEEE Communications Magazine*, July 2014.
- [69] H. Elgala, R. Mesleh and H. Haas, "Indoor Optical Wireless Communication: Potential and State-of-the-Art," *IEEE Communication*, vol. 49, no. 9, pp. 56–62, September 2011.
- [70] S. Rajagopal, R. D. Roberts and Sang-Kyu Lim, "IEEE 802.15.7 Visible

Light Communication: Modulation Schemes and Dimming Support,” *IEEE Communications Magazine*, March 2012.

[71] A. C. Boucouvalas, “Indoor Ambient Light Noise and Its Effect on Wireless Optical Links,” *IEE P.-Optoelectron.*, vol. 143, no. 6, pp. 334–38, December 1996.

[72] A. M. Khalid *et al.*, “1-Gb/s Transmission over a Phosphorescent White LED by Using Rate-Adaptive Discrete Multitone Modulation,” *IEEE Photon. J.*, vol. 4, no. 5, pp. 1465–73, October 2012.

[73] K. Cui, J. Quan and Z. Xu, “Performance of Indoor Optical Femtocell by Visible Light Communication,” *Opt. Commun.*, vol. 298–299, pp. 59–66, July 2013.

[74] D. C. O’Brien *et al.*, “Visible Light Communication: Challenges and Possibilities,” *IEEE 19th Int’l. Symp. PIMRC*, September 2008.

[75] H. Urabe *et al.*, “High Data Rate Ground-to-Train Free- Space Optical Communication System,” *Optical Engineering*, Special Section on Free-Space Laser Communications, vol. 51, no. 3, March 2012.

[76] S. Okada *et al.*, “On-Vehicle Receiver for Distant Visible Light Road-to-Vehicle Communication,” *2009 IEEE Intelligent Vehicles Symp.* , pp. 1033–38, June 2009.

[77] “The Colour Science Association of Japan,” *Handbook of Colour Science*, 2nd Ed. University of Tokyo Press, 1998.

[78] A.J. Fisher , "A photometric specification for vehicular traffic signal lanterns: Part. 1 luminous intensity necessary for the detection of signals on the line of sight," Institute of Highway and Traffic Research University of New South Wales, 1969.

[79] G. Wyszecki and W.S. Stiles, “Colour Science”, *New York: Wiley*, 2nd Ed., 1982.

- [80] A. Carl, "New ITE Standards for Traffic Signal Lights," Intelligent Transportation Systems, 2005.
- [81] Institute of Transport Research, "Comparison of LED Traffic Signal Specifications," <http://www.lrc.rpi.edu/programs/lighting/Transformation/led/LEDTrafficSignalComparison.asp>, 2009.
- [82] J. R. Barry, J. M. Kahn, E. A. Lee and D. G. Messerschmitt, "High-speed nondirective optical communication for wireless networks," *Network, IEEE*, vol. 5, pp. 44-54, 1991.
- [83] J. M. Kahn and J. R. Barry, "Wireless infrared communications," *Proceedings of the IEEE*, pp. 265-298, 1997.
- [84] I. Moreno, C.C. Sun and R. Ivanov, "Far field condition for light emitting diode arrays," *Applied Optics*, vol. 48, no.6, pp. 1190-1197, 2009.
- [85] N. Kumar, L.N. Alves and R.L. Aguiar, "Design and analysis of the basic parameters for traffic information transmission using VLC," in *Proceedings of IEEE Wireless Communication, Vehicular Technology, Information Theory and Aerospace & Electronic Systems Technology, Wireless VITAE'2009*, pp. 798-802, 2009.
- [86] N. Kumar, L. Nuno, L.N. Alves and R. L. Aguiar, "LED-based Traffic Light Emitter Model for Road Safety Applications," Submitted to *Journal of Transportation Research: Part C*, 03 March 2011.
- [87] G. Corbellini, K. Aksit, S. Schmid, S. Mangold and T. R. Gross, "Connecting Networks of Toys and Smartphones with Visible Light communication," *IEEE Communications Magazine*, July 2014.
- [88] A. Tsiatmas, F.M.J. Willems and C.P.M.J. Baggen, "Square Root Approximation to the Poisson Channel," *Proc. IEEE ISIT*, 2013, pp. 1695–99.
- [89] A. M. Khalid *et al.*, "1-Gb/s Transmission over a Phosphorescent White LED by Using Rate-Adaptive Discrete Multitone Modulation," *IEEE Photon. J.*, vol. 4, no. 5, Oct. 2012, pp. 1465–73.

- [90] J.M. Kahn and J.R. Barry, "Wireless Infrared Communications," *Proc. IEEE*, vol. 85, no. 2, pp. 265–98, February 1997.
- [91] M. Gebhart, E. Leitgeb and J. Bregenzer, "Atmospheric effects on optical wireless links," in *Telecommunications, ConTEL'2003. Proceedings of the 7th International Conference*, vol.2, pp. 395-401, 2003.
- [92] S.J. Urachada, K. Yasuo, I. Akira and A.R. James, "Channel modeling for optical wireless communication through dense fog," *Journal of Optical Networking*, vol. 4, pp. 291-299, 2005.
- [93] S. Chandrasekhar, "Radiative Transfer", Clarendon, 1950.
- [94] A. Ishimaru, "Wave Propagation and Scattering in Random Media", IEEE Press Series in Electromagnetic Theory, 1997.
- [95] H. Park and J.R. Barry, "Modulation analysis for wireless infrared communications," 1995. *ICC '95 Seattle, 'Gateway to Globalization', IEEE International Conference on Communications*, vol. 2, pp. 1182 - 1186, 1995.
- [96] A.J.C. Moreira, R.T. Valadas and A.M de Oliveria Duarte., "Optical interference produced by artificial light," *Wireless Networks*, vol. 3, pp. 131-140, 02 May 1997.
- [97] S. Hidemitsu, H. Shinichiro and M. Nakagawa, "Experimental Investigation of Modulation Method for Visible-Light Communication," *IEICE Trans. Commun.*, vol. E89-B, pp. 3393-3400, 2006.
- [98] K.-C. Chen, T.-Y. Cheng, "Signaling Methods of IR PHY," Submitted to IEEE 802.11 Standardization Project, September 1993.
- [99] S. Hranilovic, "Wireless Optical Communication Systems," Springer, 2005.
- [100] T. O'Farrell and M. Kiatweerasakul, "Performance of a spread spectrum infrared transmission system under ambient light interference," in *Personal, Indoor and Mobile Radio Communications, The Ninth IEEE International Symposium*, pp. 703-707 vol.2, 1998.

[101] H. Burchardt, N. Serafimovski, D. Tsonev, S. Videv and H. Haas, “VLC: Beyond Point-to-Point Communication,” *IEEE Communications Magazine* , July 2014.

[102] T. Yamazato, I. Takai, H. Okada, T. Fujii, T. Yendo, S. Arai, M. Andoh, T. Harada, K. Yasutomi, K. Kagawa and S. Kawahito, “Image-Sensor-Based Visible Light Communication for Automotive Applications,” *IEEE Communications Magazine* , July 2014.

[103] K. Navin, L.N. Alves and R.L. Aguiar, ”Traffic Light as Road Side Unit for Road Safety Information Broadcast using Visible Light Communication”, for the book *Roadside Networks for Vehicular Communications: Architectures, Applications and Test Fields*, Publisher. IGI Global, April 2011.

[104] IEEE 802.11p, ”Wireless Access in Vehicular Environment (WAVE)”, IEEE, 2010.

[105] Y. Wang, A. Ahmed, B. Krishnamachari and K. Psounis, “IEEE 802.11p Performance Evaluation and Protocol Enhancement,” *Proceedings of the 2008 IEEE International Conference on Vehicular Electronics and Safety Columbus*, OH, USA, 22 September 2008.

[106] ns-3 project, “ns-3 manual,” 05 March 2014.

[107] L. Cheng, B.E. Henty, D.D. Stancil, F. Bai and P. Mudalige, “Mobile Vehicle-to-Vehicle Narrow-Band Channel Measurement and Characterization of the 5.9 GHz Dedicated Short Range Communication (DSRC) Frequency Band,” *IEEE journal on selected areas in communications*, vol.25, no.8, October 2007.